

Medical University of South Carolina

MEDICA

MUSC Theses and Dissertations

2016

Diffusion MRI and Pharmacological Enhancement of Motor Recovery after Stroke

Rachel Ann Weber

Medical University of South Carolina

Follow this and additional works at: <https://medica-musc.researchcommons.org/theses>

Recommended Citation

Weber, Rachel Ann, "Diffusion MRI and Pharmacological Enhancement of Motor Recovery after Stroke" (2016). *MUSC Theses and Dissertations*. 441.

<https://medica-musc.researchcommons.org/theses/441>

This Dissertation is brought to you for free and open access by MEDICA. It has been accepted for inclusion in MUSC Theses and Dissertations by an authorized administrator of MEDICA. For more information, please contact medica@musc.edu.

**Diffusion MRI of Peri-infarct Tissue and Pharmacological Enhancement of
Recovery After Stroke**

Rachel Ann Weber

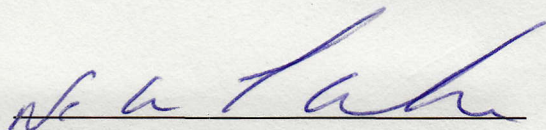
A dissertation submitted to the faculty of the Medical University of South Carolina in
partial fulfillment of the requirements for the degree of Doctor of Philosophy in the
College of Graduate Studies.

Department of Neurosciences

2016

Approved by:

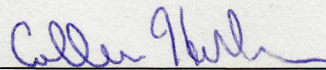
Chairman, Advisory Committee



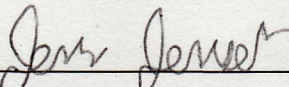
DeAnna L. Adkins



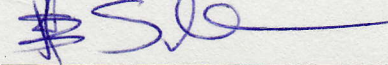
Andy Shih



Colleen Hanlon



Jens Jensen



Rick Schnellmann

ACKNOWLEDGEMENTS

I would like to thank my dissertation advisor and mentor, Dr. DeAnna Adkins for the support and mentorship you have provided me throughout my time in graduate school. You have been my strongest advocate and continue to push me to be the best scientist possible. I would also like to thank my committee members: Drs. Andy Shih, Jens Jensen, Colleen Hanlon, and Rick Schnellmann for providing me with helpful feedback and support. I have had the opportunity to form close relationships with each of my committee members individually, and I appreciate the consideration they have shown for my personal and professional development. I would also like to thank Elyse Summers, the former research assistant in the Adkins Lab, for being an outstanding friend, providing emotional support throughout graduate school, and helping me conduct experiments.

I especially want to thank my husband, Zac Manahan, his devotion during all the ups and downs of graduate school. He consistently remained invested in me as a scientist and supported me at all times. I would like to thank my family, especially my mom, for giving me unconditional love, encouragement, and always pushing me. Even from across the country, the love and support you provided helped me to achieve my goals.

The friends I have made since moving to Charleston have been crucial in making my time in Charleston and MUSC unforgettable. I want to thank Marcie Parkash for being my personal and emotional support system in all aspects of my life.

I could not have been as productive, motivated, and sane throughout graduate school without all of you. Thank you!

TABLE OF CONTENTS

ACKNOWLEDGEMENTS.....	i
LIST OF TABLES.....	v
LIST OF FIGURES.....	vi
ABSTRACT.....	viii
CHAPTER 1: INTRODUCTION.....	2
Ischemic Stroke.....	3
Animal Models of Ischemic Stroke.....	5
MCAO.....	5
Photothombic.....	6
Endothelin-1.....	6
Motor Learning-Dependent Plasticity.....	7
Motor Cortex.....	8
Dorsal Striatum.....	10
Sensory Cortex.....	11
Spontaneous and Experience-Induced Stroke Induced Plasticity.....	12
Stroke Rehabilitation.....	12
Diffusion MRI: Measures and Modeling.....	14
Diffusion Tensor Imaging (DTI).....	15
Diffusion Kurtosis Imaging (DKI).....	16
White Matter Tract integrity (WMTI) and Tract Based Spatial Statistics (TBSS).....	16
Diffusion MRI and Ischemic Injury.....	17
Diffusion MRI and Rehabilitative Training.....	18
Mitochondria Homeostasis.....	19
Mitochondria Biogenesis.....	19

Mitochondria Injury and Cerebral Ischemia.....	21
Mitochondria Function and Biogenesis, Neuronal Survival, Neuronal Remodeling.....	22
Effects of β_2 -Adrenergic Receptor Agonist on Learning and Recovery from Stroke.....	23
Conclusions and Research Directions.....	23
CHAPTER 2: CHANGES IN TISSUE DIFFUSION PROPERTIES FOLLOWING ACUTE STROKE.....	25
Introduction.....	25
Methods.....	27
Results.....	31
Discussion.....	40
CHAPTER 3: CHANGES IN TISSUE DIFFUSION PROPERTIES FOLLOWING REHABILITATION IN EXPERIMENTAL STROKE ANIMALS.....	46
Introduction.....	46
Methods.....	47
Results.....	50
Discussion.....	56
CHAPTER 4: CHARACTERIZING MITOCHONDRIA DYSFUNCTION AFTER STROKE AND RESCUING MITOCHONDRIA FUNCTION TO PROMOTE MOTOR RECOVERY.....	60
Introduction.....	60
Methods.....	63
Results.....	69
Discussion.....	87
CHAPTER 5: DISCUSSION AND CONCLUSIONS.....	98
Diffusion MRI Used as a Predictor After Stroke.....	98
Formoterol as a Potential Pharmacotherapy Following Stroke.....	104
Proposed Mechanism of Action.....	107

Future Directions.....	107
Conclusions.....	108
REFERENCES.....	110

List of Tables

Chapter 2

Table 2.1. Large sensorimotor cortical stroke dMRI and surface densities results.....34

Table 2.2. Moderate focal cortical stroke dMRI and surface densities results.....39

Chapter 3

Table 3.1. dMRI metric changes following a cortical stroke and rehabilitation training.....52

Table 3.2. dMRI metric changes following skilled forelimb training.....56

Chapter 4

Table 4.1. Primer pairs used for qRT-PCR.....66

List of Figures

Chapter 1

Figure 1.1. Cortical Motor Map Reorganization.....10

Figure 1.2. Regulation of Mitochondria Homeostasis and Biogenesis.....21

Chapter 2

Figure 2.1 Lesion Core and Peri-lesion dMRI Results.....32

Figure 2.2 Surface Density of GFAP.....33

Figure 2.3 Behavioral Impairments Following Stroke.....35

Figure 2.4 Lesion Core and Peri-lesion dMRI Results.....36

Figure 2.5 Surface Density and Correlations of GFAP and dMRI.....37

Figure 2.6 Surface Density of SMI312 and MAP2.....38

Figure 2.7 Behavioral Impairment Post Stroke.....40

Chapter 3

Figure 3.1 Peri-lesion dMRI Results Following RT.....51

Figure 3.2 Animals that Undergo RT have Greater Functional Improvement.....53

Figure 3.3 FA Increased in Naïve Animals.....54

Figure 3.4 MK Increased in Naïve Animals.....54

Figure 3.5 Axonal Water Fraction Increased in Naïve Animals.....55

Chapter 4

Figure 4.1 Stroke Induced Motor Impairment.....70

Figure 4.2 Decreased Respiratory Chain Gene Expression and mtDNA Content in Ipsilesional Motor and Sensory Cortex.....71

Figure 4.3 Transitory Changes of Mitochondrial Encoded Transcripts in Ipsilesional Striatum.....72

Figure 4.4 Reduced Mitochondrial Encoded Protein Expression in the Ipsilesional Cortex and Striatum.....73

Figure 4.5 UCP2 Activation in the Ipsilesional Cortex and Striatum.....74

Figure 4.6 Gene Expression of Inflammatory Mediators and Macrophages in the Ipsilesional Cortex and Striatum.....	75
Figure 4.7 Caspase 3 Cleavage and GAP43 Expression in Ipsilesional Cortex and Striatum.....	76
Figure 4.8 Behavioral Performance after Formoterol Treatment.....	78
Figure 4.9 Ipsilateral Motor and Sensory Cortex Markers Following Formoterol Treatment.....	79
Figure 4.10 Ipsilateral Striatum Markers Following Formoterol Treatment.....	80
Figure 4.11 Protein Expression Acutely After Formoterol Treatment.....	81
Figure 4.12 UCP2 Transcript Levels Following Formoterol Treatment.....	82
Figure 4.13 IL-6 and F4/80 Transcript Levels Following Formoterol Treatment.....	83
Figure 4.14 Cleaved Caspase 3 and GAP-43 Expression After Formoterol Treatment..	84
Figure 4.15 0.5mg/kg Formoterol and RT were not Different from Vehicle.....	85
Figure 4.16 1.0mg/kg Formoterol and RT were not Different from Vehicle.....	85
Figure 4.17 0.1mg/kg Formoterol and RT was Most Effective to Enhance Motor Recovery.....	86
Chapter 5	
Figure 5.1 0.1mg/kg Formoterol in Naïve Animals.....	106

ABSTRACT

RACHEL ANN WEBER. Diffusion MRI and Pharmacological Enhancement of Motor Recovery After Stroke. (Under the direction of DEANNA L. ADKINS)

The primary goal of these studies is to enhance recovery of motor function following stroke and to understand the relationship between dMRI measures and the cellular, functional, and behavioral changes acutely and chronically following rehabilitation. ***We hypothesize that dMRI will be a sensitive tool to identify microstructural changes acutely and chronically following stroke and that promoting mitochondria biogenesis will lead to better functional recovery and induce structural and functional plasticity following rehabilitative training.*** Towards this goal, we used a combination of sensitive behavioral, immunohistochemical and mitochondrial-related molecular markers, and diffusion magnetic resonance imaging (dMRI) to investigate the time course of acute and chronic stroke effects.

We were able to detect acute changes in dMRI metrics and correlate those changes with functional and morphological plasticity following stroke. Our work has shown that mean kurtosis, a dMRI metric, increased acutely after stroke and persists days post-stroke in the lesion core. We found strong correlations between mean diffusivity and astrogliosis in the perilesional stroke area. There were no correlations between dendritic and axonal surface densities and dMRI metrics acutely following stroke. However, behavioral-induced and learning-induced neural plasticity was not detected with dMRI changes chronically in perilesional grey matter or white matter.

Our studies have revealed mitochondria dysfunction that persists for at least six days post stroke in ipsilesional cortex and striatum following a focal sensorimotor (SMC) ischemic lesion. Therefore, we proposed that pharmacologically enhancing mitochondria function and biogenesis would promote recovery after stroke when administered early after stroke. We found that giving a drug known to induce mitochondria biogenesis,

formoterol, a FDA approved long-lasting β_2 -adrenergic receptor agonist, twenty-four hours after SMC ischemic lesions caused a full restoration of markers of mitochondria function in the striatum three days post stroke and stimulates a partial recovery of functional markers in the cortex six days post-stroke. Our studies revealed that animals given formoterol (0.1mg/kg) combined with motor rehabilitative training (RT) daily for 15 days leads to better recovery of motor function than animals given vehicle treatment and RT. These data demonstrate that stimulating mitochondria biogenesis acutely after stroke enhances functional motor recovery.

CHAPTER 1: INTRODUCTION

Ischemic stroke is a leading cause of death in the world, and a majority of stroke survivors are left with long-lasting motor deficits. The primary goals of the following studies were 1) to enhance recovery of motor function via stimulating mitochondria biogenesis following stroke and 2) to understand the relationship between dMRI measures and cellular, functional, and behavioral changes acutely and chronically. Stroke-induced neural dysfunction is the result of neuronal injury and death; dMRI may be used as a prognostic tool to determine imaging biomarkers of recovery of motor function after we have a better understanding of the morphological changes that correspond with changes in dMRI metrics. In Chapter 2, we present the results of studies examining acute stroke-induced effects on diffusion properties of water in lesion and perilesional tissue using several sensitive dMRI metrics. We then investigated how these dMRI measures correspond to alterations in structural changes in axons, dendrites, and glia. The goal was to identify potential cellular structural changes that may be driving changes in water diffusion and thus the changes in dMRI. We also examined the relationship between dMRI measures and rehabilitation-induced functional recovery.

In Chapter 4, we examined whether we could improve stroke recovery through pharmacological manipulation. Currently, drug therapy following stroke is limited to tissue plasminogen activator (TPA), which breaks down blood clots, must be administered within six hours of a stroke, and when administered early reduces the overall size of the ischemic lesion. This window is normally too short and TPA has several severe side effects. Additionally, TPA only treats the initial phase of the injury and therapies are needed that also stimulate neuronal recovery in vulnerable tissue connected to the lesion core and increase functional recovery. One possible means to support this vulnerable tissue, the perilesional area, is to stabilize mitochondrial homeostasis and potentially increase mitochondrial biogenesis. In the following studies we examined the time course of

mitochondria dysfunction acutely in ipsilesional cortex and striatum following a focal sensorimotor (SMC) ischemic lesion. We then examined whether formoterol, a FDA approved long-lasting β_2 -adrenergic receptor agonist, would enhance mitochondrial function and biogenesis in perilesional tissue and lead to greater recovery after stroke. Formoterol has been shown to induce mitochondrial biogenesis following ischemic injury in the kidney. To determine recovery of mitochondrial function, we used a well-established battery of markers of mitochondrial health. Because neurons remain dysfunctional for days and weeks after stroke, we also examined promoting mitochondrial health during rehabilitative training to enhance the efficacy of well-established rehabilitative training interventions.

We hypothesized ***that dMRI would be a sensitive tool to identify microstructural changes acutely and chronically following stroke and that promoting mitochondrial biogenesis would lead to better functional recovery and induce structural and functional plasticity following rehabilitative training.*** Towards these aims, we used sensitive behavioral, immunohistochemical, and mitochondrial-related molecular markers, in combination with diffusion magnetic resonance imaging (dMRI) to investigate the time course of acute and chronic stroke effects. The studies discussed below have been promising for stroke recovery and understanding early biomarkers post stroke.

Outlined below is the basic premise of these studies, starting with the pathophysiology of stroke and animal models of stroke. Learning-dependent plasticity, stroke-induced plasticity, and plasticity following stroke rehabilitation are highlighted to understand the functional and structural plasticity mechanisms we plan to examine in the studies within this dissertation. Lastly, aspects of dMRI and mitochondrial function and biogenesis are discussed to understand the building blocks of the subsequent studies.

Ischemic Stroke

A stroke occurs from an interruption of blood supply to the brain leading to cell death and dysfunction. Annually, roughly 800,000 people suffer from a new or recurrent stroke (Association 2015). An ischemic stroke, which accounts for 87% of all strokes, occurs when blood clots or plaques (fatty deposits and cholesterol) block the brain's blood flow. Hemorrhagic stroke, accounting for 13% of all strokes, occurs when blood seeps into brain tissue from blood vessel rupture or an aneurysm that bursts. Although ischemic strokes are more common, hemorrhagic strokes have a higher mortality rate. The studies included in this dissertation used an animal model of ischemic stroke, to model the more commonly occurring type of stroke.

The brain comprises 2% of total body weight but receives 15-20% of cardiac output, 20% of total body oxygen, and 25% of total body glucose (Mergenthaler, Lindauer et al. 2013). Normal blood flow to the brain delivers oxygen, glucose, and nutrients while removing carbon dioxide, lactic acid, and metabolites. Unlike the majority of other cells in the body, neurons almost exclusively use aerobic mechanisms to produce energy, in the form of adenosine triphosphate (ATP), namely by means of oxidative metabolism of glucose. The brain burns glucose instead of storing it for future use and lacks the ability to store creatine phosphate and glycogen (Mergenthaler, Lindauer et al. 2013), and therefore must rely upon a continuous supply of oxygen. Consequently, the brain is highly vulnerable to disrupted blood flow and damage can begin within 4-5 minutes of oxygen deprivation and 10-15 minutes of glucose deprivation.

Acute cell death within the lesion core can be caused by upregulated calcium, tissue acidosis, and free radical production. The large increase in calcium inside neurons occurs in part because without ATP, calcium export to the extracellular environment by ATP-dependent calcium pumps and the sodium/calcium exchanger can no longer occur (Woodruff, Thundyil et al. 2011). Without calcium movement out of the cell, cell death pathways will be activated. Edema, inhibition of hydrogen extrusion, inhibition of lactate

oxidation, and impairment of mitochondrial respiration all lead to tissue acidosis (Anderson and Sims 1999). Additionally, anaerobic metabolism of glucose is initiated during stroke, leading to a rise in lactate production and a fall in pH levels. Insufficient oxygen to accept electrons via the mitochondria electron transport chain causes free radical formation, which exacerbates damage to proteins, DNA, lipids, and fatty acid components of the cell membrane (Duchen 2000, Kann and Kovacs 2007). Within minutes to hours after injury, apoptosis starts to occur, normally due to calcium influx and mitochondria dysfunction (Duchen 2000). Degeneration of distal axons, also known as Wallerian degeneration occurs days to weeks following injury, due to onset of deleterious metabolic pathways which leads to expansion of infarct size and worsening of clinical outcomes (Borgens and Liu-Snyder 2012). The area undergoing secondary injury that surrounds the core of the ischemic lesion is termed the penumbra.

Animal Models of Ischemic Stroke

Middle Cerebral Artery Occlusion (MCAO)

The middle cerebral artery occlusion (MCAO) method is the most common and widely used stroke model to date. Many argue that this method is the most comparable to human stroke because the middle cerebral artery is often occluded in humans (Carmichael 2005). There are many methods used to induce a MCAO. One common MCAO method is to temporarily tie off the common carotid artery and a suture is inserted into the internal carotid artery to block the origin of the MCA at the circle of Willis for a predetermined period of time or permanently. By 12 hours after occlusion, irreversible cortical and striatal damage is induced (Liu and McCullough 2011), although apoptosis peaks at 24-48 hours post stroke (Linnik, Miller et al. 1995, Chen, Jin et al. 1997). This technique does not require a craniotomy and can be done in a high throughput manner (Carmichael 2005, Liu and McCullough 2011). MCAO strokes in rodents can come with a high mortality rate that is increased in aged and high risk (high blood pressure for example) animals (Liu and

McCullough 2011). Lastly, this model may be a poor model of human strokes because of the extremely different lesion sizes produced in rodents compared to humans. A MCAO stroke in rodents can cause damage throughout the entire sensory and motor area of the forelimb region as well as a majority of striatum, hippocampus, and other subcortical structures. This severe of a stroke is not often seen in humans and would cause death.

Photothrombosis

The photothrombotic stroke model is induced by photo-activation of an injected light sensitive dye in an animals' blood stream. Once the dye becomes active, singlet oxygen is generated and induces endothelial damage and platelet aggregation, resulting in disrupted blood flow at the site of injury and in downstream tissues perfused by the occluded arteries (Carmichael 2005, Labat-gest and Tomasi 2013). A strong immune response resulting in T-cell activation, cytokine release, and microglia upregulation, is seen within days following ischemia (Schroeter, Jander et al. 1997, Jander, Schroeter et al. 2000). Advantages of this method is the ability to stereotaxically photo-activate a specific region of the brain such as a barrel field, the small and focal lesions that are produced, and the minimal amount of surgical procedures required (Carmichael 2005). The greatest disadvantage of the photothrombotic stroke model is the lack of penumbra development, especially because the penumbra is the target for a large number of stroke therapeutics (Labat-gest and Tomasi 2013).

Endothelin-1 (ET-1)

Endothelin-1 is a vasoconstricting peptide that is produced endogenously and can be infused or injected exogenously to cause ischemia. Endothelin-1 produces highly reproducible and focal ischemic lesions (Adkins, Voorhies et al. 2004). As with any stroke model there are limitations. There are ET-1 receptors located on both neurons and glia, and application of ET-1 can alter cell morphology and interfere with the interpretation of neural repair experiments through receptor-mediated signaling effects (Nakagomi, Kiryu-

Seo et al. 2000, Carmichael 2005). Biernaskie and colleagues demonstrated that ET-1 injected near the MCA reduced blood flow in the cortex for 16 hrs and in the striatum for 7 hrs inducing ischemic lesions with a final infarct size identifiable at 48 hrs with T2-weighted MRI (Biernaskie, Corbett et al. 2001). The evolution of ET-1 ischemia in rodent models is thought to mimic the subacute onset of human ischemia (Marchal, Young et al. 1999, Biernaskie, Corbett et al. 2001). Therefore it is a good model to examine pathway disruptions and ultimately to test potential human therapeutics.

All experimental strokes in this dissertation were induced using an ET-1 model of ischemia in adult rats due to the reproducible and focal lesions produced and penumbra present.

Motor Learning-Dependent Plasticity

We know that motor learning alters brain function and drives neural remodeling in healthy brains (Kleim, Hogg et al. 2004, Adkins, Boychuk et al. 2006). Motor learning is also an effective form of rehabilitative training that leads to behavioral improvements and neural plasticity (Whishaw, Pellis et al. 1991, Alaverdashvili and Whishaw 2013). However, rehabilitation training often is insufficient and individuals continue to suffer incomplete recovery (Maldonado, Allred et al. 2008). One of the primary goals of the following studies is to investigate whether a potential pharmacological treatment can enhance the effects of rehabilitation training in an animal model of stroke.

There are conflicting reports on the definition of motor learning; some believe no definition is needed (Krakauer 2006), while others give very specific definitions (Wolpert, Ghahramani et al. 2001, Wise 2005). We have operationally defined motor learning as “a change in behavior that takes place following training on a specific task”. Motor learning occurs through the cortico-striatal system and plasticity following learning takes place throughout the nervous system, however the work here will focus on both the motor and

sensory cortex and striatum (Doyon and Benali 2005). While a majority of this review of motor learning plasticity is taken from animal reports, similar processes occurs in humans as well (Zatorre, Fields et al. 2012).

Motor Cortex

The primary motor cortex is organized with a physical representation of the body called the homunculus and is arguably the most studied areas in association with motor learning. The motor cortex undergoes functional and structural plasticity following motor learning. Several studies have shown that following training on a motor task, synapse formation and immediate early gene upregulation occurs in the primary motor cortex of rats. New synapses that form have a higher efficiency that is correlated with task retention (Kleim, Lussnig et al. 1996, Rioult-Pedotti, Friedman et al. 2000, Kleim, Hogg et al. 2004, Rioult-Pedotti, Donoghue et al. 2007, Harms, Rioult-Pedotti et al. 2008). Additionally, within one hour of training animals on a new task, new spines form on dendritic spines in the primary motor cortex that stabilize following additional training and persist for at least 5 months after training stops (Xu, Yu et al. 2009). Synapse formation was task-specific, animals were tested on two skilled forelimb reaching tasks, and each task tested produced a different cluster of new spine formation (Xu, Yu et al. 2009).

Performance of the learned motor skill and the resulting changes are dependent on protein synthesis (Kleim, Bruneau et al. 2003). Brain-derived neurotropic factor (BDNF) is one neurotropic factor involved in this plasticity. In rodents, BDNF has been found to play a role in learning dependent long-term potentiation (LTP) (Figurov, Pozzo-Miller et al. 1996, Aicardi, Argilli et al. 2004), a long-lasting strengthening of synapses that occurs following learning. BDNF has a well-known single nucleotide polymorphism (SNP), Val66Met that has been shown to play a role in several brain functions and emotions: anxiety (Chen, Jing et al. 2006, Martinowich, Manji et al. 2007), learning (Soliman, Glatt et al. 2010), episodic memory (Egan, Kojima et al. 2003), depression (Martinowich, Manji

et al. 2007), and others. This polymorphism seems to also play a role in motor dependent learning plasticity (Kleim, Chan et al. 2006, Cheeran, Talelli et al. 2008). Several reports indicate that humans with the Met allele, show decreases in corticospinal excitability and experience-dependent motor learning plasticity (Adkins, Boychuk et al. 2006, Kleim, Chan et al. 2006, Cheeran, Talelli et al. 2008). Other factors associated with learning dependent motor plasticity are still under investigation.

Rat primary motor cortex is organized into areas devoted to particular movements and can be further divided into motor maps based on specific movements (Neafsey, Bold et al. 1986), similar to the human homunculus. In rodents the sensory and motor cortices overlap in areas representing the forelimbs and hindlimbs, therefore throughout our studies we will target the forelimb area of the sensorimotor cortex (SMC). Additionally, there are two primary motor areas of importance for these studies: the caudal forelimb area (CFA) and the rostral forelimb area (RFA). The CFA is thought to represent the primary motor area, whereas the RFA is akin to the primate premotor cortex (Kleim, Barbay et al. 1998). Motor maps have now been extensively studied in rats and primates (Nudo, Milliken et al. 1996, Tennant, Adkins et al. 2012, Tennant, Kerr et al. 2015). Animals trained on a motor learning task, such as the single pellet reaching task, have increases in motor map representations following learning that correspond to the specific motor areas targeted by training (Adkins, Boychuk et al. 2006). The synaptic changes referred to in the paragraph above occur within hours, however the reorganization of cortical representations takes longer to become persistent. Animals trained on a skilled reaching task for 10 days show a reorganization of the motor maps compared to animals that practice to reach for a pellet out of reach resulting in unskilled reach training (Kleim, Hogg et al. 2004). Specifically, these animals show an increase in the proportion of caudal forelimb area represented by digits and wrist and a decrease in elbow/shoulder representations following training (Kleim, Barbay et al. 1998, Kleim, Hogg et al. 2004).

Additional evidence for specificity with increased motor maps comes from studies performed on squirrel monkeys. Monkeys first trained on a skilled digit task that caused an expansion of the digit motor representation were subsequently trained on a wrist specific task causing a decrease of the previously expanded digit map representation and an increase in the wrist motor representation as observed in the same animals (Nudo, Milliken et al. 1996, Adkins, Boychuk et al. 2006).

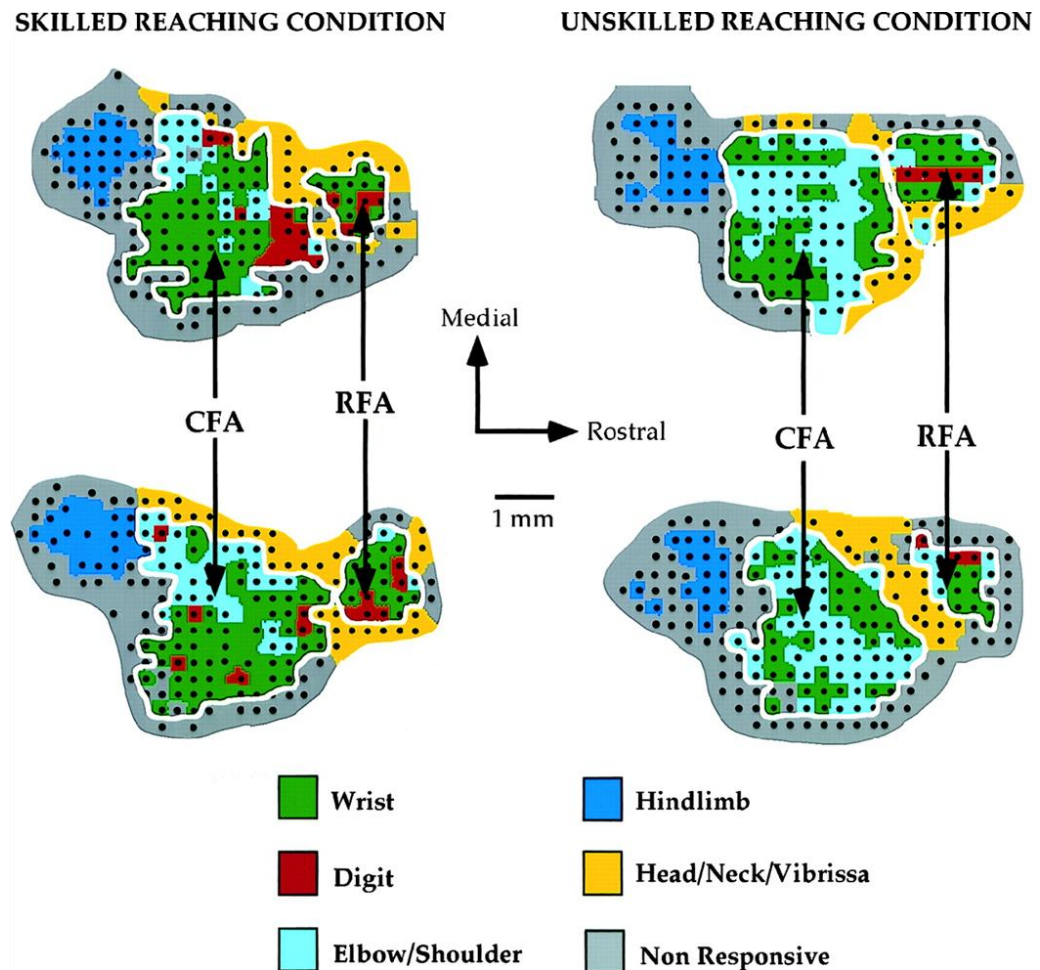


Figure 1.1. Cortical Motor Map Reorganization.

Motor representations of the wrist and digits increase following skilled reaching in the caudal forelimb area, whereas the elbow/shoulder representations decrease. In the unskilled reaching condition, there was no change. Adapted from Kleim et al. *J Neurophysiol.* 1998 Dec;80(6):3321-5.

Dorsal Striatum

Cortical pyramidal neurons from layer V in the motor cortex project to the dorsal striatum (caudate and putamen), this vital connection has pushed researchers to understand plasticity in the dorsal striatum following motor learning, which is thought to be involved in several aspects of motor learning. One group examined neuron recruitment during a motor task and found throughout motor learning trials, an increased number of striatal neurons were active as measured by multielectrode arrays (Costa, Cohen et al. 2004). This process was similar to patterns of activity they observed in the motor cortex. Once a motor learning task has been mastered, cortical and dorsal striatal neurons changed their firing pattern in parallel (Costa, Cohen et al. 2004). Secondly, researchers have found that the striatum is involved after the motor learning of a specific task has been acquired and likely important for long-term storage of the learned movement sequences learned (Ungerleider, Doyon et al. 2002). Dang and colleagues recently found that knocking out NMDA subunit 1, a receptor known to be essential for LTP, in the striatum impairs motor learning but does not have an effect on striatal neuronal morphology (Dang, Yokoi et al. 2006). Lastly, several research groups have shown that lesions in the dorsal striatum cause impairments in motor learning (Featherstone and McDonald 2005).

Sensory Cortex

Motor learning does not exclusively rely on the motor cortex and the striatum. A lesion in the sensory cortex resulted in an animal's inability to learn a new motor skill; however, these lesions had no effect on existing motor skills learned prior to the lesion (Sakamoto, Arissian et al. 1989, Pavlides, Miyashita et al. 1993). Several stimulation studies have attempted to understand the role of the sensory cortex in animals and humans. Microstimulation of the sensory cortex caused an increase in excitatory post synaptic potentials (EPSPs) in the motor cortex, therefore the sensorimotor connection is likely essential to motor learning (Sakamoto, Porter et al. 1987). While human subjects attempted to learn a new motor task, researchers have used repetitive transcranial

magnetic stimulation (rTMS) to inhibit the sensory cortex which resulted in subjects performing worse on the motor task than participants receiving sham stimulation (Vidoni, Acerra et al. 2010).

Spontaneous and Experience Induced Stroke Induced Plasticity

It is important to understand spontaneous- and experience-induced plasticity following a stroke in order to appreciate how learning-induced plasticity may promote regenerative processes and behavioral recovery. Experience-dependent and spontaneous stroke-induced plasticity can be enhanced through motor learning and rehabilitation. Although these changes occurred following strokes without any specific rehabilitation or motor learning, these studies notably allowed animals to use their impaired limb through experiences in their home cages. Within days after stroke, growth factors, cell adhesion molecules, axonal guidance, and cytoskeleton modifying molecules are increased compared to sham animals (Li, Overman et al. 2010). As early as three weeks after stroke, axonal sprouting occurs in the cortical areas surrounding and connected to the lesion (Carmichael, Wei et al. 2001). Axonal sprouting is essential for recovery post stroke; induction of axon sprouting can enhance recovery whereas inhibiting sprouting can inhibit recovery (Carmichael, Kathirvelu et al. 2016). Axonal sprouting occurs in the contralateral cortex in corticospinal neurons (Carmichael, Kathirvelu et al. 2016) and in contralesional cortical neurons that cross the corpus callosum and innervate the ipsilesional striatum (Carmichael and Chesselet 2002, Riban and Chesselet 2006). Dendritic spine remodeling occurs within two weeks after stroke in cortical areas surrounding a photothrombotic stroke in somatosensory cortex (Brown, Boyd et al. 2010), one report shows an increase in synaptic connections in neurons even 2-3mm from the lesion (Mostany, Chowdhury et al. 2010).

Stroke Rehabilitation

About one-third of all stroke patients have persistent motor disabilities following a stroke (Kelly-Hayes, Robertson et al. 1998). Timely and appropriate rehabilitation interventions are desperately needed to increase motor function in these patients. The age of the individual (Tennant, Adkins et al. 2012), intensity of the training (Bell, Wolke et al. 2015), and size and location of the lesion have all been found to influence the effectiveness of rehabilitative training. Studies have shown that behavioral dependent brain plasticity following a stroke in the remaining motor cortex and the rostral forelimb area are vital for recovery of motor function (Nudo 2013). Following incomplete motor cortical strokes, the remaining motor cortex, part of the perilesional area, undergoes robust functional and structural plasticity following a stroke. Animals that receive rehabilitation training have preservation of the forelimb area of the motor cortex and this motor map expands (Nudo 1997). However, when animals do not receive rehabilitation training following stroke, there is a greater loss of the motor map of the forelimb area of the motor cortex (Nudo 1997, Nudo 2006). The striatum also undergoes plasticity changes after a SMC ischemic lesion (Carmichael and Chesselet 2002).

Motor learning is when a change in behavior occurs following training on a specific task. Skilled motor learning can be defined as the acquisition and refinement of a combination of movement sequences (Adkins, Boychuk et al. 2006). Dendritic and synaptic morphology of the motor cortex is altered after specific learning tasks such as skilled forelimb training (Jones, Chu et al. 1999, Kleim, Freeman et al. 2002, Harms, Rioult-Pedotti et al. 2008). Additionally, there is an increase in dendritic density, which likely represents greater capacity or greater functional ability after skilled forelimb training. The single-pellet reaching task (SPR), a skilled forelimb training task that alters the non-injured brain and is used as a rehabilitation training task in animal models of brain injury. The task requires rats to reach through a narrow window and retrieve a flavored pellet (Whishaw and Pellis 1990). The SPR task has been shown to have very similar kinematic

movements to humans reaching for an object (Karl and Whishaw 2013) and one can examine qualitative gross and fine motor movements through slow-motion video replay. Animals that are trained on the SPR task have greater motor improvement compared to animals that receive control procedures, such as eating flavored pellets off the ground; however these animals only recover sub optimally (Maldonado, Allred et al. 2008). Previously, our lab and others have found that pairing rehabilitation with drug treatments or cortical stimulation enhances rehabilitation compared to rehabilitation alone following ischemic stroke and traumatic brain injury (Adkins-Muir and Jones 2003, Adkins and Jones 2005, Adkins, Campos et al. 2006, Adkins, Hsu et al. 2008, Jones and Adkins 2015). It is known that these skilled motor tasks result in reorganization of the movement representations within the motor cortex and induce cortical plasticity, such as synaptogenesis and dendritic plasticity (Adkins-Muir and Jones 2003, Adkins, Voorhies et al. 2004, Kleim, Hogg et al. 2004). These plastic changes are likely resulting in long-term potentiation like changes in the motor cortex (Rioult-Pedotti, Friedman et al. 2000, Hodgson, Ji et al. 2005) and represent motor learning within the cortex.

Diffusion MRI: Measures and Modeling

One of the goals of these studies was to improve stroke recovery and to determine the usefulness of diffusion magnetic resonance imaging (dMRI) clinically to predict recovery in the acute and chronic phase post stroke. Diffusion MRI allowed us to non-invasively examine an animal model of stroke and understand functional and structural plasticity mechanisms occurring acutely and chronically in the process of recovery. The methods and techniques discussed below are commonly used in the clinic every day.

Diffusion MRI is a brain imaging method that measures the diffusion of water within tissue as a means to non-invasively visualize and understand the pathophysiology of neurological disorders, particularly stroke. The first dMRI images were presented in 1985 (Le Bihan, Breton et al. 1986) and began to be used commonly in the early 1990s by

clinicians to visualize water diffusion in the brain, once the methods became more reliable and motion artifacts were more controlled by using an echo-planar imaging (EPI) sequence (Turner, Le Bihan et al. 1990). Now, dMRI largest clinical application is assessing patients presenting with a stroke (Alexander, Lee et al. 2007). Unfortunately, the mechanisms underlying dMRI changes following stroke are still poorly understood, specific examples are discussed below. In Chapter 2 of this dissertation, we attempt to determine some of the cellular structural changes that may alter dMRI following stroke.

Diffusion Tensor Imaging (DTI)

Water molecules diffusing through a biological tissue move in a random pattern described the diffusion displacement probability density function (dPDF). The mean square displacement of the dPDF is, in general, proportional to the diffusivity. The particular dMRI method known as diffusion tensor imaging (DTI) is based on approximating the dPDF by a Gaussian (or normal) distribution. In this case, the only information that can be inferred from the dMRI data is the diffusivity and related quantities. Since the diffusion in brain can depend on direction, especially in white matter, this includes metrics of diffusion anisotropy that quantify to degree of directionality.

DTI has largely been used to investigate changes within white matter, although reports have also demonstrated its ability to assess changes in grey matter. While the sensitivity of DTI to changes in microstructure are well documented, there is still debate regarding which underlying molecular and structural mechanisms are actually being detected (Le Bihan 2003). DTI provides four primary measures that we analyzed throughout these studies. 1) Mean diffusivity (MD) is the diffusivity averaged over all possible directions. 2) Fractional anisotropy (FA) is the most commonly used measure for diffusion anisotropy, which is commonly used in white matter tracts as a marker of myelination and axonal density. 3) Axial diffusivity is the maximum diffusivity over all possible diffusion directions. 4) Radial diffusivity is the average diffusivity over all

directions perpendicular to the direction of maximal diffusivity. These four metrics are not independent quantities since the mean diffusivity can be determined from the axial and radial diffusivities.

Diffusional Kurtosis Imaging (DKI)

Because DTI assumes the dPDF to be Gaussian, its ability to characterize tissue microstructure is generally incomplete, particularly in complex media such as brain tissue. Diffusional kurtosis imaging (DKI) is a generalization of DTI that allows for the possibility of non-Gaussian diffusion and thereby provides a more comprehensive description of the diffusion dynamics. In particular, DKI yields several additional metrics that quantify the degree of diffusional non-Gaussianity. DKI also estimates the diffusivity metrics that are available with DTI, but with improved accuracy.

There are three primary DKI measures we used in these studies Mean kurtosis (MK) is the mean directional kurtosis over all possible directions that the diffusion gradient is applied. Axial kurtosis is the maximum kurtosis over all possible diffusion directions and radial kurtosis is the average kurtosis over all directions perpendicular to the direction of maximal kurtosis.

White Matter Tract Integrity (WMTI) and Tract Based Spatial Statistics (TBSS)

To investigate rehabilitation (motor training) induced white matter changes following stroke (Chapter 3), we used two different analytical methods: white matter tract integrity (WMTI) and tract based spatial statistics (TBSS). White matter tract integrity assumes that there are two compartments that do not exchange water: the intra-axonal space and the extra-axonal space (Fieremans, Jensen et al. 2011). The intra-axonal space (IAS) includes long-cylinder like processes with a majority of these being myelinated axons. At the same time, other processes might contribute to the IAS including unmyelinated axons and dendrite processes. The extra-axonal space (EAS) is the remainder of space and is essentially cerebrospinal fluid and a majority of glia cells that

are thought to be highly permeable to water. A second assumption within this model is that the processes are mainly aligned in a single general direction for any given imaging voxel (Fieremans, Jensen et al. 2011). In our rehabilitation studies in Chapter 3, we sought to understand changes that happened in white matter, particularly the corpus callosum, post rehabilitation. Four primary metrics were used in the white matter model: 1) Axonal water fraction was used to measure axonal density. 2) The intrinsic intra-axonal diffusivity inside axons used as a marker of axonal injury. 3) The extra-axonal axial diffusivity and 4) the extra-axonal radial diffusivity served as markers of changes in extra-axonal space.

Tract based spatial statistics (TBSS) was first introduced in 2006 and allowed for a whole brain automatic investigation of white matter with less alignment and smoothing issues than previous methods (Smith, Jenkinson et al. 2006). Briefly as described in Smith et al., in a common brain scan, the target, is used to align all subject's FA images onto the target and create a mean FA which will become the FA skeleton. Next, each subject's FA image is projected onto the skeleton and voxelwise statistics are conducted across groups and subjects. A recent study utilized TBSS to investigate white matter changes in the corpus callosum in healthy rats following a skilled reaching task (Sampaio-Baptista, Khrapitchev et al. 2013). In Chapter 3, we used TBSS to examine white matter changes in the corpus callosum following stroke and rehabilitation.

Diffusion MRI and Ischemic Injury

As mentioned above, dMRI over the past 25 years has been shown to be a valuable tool for the investigation and assessment of several neurological disorders, including stroke. Advanced diffusion MRI (dMRI) techniques, such as DKI, are highly sensitive to microstructural changes in the brain and provide unique information about white matter connectivity and integrity and thus may be of great prognostic value. Within the lesion core, numerous studies have discovered that MD decreases within hours of an ischemic stroke and begins to renormalize 5-7 days post lesion (Alexander, Lee et al.

2007). Neuronal beading, a process that occurs following stroke, has been shown to restrict water movement and is currently the leading hypothesis for the reduction of MD in the lesion core (Budde and Frank 2010). More recently identified and less studied or understood is the increase in MK seen hours following stroke and persisting at least one day following stroke (Hui, Du et al. 2012). Surrounding the lesion core is an area termed the penumbra or perilesional area where cells can remain viable for several hours to days following ischemia, making the tissue vulnerable for clinical intervention. Our work discussed in the upcoming chapters will examine dMRI in the penumbra and the mechanisms underlying any changes.

Diffusion MRI and Rehabilitative Training

Diffusivity metrics, especially fractional anisotropy (FA), have been extensively used to understand motor training effects on white matter tracks in healthy and diseased brains (Sampaio-Baptista, Khrapitchev et al. 2013, Wang, Casadio et al. 2013, Bonzano, Tacchino et al. 2014). In 2013, rodents performing a skilled reaching task showed an increase in white matter myelination in the corpus callosum, assessed with TBSS, that was positively correlated with reaching performance (Sampaio-Baptista, Khrapitchev et al. 2013). Other groups have seen that different reaching tasks increase FA in healthy human subjects (Wang, Casadio et al. 2013). While DTI metrics have been used to understand changes following rehabilitative training, less work has been conducted examining grey matter changes following rehabilitation nor has DKI been used to examine these changes. DKI is thought to be more sensitive post injury because it accounts for non-Gaussian water disruption movement through injured tissue. The following studies aim to understand how these metrics change post chronic stroke and after rehabilitative training and the relationship of diffusion metrics and motor recovery post stroke. The degree of motor impairment after stroke is a potential prognostic indicator of recovery of motor function (Stinear 2010), imaging biomarkers that could provide reliable assessment therefore

would be extremely useful. Additionally, there is likely a time frame during which the brain is more amenable to rehabilitative intervention (Allred, Kim et al. 2014), biomarkers that can provide early assessment of the patient's potential to motor recovery may be key to improving the outcome of rehabilitation.

Mitochondria Homeostasis

Mitochondria are highly susceptible to ischemic injury and mitochondria dysfunction can lead to increased cell death. One possible means to support perilesional tissue is to stabilize mitochondrial homeostasis and potentially increase mitochondrial biogenesis. In Chapter 4, we examined mitochondria acutely post stroke in ipsilesional cortex and striatum following a focal SMC ischemic lesion and pharmacologically enhanced mitochondria function and biogenesis to promote recovery after stroke when administered early after stroke. Mitochondria contain their own genome and are semi-autonomous organelles that code for 13 proteins for respiratory complexes, 22 tRNAs, and 2 rRNAs. Other essential proteins are synthesized in the cytosol and transported into the mitochondria. Mitochondria are the energy producing organelles of the cell that produce ATP via metabolic substrates. Mitochondria homeostasis is a balance between mitochondria biogenesis (growth and division of mitochondria) and mitophagy (mitochondria-selective autophagy) (Palikaras and Tavernarakis 2014). Coordination of these two processes is vital to overall health, several disorders occur following inadequate mitochondria homeostasis (Malpass 2013). The work within this dissertation will focus on mitochondria biogenesis and those mechanisms will be reviewed here more extensively.

Mitochondria Biogenesis (MB)

Mitochondria biogenesis requires incredible coordination, resulting in roughly 1,000 proteins synthesized by the nucleus and assembling with mitochondrial encoded proteins within the mitochondria (**Figure 1.2**) (Ventura-Clapier, Garnier et al. 2008). Additionally, mitochondria fusion and fission processes must be coordinated (discussed

below). MB is triggered by multiple different environmental factors, one being rehabilitation training and exercise which is discussed below. Peroxisome proliferator-activated receptor gamma co-activator 1-alpha (PGC-1 α), a transcription factor, is considered the master regulator of MB and mitochondrial function. PGC-1 α is highly expressed in areas undergoing a high amount of oxidative phosphorylation (i.e., heart and skeletal muscle) (Ventura-Clapier, Garnier et al. 2008) and has an important role in the CNS (Lin, Wu et al. 2004, Cui, Jeong et al. 2006). PGC-1 α is unable to bind to DNA directly, but does interact with transcription factors including nuclear respiratory factor (NRF), particularly NRF1 and NRF2 which are vital for MB and respiration (Wu, Puigserver et al. 1999).

NRFs are linked to the transcriptional control of multiple mitochondrial genes. The nuclear-encoded mitochondrial transcription factor A (Tfam) has binding sites for both NRF1 and NRF2 (Ventura-Clapier, Garnier et al. 2008). Replication and transcription within the mitochondria are regulated by Tfam, which binds to two sites on mitochondria DNA (mtDNA). One group was able to show that the levels of mtDNA are proportional to Tfam levels (Ekstrand, Falkenberg et al. 2004, Clay Montier, Deng et al. 2009). One marker of mitochondria dysfunction is decreased levels of mtDNA, which is associated with disease. As mentioned above, most of the mRNAs in the mitochondria genome encode oxidative phosphorylation subunits. Two of these mitochondria-encoded subunits are cytochrome c oxidase subunit 1 (COX1) and NADH dehydrogenase, subunit 1 (ND1), which will be studied in detail in the subsequent studies in Chapter 4. COX1 is essential for assembling complex IV, while ND1 is essential for assembling complex 1 of the oxidative phosphorylation pathway.

Briefly, mitochondria fission and fusion are processes that occur for growth, movement, and maintenance of healthy mitochondria. Proteins are located on the outer and inner membranes of the mitochondria and are part of the dynamin family (Ventura-Clapier, Garnier et al. 2008). Dysfunctional fission and fusion processes have been linked

to several disorders (van der Blik, Shen et al. 2013). Although not examined further in this work, both processes are vital for properly functioning mitochondria.

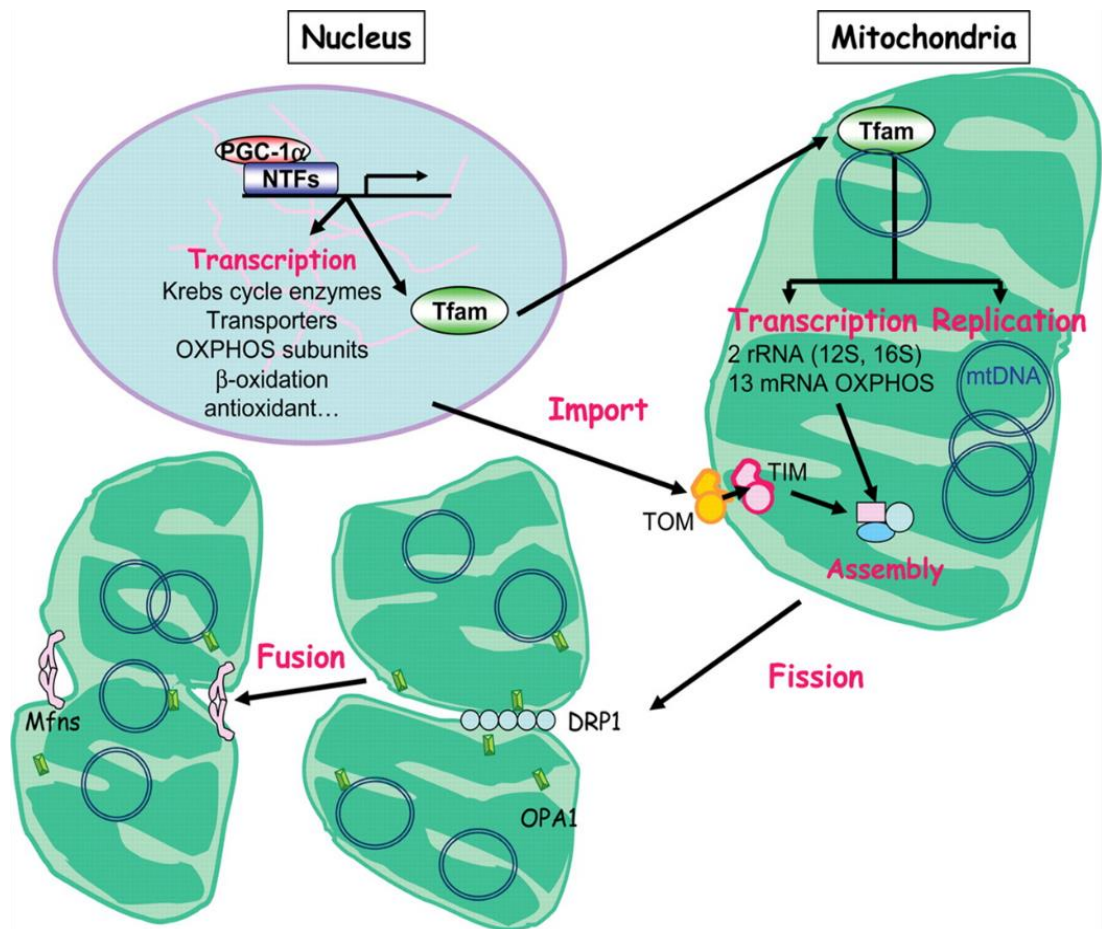


Figure 1.2. Regulation of mitochondria homeostasis and biogenesis.

PGC-1 α activates nuclear transcription factors (NTFs) leading to transcription of nuclear-encoded proteins and of the mitochondrial transcription factor Tfam. Tfam activates transcription of oxidative phosphorylation subunits and replication of the mitochondrial genome. Mitochondrial fission and fusion occurs allowing division and proper mitochondria organization.

Adapted from Renée Ventura-Clapier et al. *Cardiovasc Res* 2008;79:208-217.

Mitochondria Injury and Cerebral Ischemia.

Neurons are energetically demanding and use a large amount of ATP to maintain ion gradients across cell membranes and for neurotransmission. A majority of neuronal ATP is generated via mitochondria oxidative phosphorylation, therefore properly functioning mitochondria and oxygen supply are vital for normal neuronal communication and activity (Kann and Kovacs 2007). Mitochondria are also involved in neuronal calcium

regulation by sequestering calcium and act as a calcium buffer within the cell (Kann and Kovacs 2007). Additionally, mitochondria are mobile throughout the neuronal segment, and therefore can be in areas with high metabolic demands such as an active growth cone or the synapse (Kann and Kovacs 2007). Mitochondria are highly susceptible to even a mild decrease in blood flow, resulting in no change in ATP production but a decrease in respiration and impaired activity of electron transport chain complexes (Allen, Almeida et al. 1995). Cerebral ischemia results in a massive influx of glutamate and calcium and a depletion in energy stores, resulting in glutamate excitotoxicity, mitochondria dysfunction, and induction of apoptotic pathways (Duchen 2000). The induction of apoptotic pathways has been shown to depend on mitochondria function (Ankarcrona, Dypbukt et al. 1995) and decreases in mitochondria respiration are seen acutely following cerebral ischemia (Anderson and Sims 1999). Mitochondria dysfunction can lead to metabolic failure, oxidative stress, and impaired calcium buffering following reperfusion (Fiskum, Murphy et al. 1999).

Mitochondria Function and Biogenesis, Neuronal Survival, Neuronal Remodeling.

Mitochondria are known to play a role in axonal growth and dendritic remodeling (Cheng, Hou et al. 2010), therefore increasing healthy mitochondria function and inducing mitochondria biogenesis following stroke may be essential for promoting structural and functional plasticity of the perilesional SMC. Mitochondria biogenesis (MB) can be induced by exercise training in naïve and post-stroke animals and can lead to decreased in lesion size and fewer behavioral impairments following stroke (Steiner, Murphy et al. 2011, Zhang, Wu et al. 2012). It is likely that MB promotes energetic support during other forms of post stroke treatment, such as rehabilitation training, which has also been shown to induce structural and functional neural remodeling following stroke (see *Stroke Rehabilitation*). Remaining motor cortex and striatum are vital for recovery of motor function following ischemic stroke, in fact the majority of functional and structural plasticity

occurs in the remaining SMC (Jones and Adkins 2015). Furthermore, the remaining SMC served as the target for therapeutic interventions, as will be described in Chapter 4.

Effects of β_2 -Adrenergic Receptor Agonists on Learning and Recovery from Stroke

Stimulation of β_2 -adrenergic receptors has been shown in previous studies to promote mitochondria biogenesis and cause learning. Therefore it is theorized that these agonists may also aid recovery from stroke. β_2 -adrenergic receptors are located throughout the central nervous system (CNS) and peripheral nervous system (PNS), whereas β_1 -adrenergic receptors are primarily located in the cardiac tissue. Activation of β_2 -adrenergic receptors and exercise have been shown to increase levels of PGC-1 α and induce mitochondria biogenesis in the kidney and skeletal muscle (Miura, Kai et al. 2008, Wills, Trager et al. 2012). One non-FDA approved β_2 -adrenergic receptor long lasting agonist, Clenbuterol, has been shown to have anti-inflammatory and neuroprotective effects through the induction of neurotrophic factors such as nerve growth factor (NGF) (Gleeson, Ryan et al. 2010). Due to the number of side effects and lack of FDA approval, Clenbuterol is not an ideal, or clinically relevant agent with which to model the activation of β_2 -adrenergic receptors. Formoterol, on the other hand, is FDA approved and has a better side effect profile. Formoterol crosses the blood brain barrier and has been shown to increase cognitive function and dendritic complexity in a Down Syndrome model (Dang, Medina et al. 2014). There have been no previous investigations of the use of formoterol to stimulate mitochondria biogenesis following stroke and whether that use will lead to similarly enhanced behavioral and structural changes, as have been seen in a Down Syndrome model.

Conclusions and Research Directions

The purpose of the studies described in this dissertation is to better understand the relationship between acute and chronic stroke tissue biophysics and morphology and novel imaging metrics, behavioral outcomes, and mitochondria biogenesis. There are

limited prognostic tools or biomarkers to determine if individuals will recover motor function or respond well to rehabilitation treatments following stroke. Magnetic resonance imaging (MRI) has revealed some common characteristics in brain activation patterns that indicate level of motor recovery following stroke and has been shown, to a limited degree, to reveal training-induced changes. Diffusional MRI techniques, such as DTI and DKI, are highly sensitive to microstructural changes in the brain and provide unique information about white matter connectivity and integrity which will likely be of great prognostic value.

Mitochondria dysfunction leads to increased cell death and correlates with the magnitude of the infarct (Dirnagl, Iadecola et al. 1999, Chan 2005). Stimulating mitochondria function via promotion of mitochondria biogenesis (MB) may increase neuronal survival, reduce lesion size, and enhance behavioral recovery. Currently, post-stroke pharmacology treatment is limited to TPA, which has a small window of effectiveness and several side effects, including hemorrhage and death. Better therapies are needed to advance patient recovery, stimulate neuronal survival, and promote structural and functional plasticity following injury.

These studies within this dissertation aimed to examine the acute and chronic microstructural changes following stroke and to understand how mitochondria biogenesis leads to improved recovery and structural and functional plasticity following rehabilitative training. We hypothesized ***that dMRI is a sensitive tool to identify microstructural changes acutely and chronically following stroke and that promoting mitochondria biogenesis would lead to better functional recovery and induce structural and functional plasticity following rehabilitative training.*** To accomplish this hypothesis, we used a combination of sensitive behavioral, immunohistochemical, and mitochondrial related molecular markers, plus diffusion magnetic resonance imaging (dMRI) to investigate the time course of acute and chronic stroke effects.

CHAPTER 2: CHANGES IN TISSUE DIFFUSION PROPERTIES FOLLOWING ACUTE STROKE

Introduction

Diffusion MRI (dMRI) is a clinically relevant, feasible, and promising tool to noninvasively investigate neural plasticity changes in perilesional motor areas following acute and chronic stroke. Currently, there are relatively few tools available for clinicians to noninvasively investigate changes in perilesional motor areas acutely or chronically. The ability to evaluate and understand these time-dependent microstructural changes in perilesional regions may lead to greater customization of treatment to meet individuals' unique treatment needs. Following ischemia, areas connected to the lesion core undergo time-dependent structural and functional plasticity (Carmichael, Kathirvelu et al. 2016) and experience-dependent functional recovery (Nudo, Milliken et al. 1996, Jones and Jefferson 2011). Treatments that successfully promote motor recovery likely work at least in part by enhancing neural remodeling in the perilesional cortex (Adkins-Muir and Jones 2003, Plautz, Barbay et al. 2003, Adkins, Hsu et al. 2008). After stroke, the perilesional cortex shows the most dramatic neural remodeling. Therefore our lab focused examination on the perilesional cortex to establish the relationships between dMRI measurements and underlying microstructural changes along the time course of stroke recovery. Currently, these relationships remain largely unknown. It is thought that clarification may lead clinicians to develop further individualized treatment interventions.

Diffusion MRI measures water diffusion throughout tissues. Diffusion tensor imaging (DTI) and diffusional kurtosis imaging (DKI) have previously been shown to be sensitive to molecular and structural changes in the brain (Cheung, Wang et al. 2012, Hui, Du et al. 2012, Umesh Rudrapatna, Wieloch et al. 2014). DTI estimates the diffusivity of water under the assumption that water diffusion dPDF is Gaussian. Consequently, DTI may be unable to fully capture tissue microstructural changes. Diffusional kurtosis imaging

measures tissue heterogeneity without requiring diffusion to be Gaussian. Therefore, DKI may be able to reveal more about tissue characterization and the complexity of central nervous system tissue (Jensen, Helpert et al. 2005, Lu, Jensen et al. 2006, Cheung, Wang et al. 2012, Umesh Rudrapatna, Wieloch et al. 2014). Different parts of the nervous system (axons, dendrites, cerebrospinal fluid, etc.) have different diffusion properties, and we hypothesize that by using these different diffusion properties, we can identify specific microstructural changes after stroke and link to specific quantifiable changes in diffusion metric changes.

Diffusion MRI techniques have been valuable tools for the investigation and assessment of stroke since the 1990s (Le Bihan, Breton et al. 1986). Within the lesion core, numerous studies have discovered that mean diffusivity (MD) decreases within hours of an ischemic stroke and begins to renormalize 5-7 days post lesion (Alexander, Lee et al. 2007). Neuronal beading, swelling and osmotic imbalance in neurons following stroke, has been shown to restrict water movement and is currently the leading hypothesis for the reduction of MD in the lesion core (Budde and Frank 2010). The increase of mean kurtosis (MK) in the lesion core seen within hours following stroke and persisting at least one week following stroke has been less studied and is poorly documented in the literature (Hui, Du et al. 2012). Recently, a few studies have begun to examine changes in MK acutely following stroke (Hui, Du et al. 2012, Weber, Hui et al. 2015). However current theories to explain the increase have not been directly examined. The use of dMRI techniques in perilesional grey matter, has been under examined, largely because grey matter is more heterogeneous which makes understanding water diffusivity metrics and changes more difficult. The literature thus far has focused on MD and MK either in the lesion core or white matter only these studies examined grey matter changes in perilesional cortex.

By the design of our studies, we set forth to examine changes and determine if dMRI metrics are sensitive to potential structural changes that have been related to neural degeneration and neural remodeling following acute stroke. We did this through two different studies. Initially, we induced a large stroke and examined animals post stroke at 2hrs, 24hrs, or 72hrs to get a general baseline understanding of changes in a focal motor cortical stroke model. A second follow up study examined a smaller focal lesion in animals 3hrs, 24hrs, 72hrs, and 7 days post stroke. During our second small stroke study, animals were scanned at each time point to understand the progression of the stroke over time in each individual animal.

Methods

Animals

Long Evan male rats were given food and water *ad libitum* and were kept on a 12:12-hour light:dark cycle. All work was done in accordance with the Medical University of South Carolina Animal Care and Use Committee guidelines. Animals were randomly assigned to groups in both studies. Study 1: Animals underwent dMRI scans at one of three time points following ET-1 induced stroke, 2 hours (n=7), 24 hours (n=8), 72 hours (n=9), and were sacrificed immediately after for histology analysis. Study 2: Animals received ET-1 induced strokes and underwent dMRI scans at 3 hr (n=39), 1 day (n=29), 3 days (n=19), and 7 days (n=10) post-injury. Shortly after these scans, a subset of animals were sacrificed for histology at 3 hr (n=10), 1 day (n=10), 3 days (n=9), and 7 days (n=10). For comparison, this study included sham animals (n=19) without strokes that also underwent dMRI and sacrificed for histology.

Surgical Procedures

Study 1: Animals were anesthetized with isoflurane (4-5% for induction/1-3% for maintenance) and unilateral ischemic lesions were induced via infusion of ET-1 (American Peptide, Inc) into layer V of the left FI-SMC through 4 holes drilled at 0.5 mm posterior,

2.5 mm anterior, and 3.5 and 4.6 mm lateral to bregma (Adkins, Voorhies et al. 2004). One microliter of ET-1 (0.2 $\mu\text{g}/\mu\text{L}$ in sterile saline) was injected into each hole via a Hamilton syringe (lowered to 1.5 mm DV), at a rate of 1 $\mu\text{L}/2$ minutes. Study 2: Animals were anesthetized with a cocktail of ketamine (110 mg/kg) and xylazine (70 mg/kg) and similar to *Study 1*, ET-1 was infused into layer V of the left forelimb area of the sensorimotor cortex. However, to produce a more focal and clinically relevant lesion two holes drilled at 1.0 mm posterior and 2.0 mm anterior and 4.1 mm lateral to bregma. A total of 0.6 μL of ET-1 (0.2 $\mu\text{g}/\mu\text{L}$ in sterile saline) was injected into each hole (lowered to -2.5 mm DV), at a rate of 0.6 $\mu\text{L}/\text{min}$. Sham animals were anesthetized, received a midline incision and were sutured.

Diffusion MRI

dMRI scans were acquired at various time points depending on the experiment using a 7T/30 Bruker BioSpec (Billerica, MA) animal scanner. Animals were anesthetized with isoflurane/air (4-5% for induction/1-3% for maintenance) for all dMRI scans. A standard DKI (Jensen and Helpert 2010) protocol was utilized consisting of a two shot spin-echo echo planar imaging diffusion sequence with 30 diffusion encoding directions and 5 b-values (0, 500, 1000, 1500, 2000 s/mm^2). Other imaging parameters were: TR/TE = 4750/32.5 ms, field of view = 30 \times 30 mm^2 , matrix = 128 \times 128, in-plane resolution = 0.23 \times 0.23 mm^2 , slice thickness = 1.0 mm, diffusion gradient pulse duration = 5 ms, diffusion time = 18 ms, and number of excitations = 2. A total of 19 axial slices with no interslice gap were collected.

Data presented are for MD and MK corresponding to the apparent diffusion and kurtosis coefficient, respectively, averaged over all directions (Jensen, Helpert et al. 2005). Diffusion and diffusional kurtosis tensors were calculated using diffusional kurtosis estimator (DKE), a publically available in-house software (Tabesh, Jensen et al. 2011). For *study 1 and 2* multislice regions of interest (ROIs) were manually drawn in the (1)

infarct core, (2) homologous region in the contralesional SMC, (3) perilesional layers II/III and V of the remaining MC, and (4) contralesional layers II/III and V of the FI-SMC. The perilesional regions of interest were drawn on 3 contiguous MRI slices (1-mm thick) and were inclusive of layers II/III and V.

Behavioral Assays

In order to assess ischemia-induced impairments of forelimb function and compare these to dMRI and histological measures, all animals were tested on sensitive motor tasks before injury and at post-operative time points starting at 24hrs.

Cylinder Task

The cylinder task is a sensitive measure of asymmetric forelimb use during postural support behaviors (Schallert, Fleming et al. 2000). Animals were placed in a clear cylinder, allowed to explore freely, and videotaped for 2 minutes or until there were 30 contacts made with the forelimb against the cylinder walls. Forelimb use was assessed by counting the number of times each limb was used for upright body support against the wall. Percent use was calculated as: $(1/2 \text{ both limbs} + \text{paretic limb}) / \text{total touches}$. Animals with a stroke use their paretic limb less post stroke while naïve animals will continue to use both limbs equally on the cylinder task.

Ladder Task

The ladder task was used to assess coordinated forelimb use, stepping accuracy, and limb placement. The ladder apparatus is made of two plexiglass walls, with 3mm pegs spaced 1cm apart from each other. The ladder is raised ~20cm off the ground with a neutral start cage and the animal's home cage at the end. Animals were allowed to walk freely across the ladder and videotaped for three trials. Scoring of the steps was done with slow motion video replay and based on a previously established rating scale (Metz and Whishaw). The total number of steps and missteps were calculated and scored on a scale (0-6) based on how the animal placed the forelimb on the rungs of the ladder. Errors were

counted when an animal completely missed the ladder rung and a fall occurred (score of 0) or placed the limb but when weight bearing either fell (score of 1) or slipped (score of 2). Percent error was calculated as: $(\#0+1+2)/\text{total steps}$.

Immunohistochemistry and Quantification of Tissue Densities

Following end-point MRI scans, animals were deeply anesthetized with pentobarbital (Euthasol, 100-150mg/kg, IP) and were intracardially perfused with 0.1M phosphate-buffer and 4% paraformaldehyde. Six serial rostral to caudal sets of 50 μm coronal sections were produced using a vibratome and stored in cryoprotectant. Three sets of sections were processed for immunohistochemistry (IHC) to ascertain post-injury morphological changes in the surface density of astrocytes, dendrites, and axons in the perilesional motor cortex. Astrocytes, dendrites, and axons are key structural elements that change expression acutely post stroke and likely contribute to post stroke dMRI metric changes.

Free-floating sections were processed for IHC. Tissue was incubated for 48 hrs in one of the following primary antibodies: glial fibrillary acidic protein (GFAP) for astrocytes (1:800 rabbit polyclonal), microtubule protein 2 (MAP2) for dendrites (1:500 mouse monoclonal), and pan-axonal neurofilament marker (SMI-312; 1:1000 mouse monoclonal) for axons. Following primary incubation, sections were rinsed and incubated for 2 hrs in secondary antibody at a dilution of 1:200 (horse anti-mouse for MAP2 and SMI-312; goat anti-rabbit for GFAP). Sections were incubated in peroxidase-linked avidin-bioin complex (ABC kit) for 2 hrs. Immunoreactivity was visualized using 3,3' diaminobenzidine with nickel ammonium sulfate intensification. All animals were included in each batch of IHC processing and each batch included negative control sections without primary antibody.

Microstructure Quantification

The cycloid grid intersection method (Baddeley, Gundersen et al. 1986) was used to determine surface density for the GFAP, MAP2 and SMI-312 immuno-reactive (IR)

processes. For each antibody, we sampled tissue that was represented in three adjacent MRI slices that included the forelimb area of the sensorimotor cortex. Data were obtained in three adjacent coronal sections (~600 μm apart) which included perilesional motor cortex (i.e., between approximately +1.2 and -0.26 mm anterior/posterior relative to bregma). Using ImageJ (National Institute of Mental Health, Bethesda, MD), cycloid arcs were overlaid on light microscopic images, taken at 100 \times oil immersion (final magnification=1,400 \times), of four sample regions, two adjacent sets (~250 μm) in layers II/III and two sets in layer V beginning at approximately 250 μm medial to the lesion core (towards midline), for 3 sections. Each immuno-reactive process that crossed an arc was counted. The surface density was calculated using the formula $S_v = 2(I/L)$, where S_v is the surface density, I is the total number of intersections and L is the sum of the cycloid arc lengths.

Statistical Analysis

All data are reported as mean \pm standard error of the mean (SEM). In *Study 1*, one-way ANOVAs were used to test for time point differences using SPSS software and corrected using Bonferroni post-hoc analysis. For *Study 2*, repeated analysis of variance (rANOVA) models were used to look for a relationship between histology measures by group and injury, as well as their interaction with a Scheffe's adjustment. Correlations were used to determine relationships between changes in the density of glia, dendrites, and axons with post-lesional dMRI metrics. The significance level was $\alpha=0.05$.

Results

Study 1: dMRI Reveals Different Time-Sensitive Stroke-Induced Microstructural Changes in a Large SMC Stroke

Diffusion MRI

MD was significantly different in the lesion core compared with the contralesional homologous cortex ($F_{3,29}=22.547$, $p<0.01$). Similar to previous reports (Hui, Du et al.

2012), MD in the lesion core was significantly reduced compared with the contralesional homologous cortex at 2hrs ($p < 0.01$) and 24hrs ($p < 0.01$) after stroke, but there were no longer significant differences at 72hrs. MK remained significantly elevated across all time points in the lesion core ($F_{3,29} = 31.194$, $p < 0.01$) compared with contralesional SMC at 2hrs, 24hrs, and 72hrs (p 's < 0.01). In the perilesional cortex, at 2hrs after lesion, MD was subtly but significantly decreased in remaining perilesional MC compared with pre-operative levels [$t(6) = 2.631$, $p = 0.039$]. At 24hrs and 72hrs perilesional MD was no longer significantly different from the before lesion. However, MK remained elevated in the remaining MC longer after injury compared to before lesion. Perilesional MK in the perilesional cortex was significantly increased compared with pre-operative levels at 24hrs [$t(7) = -4.479$, $p = 0.003$] and 72hrs [$t(9) = -5.761$, $p < 0.05$] after lesion.

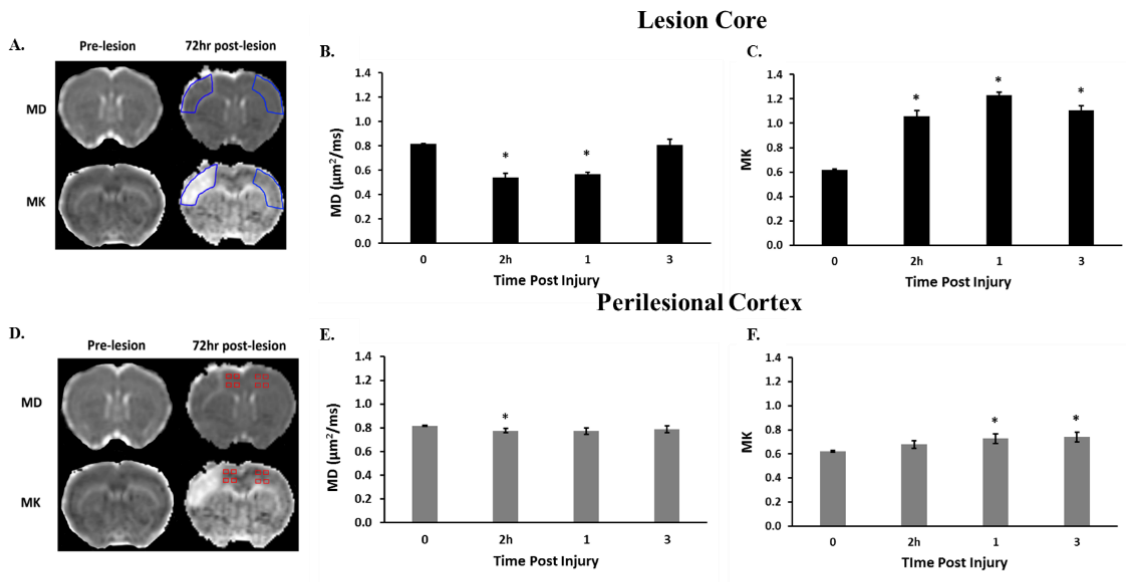


Figure 2.1. Lesion Core and Peri-lesion dMRI Results.

A. A representative image of MD and MK maps before lesion and 72hrs post-lesion. B. MD was significantly decreased at 2 and 24 hrs post stroke compared to before injury. C. MK was increase 2, 24, and 72 hrs post stroke compared to before injury. D. Representative image of MD and MK maps with perilesional ROIs. E. MD was decreased at 2 hrs post stroke compared to before injury. F. MK was increased at 24hrs and 72hrs post stroke compared to before injury.

Microstructural/histology Results

As seen in Figure 2.2, there was a significant effect of time after injury on the surface density of GFAP-immunoreactive processes in perilesional motor cortex ($F_{3,29}=26.822$, $p<0.01$). At 72hrs, there was a significant increase in GFAP-positive processes compared with the contralesional forelimb region of the SMC ($p<0.001$) and

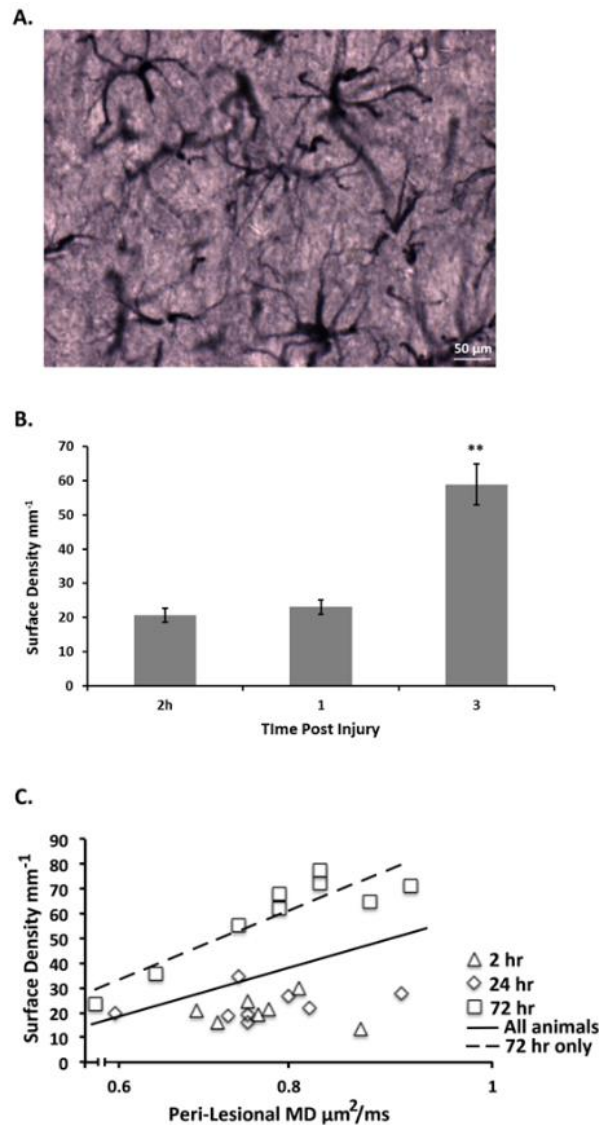


Figure 2.2. Surface density of GFAP.

A. Representative 100X image of glia density at 72hrs post-lesion in the perilesional area (scale bar=50 μ m). **B.** The surface density of glial processes was increased at 72h in the lesion hemisphere (** $p<0.005$) compared to 2 and 24hrs post-lesion. **C.** There was a significant positive correlation between GFAP surface density and perilesion MD across time-points ($r=0.416$, $p=0.043$). GFAP surface density at 72hrs time-point, when there is the greatest glia infiltration into the perilesion cortex, was highly correlated with perilesional MD ($r=0.897$, $p=0.001$).

compared with other time points (2hrs [$t(21)=-6.293$, $p<0.005$] and 24hrs [$t(21)=-6.115$, $p<0.005$]). In addition, there was a significant increase in the density of glia processes in the contralesional SMC at 72hrs compared with 2hrs ($p<0.05$). There were no significant differences between perilesional MAP2 surface densities at any acute time point compared with the contralesional SMC ($F_{2,21}=1.442$, $p=0.259$). There were no significant differences between perilesional surface densities of SMI-312 at any acute time point compared with the contralesional SMC ($F_{2,21}=0.247$, $p=0.783$).

Although MD in the perilesional cortex was no longer significantly different from contralesional SMC at 72hrs, GFAP surface density at 72hrs was highly correlated with perilesional MD ($r=0.897$; $p<0.001$, **Figure 2.2**). The return of MD to pseudonormalized levels acutely after ischemia may be due to increased astrogliosis, which is indicated by the increased surface density in GFAP, and an increase in water diffusion through these astrocytes. There was also a significant, but weak, correlation overall between MAP2 surface density in the perilesional cortex and perilesional MD ($r=0.462$; $p<0.05$).

Table 2.1. Large sensorimotor cortical stroke dMRI and surface densities results.

	Brain Region Examined	Result
MD: mean directional diffusivity	Lesion Core and Perilesional Grey Matter	1. Lesion core decreases that normalize by day 3. 2. Perilesional decreases at 2hrs then normalized
MK: mean directional kurtosis	Lesion Core and Perilesional Grey Matter	1. Lesion core increases at 2hrs-72hrs 2. Perilesional increases at 2hrs and 24hrs
GFAP: astrocytes	Perilesional Grey Matter	Increased at 72hrs
MAP2: dendrites	Perilesional Grey Matter	No change
SMI-312: axonal marker	Perilesional Grey Matter	No change

Behavioral Assessment

Unilateral ET-1 lesions to the FI-SMC resulted in lasting impairments in the forelimb opposite the lesion in the cylinder task. As seen in Figure 2.3, at 24 and 72hrs post-lesion, rats used their paretic limb for upright postural support significantly less post-

infarct compared to their non-paretic limb at 24hrs [$t(13)=4.441$, $p=0.001$] and 72hrs [$t(6)=3.399$, $p=0.015$]. Additionally, animals made significantly more limb placement errors with their paretic limb at 24hrs [$t(14)=-5.036$, $p<0.005$] and 72hrs post-injury [$t(7)=-3.531$, $p=0.012$] compared to pre-injury (**Figure 2.3**) on the ladder task. There were no significant change in errors made with the non-paretic limb.

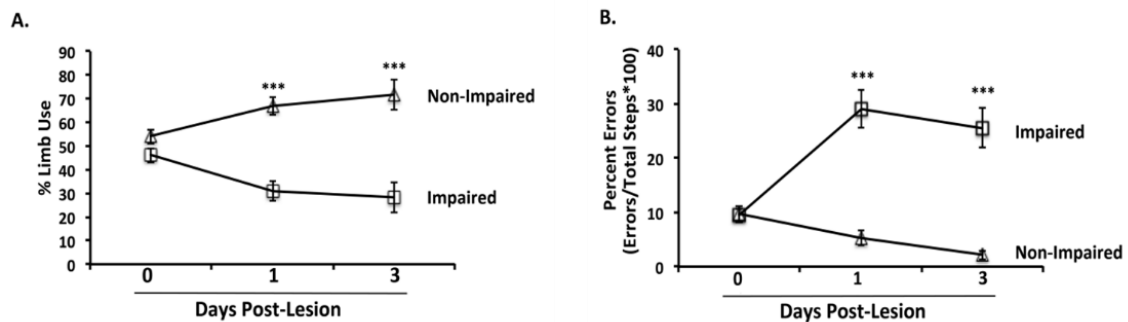


Figure 2.3. Behavioral Impairments following Stroke.

A. Animals used their impaired forelimb less on days 1 and 3 compared to their non-impaired forelimb on the cylinder task. **B.** Animals made significantly more errors on the ladder task with their impaired forelimb.

Study 2: Sensitivity of Diffusion MRI in a Moderate Motor Cortical Stroke

Diffusion MRI

Representative maps of MD and MK for a single slice from one animal sacrificed at 7 days are shown in Figure 2.4. Substantial changes within the lesion core are apparent for both metrics, which are consistent with ischemia (**Figure 2.4**). In the lesion core there was a significant time by injury interaction ($F_{149}=44.7$, $p<0.001$) and a significant decrease in MD at 3hrs ($p<0.001$) and 24hrs ($p<0.001$) compared to sham animals and pre-operative levels following stroke, which renormalized by day 3 post-injury. This result is consistent with previous data in the field (Hui, Du et al. 2012, Weber, Hui et al. 2015). Additionally, there was also a significant time by injury interaction with MK ($F_{156}=39.31$, $p<0.001$), and MK remained elevated at all time points: 3 hrs ($p<0.001$), 24 hrs ($p<0.001$),

and 72 hrs ($p < 0.001$) which is consistent with previous reports (Hui, Du et al. 2012, Weber, Hui et al. 2015).

We examined the same metrics (MD and MK) in the perilesional motor cortex (**Figure 2.4**). There was a significant injury by time interaction of MD in the perilesional cortex ($F_{133}=5.96$, $p < 0.001$) and MD was significantly decreased at 3 hrs ($p < 0.001$) post-injury compared to sham animals and pre-operative levels. There was not a significant interaction of injury and time in MK, only a significant effect of time ($F_{151}=4.781$, $p=0.001$). There was a slight increase in MK at 3 hrs ($p=0.016$) compared to pre-operative levels. These data indicate that not only are dMRI metrics sensitive to differences in the lesion core, but also are able to detect changes in the perilesional area of the motor cortex, which undergoes ischemia induced, time-dependent biochemical and structural changes (Carmichael, Kathirvelu et al. 2016).

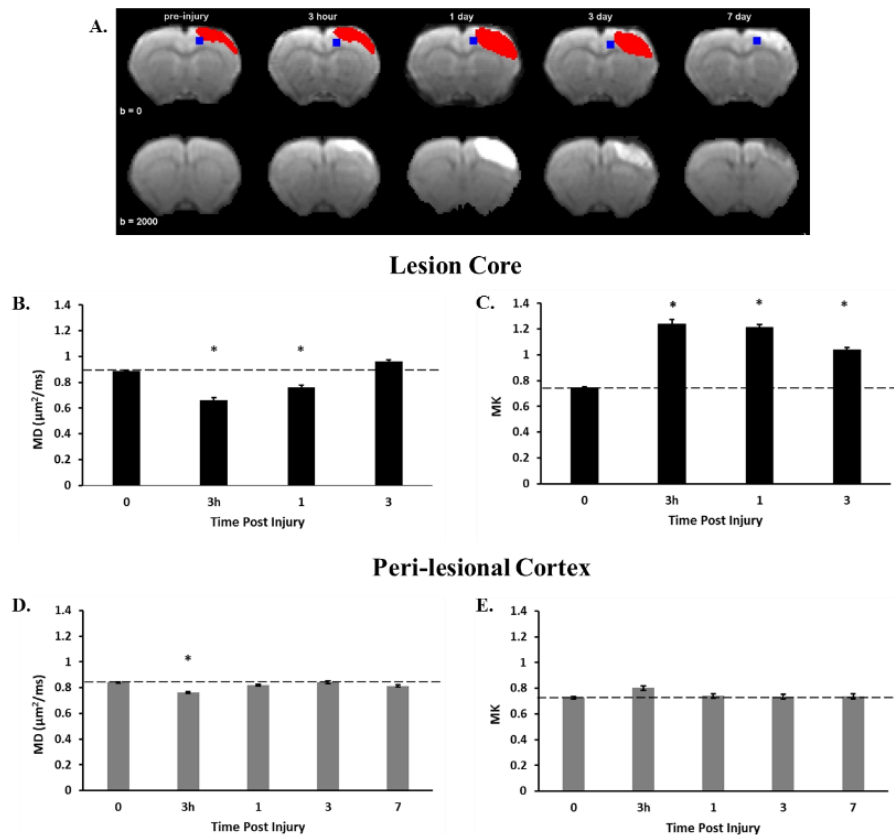


Figure 2.4. Lesion Core and Peri-lesion dMRI Results. **A.** Lesion core and peri-lesional ROIs and stroke evolution over time. **B.** MD was significantly decreased at 3 and 24 hrs post stroke compared to sham animals. **C.** MK was increase 3, 24, and 72 hrs post stroke compared to sham animals. **D.** MD was decreased at 3 hrs post stroke compared to sham animals and all other stroke timepoints. **E.** There was no difference in MK at any time point post stroke.

Histology

Lastly, we examined the surface density of glia, dendrite processes, and axons in the perilesional cortex (see **Figure 2.5**). It should be noted that by post-injury Day 3, tissue in the lesion core is likely not viable and does not react to the antibodies used in this study (**Figure 2.5A**); thus, we focused on changes in astrocytic (GFAP positive cells) and neural (dendrites and axons) structural changes in perilesional cortex and related these to dMRI metrics. There was a significant interaction of time and injury ($F_{49}=8.03$, $p<0.001$) and significant increases in the density of immuno-positive GFAP processes at 3 days ($p=0.005$) and 7 days ($p<0.001$) post-injury compared to sham animals (**Figure 2.5B**). As

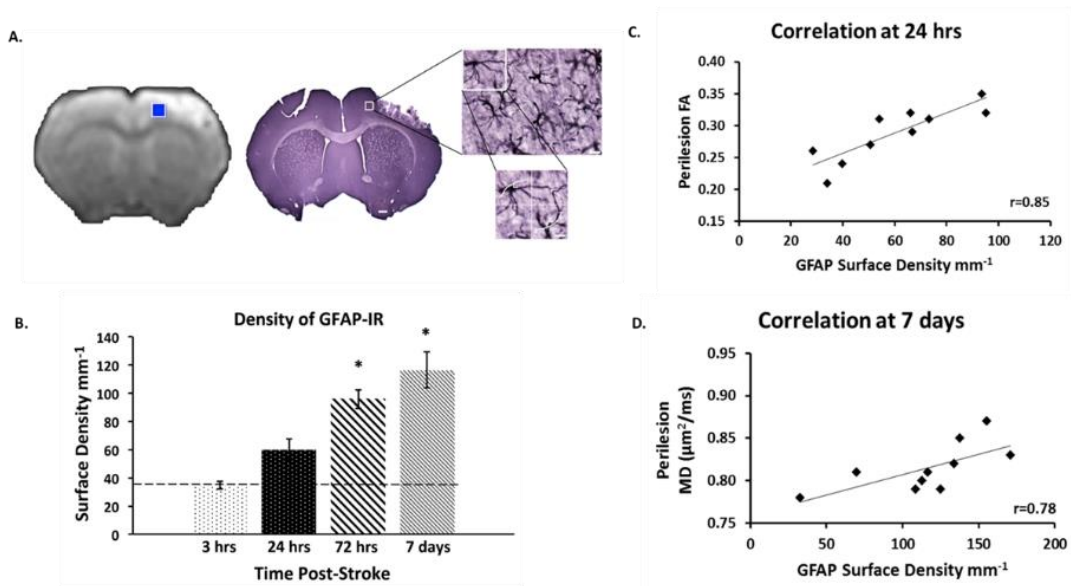


Figure 2.5: Surface Density and Correlations of GFAP and dMRI. **A.** The 7 day $b=0$ dMRI image with the perilesional ROI compared to a GFAP-stained section of sampled tissue (scale bar=0.5mm) to compare regions of sampling between dMRI and histology. The sampled region of GFAP is blown up to a 100x image to demonstrate our staining levels (scale bar=50μm). Lastly, to illustrate our quantification technique we overlaid our cycloid grid arc filter used for counting on an enlarged section of GFAP stained tissue (scale bar=50μm). **B.** Immuno-reactive GFAP staining in the perilesional cortex and the dashed line indicates sham levels. We observed an increase in GFAP at 3 days and 7 days post-injury. **C.** At 24 hrs post-injury, we found a correlation between perilesional FA and GFAP and at 7 days we found a correlation between perilesional MD and GFAP (**D.**).

seen in Figure 2.5C, there was a significant and strong positive correlation at 24 hrs between GFAP and perilesional fractional anisotropy (FA) ($r=0.85$, $p=0.001$). There was

also a significant correlation between GFAP-positive processes and perilesional MD on post-injury day 7 ($r=0.78$, $p=0.01$; **Figure 2.5D**). These data suggest that astrocytes may play a role in the return of MD to pre-stroke levels, as previously reported (Weber, Hui et al. 2015).

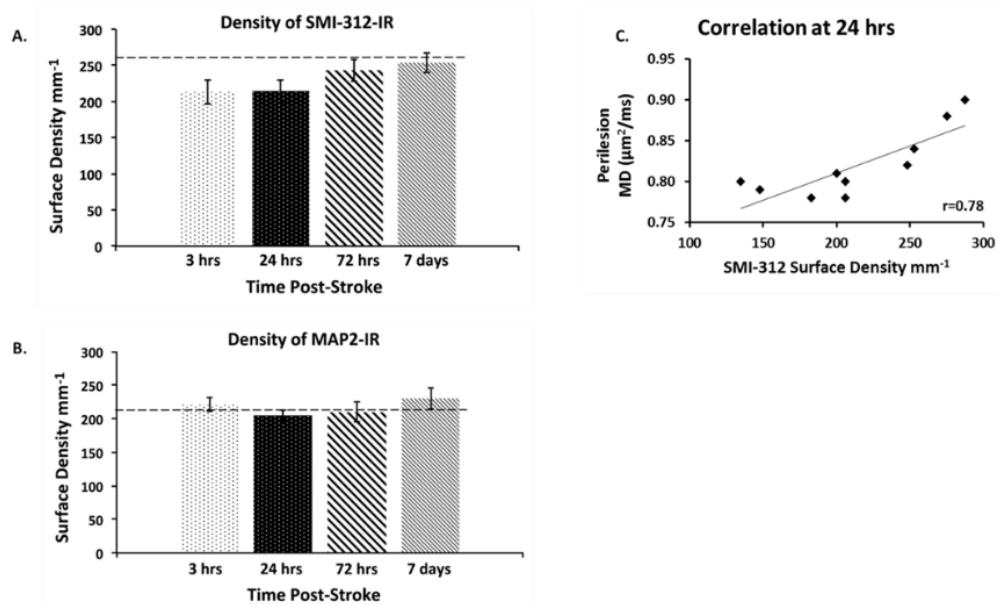


Figure 2.6: Surface Density of SMI312 and MAP2 **A.** Levels of immune-reactive SMI-312 in the peri-lesional cortex revealed no differences across time points after stroke. **B.** There was not a significant difference in MAP2 processes over the acute time after stroke, dashed line represents sham animals. Lastly, at 24 hr after stroke SMI-312 was significantly correlated with perilesional MD (**C.**).

There was not a significant interaction of time and injury in perilesional density of axon (SMI-312-positive) or dendritic (MAP2-positive) processes (**Figure 2.6 A&B**). However, at 24 hrs after injury, there was a positive correlation between the density of SMI-312-positive axons and perilesional MD ($r=0.78$, $p=0.008$; **Figure 2.6C**). Thus, these data suggest that changes in axonal and astrocyte density might be involved in some of the changes in MD and FA.

Table 2.2. Moderate focal cortical stroke dMRI and surface densities results.

	Brain Region Examined	Result
MD: mean directional diffusivity	Lesion Core and Perilesional Grey Matter	1. Lesion core decreases that normalize by day 3. 2. Perilesional decreases at 2hrs then normalized
MK: mean directional kurtosis	Lesion Core and Perilesional Grey Matter	1. Lesion core increases at 2hrs-72hrs 2. No change in the perilesional cortex
GFAP: astrocytes	Perilesional Grey Matter	Increased at 72hrs and 7 days
MAP2: dendrites	Perilesional Grey Matter	No change
SMI-312: axonal marker	Perilesional Grey Matter	No change

Behavioral Assessment

All animals were tested on behavioral tasks before stroke induction and post lesion at 24hrs, 72hrs, and 7 days (**Figure 2.7**). Behavioral testing was not performed at 3hrs due to anesthesia effects. Animals showed a reduced use of the impaired forelimb at 24hrs [t(28)=6.328, p<0.001], 72hrs [t(18)=4.917, p<0.001], and 7 days [t(9)=2.523, p=0.033] compared to pre-operative use on the cylinder task. Additionally, at 24hrs [t(28)=-6.050, p<0.005] and 72hrs [t(18)=-4.987, p=0.034] post-stroke impaired forelimb use is decreased compared to the non-impaired forelimb. At 7 days post-stroke, there is still a reduction in use of the impaired forelimb compared to the non-impaired forelimb [t(9)=-2.264, p=0.05], however there was not a significant reduction from sham animals. On the ladder task, significantly more errors were made with the impaired forelimb at all post lesion time points compared to the non-impaired forelimb: 24hrs [t(28)=7.319, p<0.001], 72hrs [t(18)=5.817, p<0.001], and 7 days [t(9)=3.851, p<0.005]. Additionally, the injured forelimb showed impairment following a stroke compared to pre-stroke assessment at 24hrs [t(28)=-6.541, p<0.001], 72hrs [t(18)=-4.616, p<0.005] and 7 days [t(9)=-2.497, p=0.034].

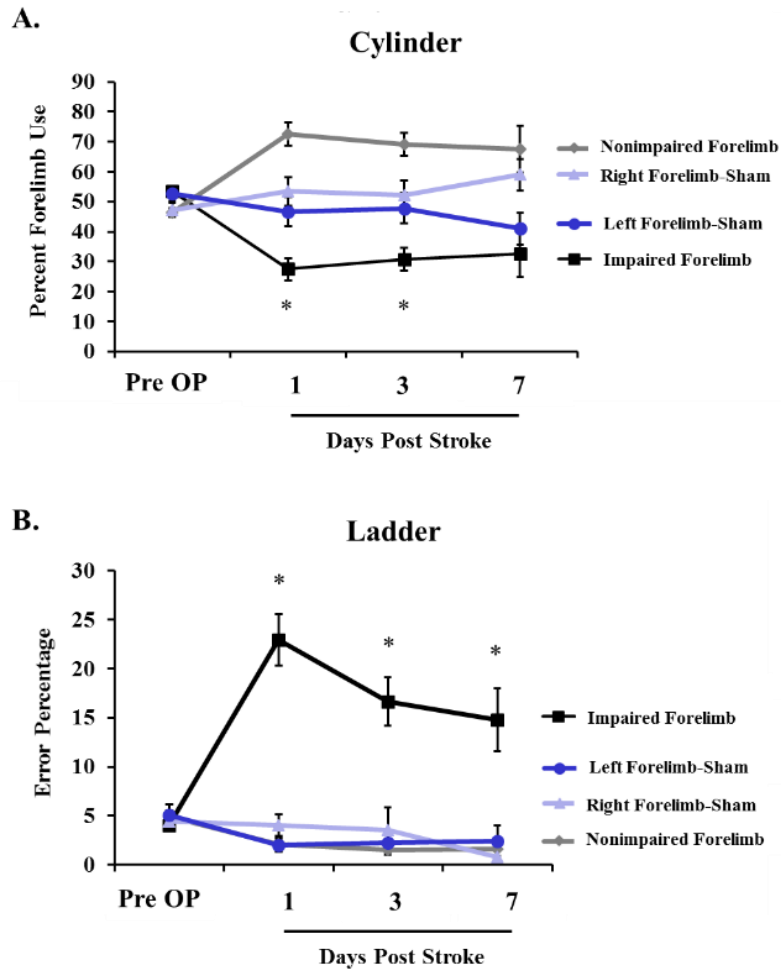


Figure 2.7. Behavioral Impairment Post Stroke
A. Animals with a stroke had reduced forelimb use on post-op days 1 and 3 compared to the nonimpaired forelimb and sham animals. **B.** There was a significant increase in error percentage with the impaired forelimb compared to the nonimpaired forelimb and sham animals.

Discussion

Study 1 and 2 revealed very similar results and provided further evidence that MK and MD reveal different but likely complimentary information about microstructural changes after stroke. Similar to previous findings (Hui, Du et al. 2012), MD in the lesion core was reduced until 24hrs after lesion, but was no longer significantly different from the contralesional SMC at 72hrs after lesion. However, MK of the lesion core remained significantly different from contralesional homotopic SMC at all time points. These findings are similar to those reported after unilateral MCAO in rats and likely reflect, as others have

reported in different models, changes in water diffusion associated with edema (Moseley, Cohen et al. 1990), axon beading (Budde and Frank 2010), and demyelination (Jiang, Zhang et al. 2010). These early changes in MD and MK in the lesion core are also likely because of other, as of yet unidentified microstructural changes. We were unable to address the underlying cause of these lesion core changes because there was rarely lesion tissue remaining during these acute time points after injury.

In these two studies, we also sought to determine whether after a focal, unilateral ET-1–induced ischemic insult to the SMC, alterations in microstructure were detectable using dMRI in the perilesional motor cortex, an area known to undergo acute and chronic changes after injury and experience-dependent changes (Carmichael, Kathirvelu et al. 2016). We observed conflicting results with MK in the perilesional cortex. In *study 1* we saw MK elevated at 72hrs post stroke, whereas in *study 2* we did not see any increase in MK in the perilesional cortex. This may be, in part, due to smaller lesions (482.44 ± 58.14 voxels) in the *study 2* compared to *study 1* (1187.88 ± 237.40 voxels) determined by ROIs drawn on T2 images and thus perilesional cortex MK responses may be less robust. Further, these data indicate that elevations in MK are not likely because of glia infiltration or acute disruption of the overall density of axons and dendrites in perilesional cortex. It is likely, but yet unexplored in this stroke model, that these ongoing elevations in MK are related to axon beading, microglia upregulation, or other microstructural changes not examined in our studies. Further studies are needed to investigate these other likely microstructural changes that underlie the time-specific changes in MK.

We observed several significant and strong correlations between density histology measures and dMRI metrics in both *study 1 and 2*. First, in our larger injury model the surface density of glia and dendritic processes in perilesional cortex was both correlated with perilesional MD. There was a substantial degree of reactive astrogliosis, as measured

by GFAP+ immuno-reactive processes, in the perilesional cortex at 72 hrs and was strongly correlated with MD at this time point. Glia, specifically astrocytes, expresses aquaporin-4 making them highly permeable to water, leading to increased water diffusion. After ischemic injury, glia infiltration can lead to greater edema; when aquaporin-4 is knocked out, there is reduced edema (Manley, Fujimura et al. 2000). Thus, the increase in astrogliosis in the perilesional cortex at 72hrs after stroke is one explanation for why MD is increased (to more normalized levels) at 72hrs after lesion. In the large stroke study, we found a statistically significant correlation between the surface density of GFAP and perilesional MD at 3 days post-lesion, but this finding is not reproduced in *study 2* ($r=0.09$). We do however show a significant correlation between GFAP and perilesional MD at 7 days in *study 2*. Again, the later time point correlation may be due to the fact that our lesions were smaller in *study 2*, which may have delayed some aspects of the injury response. These two studies suggest that astrogliosis levels may be correlated with the size of injury and the reason we do not see a correlation until 7 days post stroke in *study 2*.

Astrocyte density also correlated with perilesional FA 24hrs after stroke, but not at any other time points in *study 2*. As noted by Sofroniew and Vinters (Sofroniew and Vinters 2010), GFAP antibodies can be used as a sensitive and reliable marker that labels most CNS injury-induced reactive astrogliosis. GFAP antibodies also do not necessarily react to all astrocytes in healthy tissue nor does it reveal all the fine distal processes. Further, mild to moderate reactive astrogliosis often leads to only negligible astrocyte proliferation (Sofroniew and Vinters 2010). Thus, the observed increase in astrocyte surface density changes in this study likely does not reflect astrocyte proliferation but instead an upregulation of injury-induced GFAP astrocytes undergoing lesion induced morphological and functional changes. In other models, including traumatic brain injury, GFAP

immunoreactivity has also been associated with FA levels (Budde, Janes et al. 2011). Other models and groups have found correlations in neuronal injury models with dMRI and GFAP levels. In a rat model of TBI, Zhuo and coworkers (Zhuo, Xu et al. 2012) found evidence linking increased MK with increased GFAP immunoreactivity in gray matter. Other studies that have attempted to link reactive astrogliosis with diffusion measures report both positive (Wang, Wu et al. 2009, Falangola, Guilfoyle et al. 2014) and negative results (Umesh Rudrapatna, Wieloch et al. 2014, Guglielmetti, Veraart et al. 2016).

Perilesional surface densities of dendritic processes examined by quantifying immunoreactive MAP2 did not show a difference across post stroke time points in either study, as expected. The correlation seen in the large stroke study between perilesional MD and surface density of dendritic processes was extremely weak ($r=0.462$), but may reflect acute lesion-induced dendritic remodeling. Further investigation is needed to understand this relationship. The water permeability rates are unknown in dendritic processes and these rates likely depend on shape and size. Water permeability may be changing after ischemic damage, leading to MD detecting these changes but likely do not capture all of the changes occurring in perilesional microstructure.

Axonal remodeling after stroke has been demonstrated previously (Liu, Li et al. 2012), is linked to behavioral recovery (Liu, Li et al. 2012), and has been associated with changes in dMRI measures, primarily in white matter tracts (Jiang, Zhang et al. 2010). In our studies, we were interested in whether dMRI could capture axonal degeneration in cortical gray matter. We found conflicting correlation results in both studies. In both studies we found no significant changes after stroke in the density of axons in remaining cortex. In *study 1*, we found no significant correlations with dMRI metrics. However, we found a strong correlation very early after stroke between axonal density and FA in *study 2*. FA may be detecting axonal degeneration and axonal demyelination, which has been

proposed in other models of injury (Budde, Janes et al. 2011). Previous research has shown a link between density of axonal projections and FA in white matter tracts (Jiang, Zhang et al. 2010, Budde, Janes et al. 2011, Liu, Li et al. 2012). Further studies are needed to determine this possible relationship.

Together these data indicate that diffusional kurtosis imaging measures are sensitive to changes in tissue properties of acute perilesional cortex; however, it is still unclear whether this is because of alterations in the surface density of glia processes, dendrites, and axons. Nevertheless, glia infiltration into the perilesional cortex may underlie the normalization of diffusion properties measured by MD after lesion, but likely there are also other structural changes responsible for the apparent normalization of MD. This work is one of the first to characterize morphological changes after ischemic stroke and to relate these findings to changes in dMRI metrics. These data further support that diffusional kurtosis and diffusion tensor measures provide different but complimentary information on acute changes in perilesional cortex after stroke. There are likely several different microstructural changes underlying these two complimentary diffusion measures.

These studies pose several limitations that should be taken into consideration when interpreting the results. The majority of studies that attempt to find causal links between dMRI and histological measures have used correlations between the two, as we have done, but as the old adage states--correlations do not determine causality. Future studies would benefit from using conditional knockout or knockin animals to help determine the effects on dMRI metrics of altering the expression of different cell types or their structure. We examined three different cell types using IHC and stereological quantification, however many more factors could be contributing to changes detected by dMRI. Edema, microglia activation, inflammation, and cellular apoptosis are all likely to contribute to changes in water diffusion and thus dMRI metrics following stroke (Moseley,

Cohen et al. 1990, Budde, Janes et al. 2011, Umesh Rudrapatna, Wieloch et al. 2014). Another limitation is possible displacement of the perilesional tissue due to tissue degradation within the lesion core over the course of the experiment, which could confound the positioning of our perilesional ROIs and contribute to the variability of our measurements. MD and MK values in both studies were more variable during early time points post stroke (3hrs) compared to later time points such as 7 days.

Conclusion

In conclusion, these studies are one of the first to characterize morphological changes after ET-1–induced ischemic stroke and to relate the findings to changes in dMRI metrics. These data further support that diffusional kurtosis and diffusion tensor measures provide different but complimentary information on acute changes in perilesional cortex after stroke. There are likely several different microstructural changes underlying these complimentary diffusion metrics, though it appears that upregulation of astrocytes seem to play a role. Further investigation needs to be done to determine these time-sensitive, region-specific changes.

CHAPTER 3: CHANGES IN TISSUE DIFFUSION PROPERTIES FOLLOWING REHABILITATION IN EXPERIMENTAL STROKE ANIMALS

Introduction

While many studies have examined dMRI metric changes in the lesion core chronically following a stroke, there are no studies in animal models examining rehabilitation training induced effects on dMRI measures in peri-infarcted. Although human studies have shown differences in dMRI metrics after rehabilitation training, determining the cause of these changes has yet to be possible. Theories such as changes in myelination, increased density of axons, and others have been given to justify dMRI changes (Jiang, Zhang et al. 2010, Sampaio-Baptista, Khrapitchev et al. 2013). Our goal was to determine the microstructural changes occurring that drive these dMRI changes following rehabilitation. This work has focused on upper extremity deficits, which are the most common persistent impairments following stroke (Kelly-Hayes, Robertson et al. 1998).

Currently, physical rehabilitation is the gold standard to improve motor function and allow stroke survivors to regain independence following an ischemic stroke (Association 2014). Animal models of ischemic stroke that go through forelimb motor rehabilitative training show enhanced motor performance compared to control conditions where animals are allowed to recover in their home cage (Maldonado, Allred et al. 2008). Motor rehabilitative training via a skilled reaching task, a form of motor learning, drives more efficient neuroplastic changes throughout the cortex, especially in the perilesional area, and white matter. For example, in rodents, synaptogenesis, spine formation and elimination, and glial changes all occur in the peri-injury remaining motor cortex following a motor learning task (Adkins-Muir and Jones 2003, Kleim, Hogg et al. 2004, Xu, Yu et al. 2009). Functional plasticity also occurs after training on a skilled reaching task measured by cortical representations of motor maps. Several studies have shown increases in

forelimb representations in motor maps in the caudal forelimb area of the motor cortex following a skilled reaching task (Nudo, Milliken et al. 1996, Kleim, Barbay et al. 1998, Kleim, Hogg et al. 2004). There is support from human neuroimaging studies that motor learning causes increases in fractional anisotropy (FA) in white matter. Patients with multiple sclerosis undergoing upper limb skilled reaching rehabilitation showed preservation of corpus callosum and cortospinal tracts, measured by increases in FA (Bonzano, Tacchino et al. 2014).

In the current set of studies, we examined whether changes in dMRI metrics were sensitive to potential structural changes related to neural remodeling and better functional recovery following chronic stroke. We did this through two different studies. Our first study investigated the relationships between dMRI measures and rehabilitative-induced forelimb functional recovery following an ischemic lesion. Secondly, we aimed to understand the relationship between learning-induced plasticity and dMRI metrics in animals with no history of an ischemic lesion.

Methods

Animals

Long Evan male rats were given food and water *ad libitum* and were kept on a 12:12-hour light:dark cycle. All work was done in accordance with the Medical University of South Carolina Animal Care and Use Committee guidelines. Animals were randomly assigned to groups in both studies. Study 1: Animals received ET-1 stroke (n=30) to examine lesion induced dMRI changes and rehabilitation training effects in dMRI metrics (stroke+rehabilitation training n=15, stroke+no-rehabilitation control n=15). Study 2: Sham animals (n=19) from Chapter 2, *study 2* were compared to pre-stroke single pellet reach trained animals from Chapter 3, *study 1* to examine learning-induced changes in dMRI metrics.

Surgical Procedures

Animals in *study 1* received a cocktail of ketamine (110 mg/kg) and xylazine (70 mg/kg). A craniotomy was performed at 0.5 mm posterior and 1.5 mm anterior to bregma and 3.0 to 5.0 mm lateral to midline, and then dura was gently retracted. Four microliters (0.2 µg/µL in sterile saline) of ET-1 was applied directly on the brain surface at 1 µL/min, with a 2-minute wait between each 1 µL of ET-1 application. After the final application of ET-1 in all surgeries, the brain was left undisturbed for 5 minutes and then the holes or craniotomy was covered with gel film and UV-cured dental acrylic.

Diffusion MRI

dMRI scans were acquired at various time points depending on the experiment using a 7T/30 Bruker BioSpec (Billerica, MA) animal scanner. Animals were anesthetized with isoflurane/air (4-5% for induction/1-3% for maintenance) for all dMRI scans. A standard DKI (Jensen and Helpert 2010) protocol was utilized consisting of a two shot spin-echo echo planar imaging diffusion sequence with 30 diffusion encoding directions and 5 b-values (0, 500, 1000, 1500, 2000 s/mm²). Other imaging parameters were: TR/TE = 4750/32.5 ms, field of view = 30×30 mm², matrix = 128×128, in-plane resolution = 0.23×0.23 mm², slice thickness = 1.0 mm, diffusion gradient pulse duration = 5 ms, diffusion time = 18 ms, and number of excitations = 2. A total of 19 axial slices with no interslice gap were collected.

Data presented from the region of interest (ROI) analysis are for MD and MK corresponding to the apparent diffusion and kurtosis coefficient, respectively, averaged over all directions (Jensen, Helpert et al. 2005). Diffusion and diffusional kurtosis tensors were calculated using diffusional kurtosis estimator (DKE), a publically available in-house software (Tabesh, Jensen et al. 2011). For *study 1* multislice ROIs were manually drawn in the perilesional layers II/III and V of the remaining MC and contralesional layers II/III and V of the forelimb area of the SMC. The perilesional regions of interest were drawn on 3 contiguous MRI slices (1-mm thick) and were inclusive of layers II/III and V.

Tract Based Spatial Statistics (Study 1 and 2)

All imaging metrics derived from DKE were analyzed by using unbiased whole brain tract-based spatial statistics (TBSS) (Smith, Jenkinson et al. 2006). Prior to utilizing TBSS, Advanced Normalization Tools (ANTs, <http://stnava.github.io/ANTs>) created a study-specific atlas of evaluated FA maps to be used for independent subject image normalization and registration. The standard TBSS pipeline was followed, except the intermediary steps, where they were modified in house to use ANTs for all FA image normalization and registration purposes in the cohort. The skeleton of white matter tracts generated by the TBSS pipeline was obtained by thresholding the mean FA map at 0.2, and white matter tract integrity metrics were thresholded with the FA at 0.36. Animals utilizing their left forelimb for training (right hemisphere) were flipped to be standardized on the left, i.e. all training hemispheres were manipulated to one lateral side.

Behavioral Assays

Single Pellet Reaching (Study 1)

The single pellet reaching (SPR) task, a skilled forelimb reaching task, can be used to assess skilled learning and relearning of a skilled forelimb task following stroke. Animals were placed in a plexiglass chamber and allowed to reach through a small window in the front of the chamber. Animals reached through the window with a limb they prefer, a 1-centimeter tall platform holds a single banana flavored pellet for the animal to reach for. Each time the animal reaches for the pellet it will be scored as a success, fail, or drop (Whishaw and Pellis 1990). A success occurs when the animal reaches for a pellet and eats the pellet without dropping the pellet. Animals in the rehabilitation groups reached to a criterion of roughly 60% success rate before undergoing ET-1 induced stroke. These pre-operative animals were used to compare to naïve animals in *study 2*. After surgery, this task also served as the rehabilitation training (RT) task for animals in the RT group. For RT, animals reached for 20 minutes/day or until they completed 60 trials for 6

days/week for 21 days. Animals in the no-rehabilitation control (No-RT), following surgery, were placed in the plexiglass chamber with banana pellets to eat off the ground for 20 minutes/day for 6 days/week for 21 days.

Statistical Analysis

All data are reported as mean \pm standard error of the mean (SEM). *Study 1*, used rANOVAs to examine behavioral differences following RT with Bonferroni post-hoc corrections. For *study 1 and 2*, TBSS voxelwise statistics on all skeletonized metrics were conducted between groups in the cohort with a two-group difference GLM. The significance level was $\alpha=0.05$.

Results

Study 1: Changes in Diffusion Measures Following Experimental Stroke and Rehabilitative Training

Diffusion MRI

Animals were scanned prior to lesion, 4 days post stroke, and after 21 days (26 days post stroke) of rehabilitation training or control procedures. As in our previous studies, we first drew ROIs in the perilesional area, but did not find a significant interaction of time and/or group in MD or MK. Therefore, our ROI analysis revealed no difference of rehabilitation over time. There was a significant change over time when groups were combined in both MD ($F_2=8.042$, $p=0.001$) and MK ($F_2=8.544$, $p=0.001$) indicating a stroke effect in the diffusion metrics. With no change between groups, animals were combined to determine time point effects. MD was significantly decreased at 4 days [$t(29)=3.319$, $p<0.05$] and 26 days [$t(29)=4.459$, $p<0.05$] post stroke compared to pre-operative values. However, MK was only increased at 26 days [$t(29)=-2.591$, $p=0.015$] post stroke compared to pre-operative values.

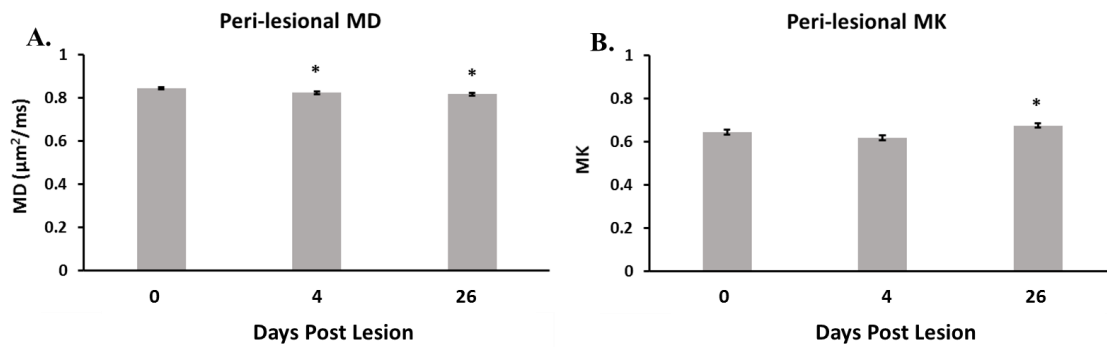


Figure 3.1. Peri-lesion dMRI Results Following RT.

Regions of interest were drawn in the peri-lesional area. RT and NoRT groups were combined for analysis because there was no difference between groups. **A.** MD was significantly decreased at 4 and 26 days post stroke compared to pre-operative levels. **B.** MK was increase at 21 days post stroke compared to pre-operative levels. Values are reported as mean \pm SEM. * $p < 0.05$.

Using the TBSS approach, we examined changes in FA along all white matter in the brain. Additionally, we ran the white matter model (WMM) to determine directionality of any FA changes seen with TBSS (details in the Introduction). Although a previously published study found an increase in FA in the corpus callosum under the motor cortex grey matter between naïve animals that underwent skilled training compared to control training conditions (Sampaio-Baptista, Khrapitchev et al. 2013), we did not find a difference in FA in any white matter tracts in the brain in stroke animals that underwent RT compared to NoRT. We used similar methods to the Sampaio-Bapitista and colleagues to examine differences between RT treated animals and control animals following stroke. We also did not find a difference in white matter tract integrity parameters in our animals following stroke and RT. We performed extensive analysis to confirm our findings, which will be highlighted in the discussion.

Table 3.1. dMRI metric changes following a cortical stroke and rehabilitation training.

	Brain Region Examined	Result
MD: mean directional diffusivity	Perilesional Grey Matter	Perilesional decreases at 4 days and 26 days
MK: mean directional kurtosis	Perilesional Grey Matter	Perilesional increases at 26 days
FA: degree of anisotropy of a diffusion process	All Cortical White Matter (via TBSS)	No change
White Matter Modeling: Axonal Water Fraction Intrinsic Diffusivity Axial Diffusivity Radial Diffusivity	All Cortical White Matter	No change

Our lack of findings in our dMRI and TBSS metrics were not due to lack of behavioral recovery on our sensitive behavioral task. After animals had an ET-1 induced lesion they were significantly impaired on the single pellet reaching (SPR) task [$t(29)=15.044$, $p<0.001$]. There was a significant effect of group by day throughout rehabilitation ($F_4=11.841$, $p<0.001$). The RT ($n=15$) animals had significantly better motor performance on week 1 [$t(28)=2.967$, $p=0.006$], week 2 [$t(28)=3.442$, $p=0.002$], and week 3 [$t(28)=5.648$, $p<0.001$] compared to NoRT animals ($n=15$).

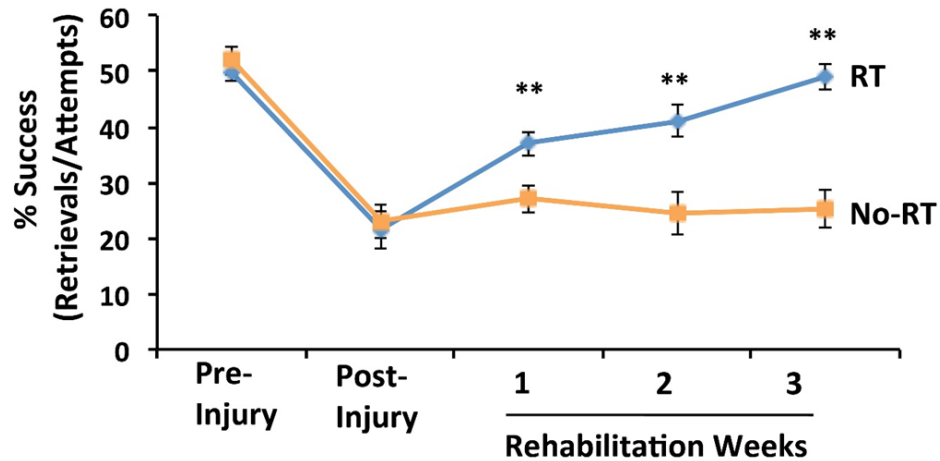


Figure 3.2. Animals that undergo RT have greater functional improvement.

After ET-1 induced stroke, all animals were significantly impaired compared to pre-op levels ($p < 0.001$). Animals performing the single pellet reaching (SPR) task improved compared to animals in the control condition on weeks 1 ($p = 0.006$), 2 ($p = 0.002$), and 3 ($p < 0.001$). Values are reported as mean \pm SEM. * $p < 0.005$.

Study 2: Changes in Diffusion Measures Following a Skilled Motor Learning Task

Sham animals (Chapter 2, *study 2*) were scanned after being handled for one week. Following pre-training on the SPR task and reaching a criterion of 60% success, animals (Chapter 3, *study 1*) were imaged. This study was conducted to understand learning-induced plasticity changes in dMRI metrics, however was not originally planned out to be completed therefore was likely not designed properly. Pre-trained animals from Chapter 3 study 1, had a varying amount of training days because all animals reach asymptotic behavior at a different pace. Once asymptotic, animals remained in their home cage to await imaging and an ischemic lesion. Animals on average were trained for 6 ± 0.53 days, with a maximum of 11 days for one animal.

TBSS analysis for all white matter tracts in the brain was performed to examine learning-induced dMRI changes. We found a significant increase in FA in the external capsule of the non-trained hemisphere of naïve animals compared to animals performing a skilled reaching task (**Figure 3.3**). Additionally, kurtosis metrics (mean kurtosis, axial

kurtosis, and radial kurtosis) show increased in the entire white matter of naïve animals compared to trained animals (**Figure 3.4**).

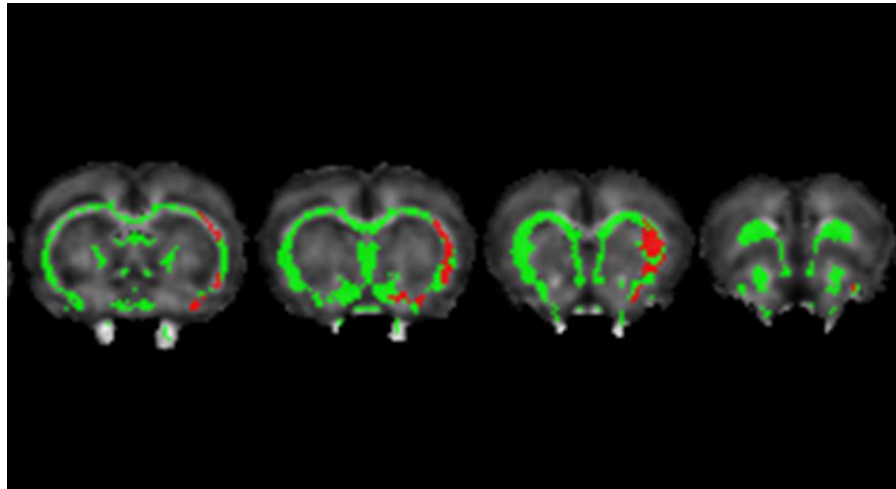


Figure 3.3. FA increased in naïve animals. Green white matter overlay is showing TBSS FA skeleton. Red areas indicate an increase in FA in naïve animals compared to trained animals. Trained hemisphere=left.

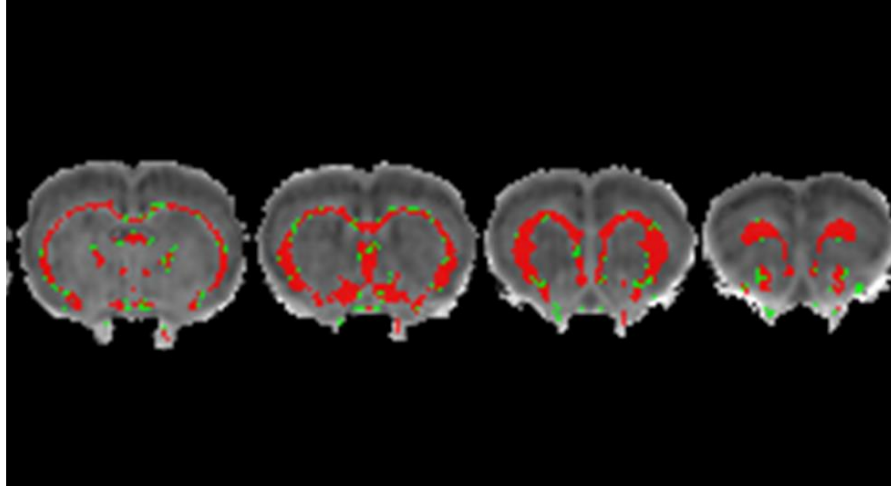


Figure 3.4. MK increased in naïve animals. Green white matter overlay is showing TBSS FA skeleton. Red areas indicate an increase in MK in naïve animals compared to trained animals. Trained hemisphere=left.

Lastly, to understand the meaning of these increases seen in naïve animals we ran the white matter model. The four primary metrics of WMM would give us more insight

into understanding these changes. We only found a significant increase in axonal water fraction in naïve animals in the corpus callosum near the forelimb region of the motor cortex compared to trained animals (**Figure 3.5**). Increases in axonal water fraction would suggest an increase in axonal density in naïve animals. Secondly, it may be the case that we are detecting reduced axonal density driven by training.

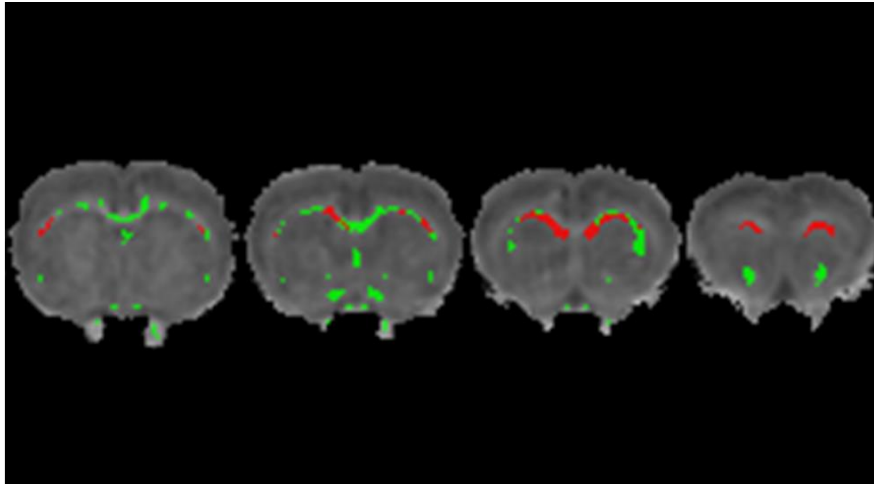


Figure 3.5. Axonal water fraction increased in naïve animals. Green white matter overlay is showing TBSS FA skeleton. Red areas indicate an increase in axonal water fraction in naïve animals compared to trained animals. Trained hemisphere=left.

Table 3.2. dMRI metric changes following skilled forelimb training.

	Brain Region Examined	Result
FA: degree of anisotropy of a diffusion process	All Cortical White Matter (via TBSS)	Naïve increase in external capsule
MK: mean directional kurtosis	All Cortical White Matter (via TBSS)	Naïve increases throughout all cortical white matter
Axial Kurtosis: diffusional kurtosis in the direction of highest diffusion	All Cortical White Matter (via TBSS)	Naïve increases throughout all cortical white matter
Radial Kurtosis: mean directional kurtosis perpendicular to the direction of highest diffusion	All Cortical White Matter (via TBSS)	Naïve increases throughout all cortical white matter
White Matter Modeling: Axonal Water Fraction Intrinsic Diffusivity Axial Diffusivity Radial Diffusivity	All Cortical White Matter	Naïve increases in the corpus callosum under the forelimb region of the sensorimotor cortex in both hemispheres of axonal water fraction

Discussion

Animals that underwent skilled reaching RT, via the SPR task, for 21 days following injury had enhanced forelimb reaching improvements compared to animals that did not have RT. Other groups have shown enhancement of motor recovery with RT and changes in structural proteins such as increases in dendritic density, synapse number, and increases in glutamate receptor number the perilesional cortex (Maldonado, Allred et al. 2008). We anticipated recovery of structural proteins would lead to dMRI metric changes and therefore enhanced behavioral recovery should have given a favorable environment to discover differences in dMRI metrics. In both the region of interest comparison of the perilesional area and TBSS analysis of white matter neither showed any differences between the two groups (RT and NoRT). Our TBSS analysis corrected the p-value for multiple comparisons, as should be done with so many comparisons. We then examined the results with uncorrected p-values to determine if there were any potential changes that

we masked by a conservative correction. The uncorrected results showed a few minute significant voxels scattered throughout the brain. These voxels were in random locations such as the tongue region of the sensory cortex that are unlikely altered by forelimb training. The TBSS analysis was unable to reveal any significant difference between groups. We ran both a ROI based analysis and TBSS analysis after RT so we were not bias in our analysis and that no possible brain region was overlooked that underwent RT induced changes in water diffusion.

Lastly, we ran white matter tract integrity parameters (WMTI) (in depth explanation in introduction) after the planned ROI based analysis and TBSS analysis following rehabilitation. We examined four different parameters: axonal water fraction, intrinsic diffusivity, axial diffusivity, and radial diffusivity. The axonal water fraction is thought to measure axonal density. The intrinsic diffusivity examines diffusion inside axons and might be a marker of axonal injury. The axial and radial diffusivities are markers of isotropic changes in extra-axonal space. Radial diffusivity is a marker for changes in the extra-axonal diffusion transverse to the fibers, which may be linked to myelin breakdown. We found no significant changes in any parameters examined; therefore, we conclude that dMRI metrics were unable to detect microstructural changes following RT despite large behavioral recovery. There is conflicting evidence in the literature investigating white matter changes using MRI and motor learning. Research groups have reported seeing differences between people performing a motor learning task and controls; correlations have been established between imaging metrics and behavior (Sampaio-Baptista, Khrapitchev et al. 2013, Bonzano, Tacchino et al. 2014). Negative results are uncommonly reported, however one group has shown that there was no changes in MRI metrics following a training task similar to our studies (Thomas, Marrett et al. 2009, Johansen-Berg 2012).

Following negative results in *study 1*, we aimed to determine if there was a difference between naïve animals and non-stroke SPR trained animals. Referencing a 2012 report from Sampaio-Baptista and colleagues (Sampaio-Baptista, Khrapitchev et al. 2013) to use the same parameters to determine if we could find motor learning induced changes using TBSS. We thus examined a subset of animals comparing sham animals (n=19) from *Chapter 2 study 2* and animals scanned before stroke induction and after SPR pre-training (n=15) from *Chapter 3 study 1*. We found a decrease in FA in the external capsule near sensory cortex in animals that trained on the SPR task compared to naïve animals. There was no correlation found between FA in this region with reaching performance in the animals that were pre-trained on the SPR task. There were also decreases throughout all cortical white matter areas in kurtosis metrics (MK, radial kurtosis, and axial kurtosis) in animals pre-trained on the SPR task. To understand what these widespread cortical changes might mean, we ran WMM parameters. In the corpus callosum under the forelimb region of the sensorimotor cortex, there was a decrease in the axonal water fraction in both hemispheres of animals who underwent SPR training compared to naïve animals (**Table 3.2**). The axonal water fraction is thought to be a marker of axonal density (Fieremans, Benitez et al. 2013), therefore an increase in axonal water fraction is thought to represent an increase in axonal density. This would suggest that naïve animals have a greater axonal density in this region compared to trained animals, which is contradictory to the literature (Johansen-Berg 2012). Due to the white matter model assumptions, if there are changes in myelination the interpretation that axonal water fraction is a marker of axonal density may not hold up. These data are therefore inconclusive, but may be indicating that dMRI metrics are not useful in examining neuroplastic changes following motor learning. This final comparison combined two

studies that were never intended to be combined and was not properly designed (see Chapter 5), therefore the results we are seeing could be an indicator of poor design.

Conclusions

In conclusion, there were no changes in diffusion metrics following stroke and rehabilitation training even though animals showed strong behavioral recovery. Additional studies will need to be completed to understand whether the lack of effect was because of the techniques used, lesion size, or experimental design (for example when animals were scanned or extent of RT).

CHAPTER 4: CHARACTERIZING MITOCHONDRIA DYSFUNCTION AFTER STROKE AND RESCUING MITOCHONDRIA FUNCTION TO PROMOTE MOTOR RECOVERY

Introduction

Ischemic strokes make up 87% of all strokes (Association 2015) and treatment for ischemic stroke patients is limited. Many studies have focused on neuroprotective drugs that are administered prior to or within minutes to hours after stroke. While only tissue plasminogen activator (TPA) has been found to be effective at reducing stroke-induced tissue loss. TPA has a small window of effectiveness (<4hr post-stroke) and can have severe consequences in hemorrhagic patients therefore, there remains a need for treatment options beyond the first few hours after stroke.

Within minutes to hours after injury, apoptosis starts to occur, normally due to calcium influx and mitochondria dysfunction (Duchen 2000). Degeneration of distal axons, also known as Wallerian degeneration occurs days to weeks following injury due to onset of deleterious metabolic pathways which leads to expansion of infarct size and worsening of clinical outcome. The area undergoing secondary injury that surrounds the core of the ischemic lesion is termed the penumbra and this peri-infarct tissue is clinically attractive due to the delayed onset of pathogenic mechanisms, which may be amenable to therapeutic interventions (Borgens and Liu-Snyder 2012). In addition to synthesizing ATP, the mitochondrion is also important in cell metabolism, calcium homeostasis, free radical production, and apoptosis (Bayir and Kagan 2008, Niizuma, Endo et al. 2009, Hoppins 2014). During the secondary phase of ischemic injury, these mitochondria-dependent pathways are disrupted leading to increased reactive oxygen species, intracellular calcium and induction of pro-apoptotic cascades (Duchen 2000, Lin and Beal 2006, Franklin 2011). Thus, the development of pharmacological agents to promote recovery of mitochondria and ATP-dependent cellular functions may limit secondary neuronal damage in peri-infarct tissue. Mitochondria abundance and the integrity of mitochondrial DNA (mtDNA) is

disrupted following subacute brain insult (Harmon, Gibbs et al. 2016) and is crucial for recovery of cellular function following ischemic injury (Stallons, Whitaker et al. 2014, Smith, Stallons et al. 2015).

Mitochondria are also known to play a role in axonal growth and dendritic remodeling (Cheng, Hou et al. 2010), therefore increasing mitochondria healthy function and inducing mitochondria biogenesis (MB) following stroke may be essential for promoting structural and functional plasticity of peri-lesional sensorimotor cortex (SMC). Mitochondria biogenesis can be induced with exercise training in naïve and post-stroke animals and leads to decreases in lesion size and behavioral impairments following stroke (Steiner, Murphy et al. 2011, Zhang, Wu et al. 2012). It is likely that MB will promote energetic support during other forms of treatment following stroke, such as rehabilitation training, which has also been shown to induce structural and functional neural remodeling following stroke. Remaining motor cortex is vital for recovery of motor function following ischemic stroke, the majority of functional and structural plasticity occurs in the remaining SMC (Jones and Adkins 2015). The remaining SMC will be our target for therapeutic intervention following ischemic stroke.

Activation of β_2 -adrenergic receptors and exercise have been shown to increase levels of PGC-1 α and induce MB in the kidney and skeletal muscle (Miura, Kai et al. 2008, Wills, Trager et al. 2012). One non-FDA approved β_2 -adrenergic receptor long lasting agonist, Clenbuterol, has been shown to induce neuroprotection, induce neurotrophic factors such as nerve growth factor (NGF), and have an anti-inflammatory effect (Gleeson, Ryan et al. 2010). Due to the number of side effects and because it is not FDA approved Clenbuterol is not an ideal way to activate β_2 -adrenergic receptors for a clinically relevant model. Formoterol however, is FDA approved, has less severe side effects, and has been shown to induce MB in the kidney (Wills, Trager et al. 2012). Formoterol crosses the blood brain barrier and has been shown to increase cognitive function and dendritic complexity

in other disease models (Dang, Medina et al. 2014). There has been no investigation of the effect of formoterol stimulating MB following stroke and whether that leads to the enhanced behavioral and structural changes.

This study had three primary aims: 1) to examine mitochondria dysregulation following an ET-1 model of stroke; 2) determine if formoterol could rescue mitochondria homeostasis markers acutely, and 3) finally if formoterol combined with rehabilitation could enhance functional recovery. Initially, we examined the subacute (up to 7 days post stroke) time course of mitochondria dysregulation by examining genes that encode for respiratory chain subunits and link these mitochondria changes to common pathological pathways such as neuroinflammation and cell death. Because previous studies have shown that rescued function of SMC is dependent on preservation of the peri-infarct motor and sensory cortex and dorsal lateral striatum, we hypothesized that ischemic injury to the SMC would result in disrupted mitochondria homeostasis and biogenesis in peri-infarct tissue in concert with neuroinflammation and cell death that would result in impaired behavior outcomes. Secondly, we hypothesized that administration of formoterol would rescue mitochondria homeostasis markers in the perilesional motor and sensory cortex and the striatum, where we examined dysfunction in our first experiment. We administered the β_2 -adrenergic receptor agonist formoterol 24 hours after injury to examine the same subacute time course of mitochondria function and investigating the same respiratory chain subunits as in experiment one. Lastly, we hypothesized that administering formoterol in combination with RT would decrease motor impairments post stroke. We injected animals at one of three different doses of formoterol 24 hours after injury in combination with rehabilitation training (RT) for 15 days to determine the optimal dosing regimen to promote maximal behavioral recovery post stroke. Additionally, we performed several experiments to understand the underlying mechanism of formoterol to enhance behavioral recovery.

Methods

Animal

Long Evans male rats (n=233, 3-4 months old) received food and water *ad libitum* and were kept on a 12:12hr light:dark cycle. For study 1 rats were randomly assigned to one of six groups that received either a sham or stroke procedure and were euthanized at one of three time points: 24 hrs (sham=10; stroke=10), 72 hrs (sham=14; stroke=22), or 144 hrs (sham=10; stroke=20). Animals in study 2 were randomly assigned to three groups: stroke+0.1mg/kg formoterol (n=26), stroke+vehicle (n=25), or sham (n=16). Lastly, animals in study 3 were randomly assigned to eight groups: rehabilitation+vehicle (n=9), no rehabilitation+vehicle (n=10), rehabilitation+0.1mg/kg (n=9), no rehabilitation+0.1mg/kg (n=10), rehabilitation+0.5mg/kg (n=10), no rehabilitation+0.5mg/kg (n=9), rehabilitation+1.0mg/kg (n=10), or no rehabilitation+1.0mg/kg (n=9). Animals that did not display behavioral impairment in study 3, which was defined as less than a 20% change from pre-stroke assessment, were excluded from the study (n=4). All animal protocols followed the National Institutes of Health (NIH) Guide for the Care and Use of Laboratory Animals, and were approved by the Medical University of South Carolina Animal Care and Use Committee.

Surgical Procedures

For all three experiments rats were anesthetized with ketamine (1.1mg/kg I.P.) and Xylazine (0.7mg/kg I.P.). Unilateral ischemic lesions were induced via ET-1 (American Peptide, Inc) applied to the cortical surface of the forelimb area of the SMC (FI-SMC). Briefly, a craniotomy was performed at 1.0 mm posterior and 2.0 mm anterior to bregma and 3.0–5.0 mm lateral to midline and dura was gently retracted. ET-1 was applied on the brain surface at approximately 1ul/min, with a 2 min wait between applications using a total of 4ul. After the final 1ul of ET-1, the brain was left undisturbed for 5 minutes and

then the craniotomy was covered with gel film (Invotec International) and dental acrylic. Sham animals had all procedures up to craniotomy. All animals received buprenorphine (0.5mg/kg S.C.) prior to incision for pain.

Behavioral Tasks

Ladder Task (Study 1 and 2)

To assess ischemia-induced impairments of forelimb function and compare these to mitochondria homeostasis markers, all animals were tested on the ladder task on days 0, 1, 3, and 6. The ladder task was used to assess coordinated forelimb use, stepping accuracy, and limb placement and is sensitive to motor cortex damage (Metz and Whishaw 2009). The ladder apparatus is made of two plexiglass walls, with 3mm diameter pegs spaced 1cm apart from each other. The ladder is raised ~20cm off the ground with a neutral start cage and the animal's home cage at the end. Through slow-motion video replay, all forelimb placements were qualitatively scored on a 0-6 rating scale over three trials (three traverses across the ladder). A perfectly placed limb received a score of 6 and a partial placed limb, such as just one digit on the rung, scores a 5. Errors were scored as follows: 0 = limb missed the ladder rung and the limb fell through the rungs; 1 = the limb was placed the limb but when weight bearing either fell (score of 1) or slipped (score of 2) (Metz and Whishaw 2009). Percent errors was calculated as: $\text{sum of errors (0+1+2)} / (\text{total steps})$ per test day.

Single Pellet Reaching (SPR) Task (Study 3)

Animals were placed in a plexiglass chamber and allowed to reach through a small window in the front of the chamber. Animals reached through the window with a limb they prefer and a 1-centimeter tall platform holds a single banana flavored pellet for the animal to reach for. Each time the animal reached for the pellet it was scored as a success, fail,

or drop (Whishaw and Pellis 1990). Animals must reach a criterion of roughly 60% success rate before undergoing ET-1 induced stroke. After surgery, animals were allowed to recover for two days. On the third day, behavioral assessment was conducted using the single pellet reaching task and this task served as the rehabilitation training task. Animals reached for 20 minutes/day or until they complete 60 trials for 6 days/week for 15 days.

Tissue Collection (Study 1 and 2)

Animals were deeply anesthetized with Euthasol (0.1mg/kg) and brains were removed to obtain fresh tissue punches from the ipsilesional sensory and motor cortex and the striatum. Samples were taken medial and anterior to the injury based on specific lesions and anatomical observation, no tissue was sampled that contained the lesion core. Tissue was placed on dry ice to preserve mRNA and protein levels. Samples remained in a -80 freezer until RNA isolation or western blot analysis was performed. We choose to investigate the motor and sensory cortex that did not include the lesion core because these areas are highly connected to the primary area of injury, undergo secondary degeneration, and are important for recovery of sensorimotor function following caudal forelimb injuries and thus are targets for future intervention (Jones, Chu et al. 1999, Carmichael 2003, Nudo 2013).

RNA Isolation and Real-Time PCR (Study 1 and 2)

Total RNA was extracted from cortex and striatum using TRIzol reagent (Invitrogen) according to the manufacturer's protocol. Reverse transcription was performed using the RevertAid First Strand cDNA kit (Thermo Fisher Scientific) with 0.5-1 ug of RNA. 5 uL of cDNA template was used to amplify PCR products using 2x Maxima SYBR green qPCR master mix (Thermo Fisher Scientific). The primer sequences used in the qPCR protocol are listed in **Table 4.1**. Fold changes in mRNA expression were

normalized to tubulin were calculated using the $\Delta\Delta$ - Ct analysis method (Wills, Trager et al. 2012). Tubulin has been established to be a relevant control used to determine changes in mitochondria genes (Wills, Trager et al. 2012, Harmon, Gibbs et al. 2016).

Table 4.1. Primer pairs used for qRT-PCR.

Gene	Primer Sequence	
PGC-1 α	Sense	5'-AGGAAATCCGAGCGGAGCTGA-3'
	Antisense	5'-GCAAGAAGGCGACACATCGAA-3'
NDUFS1	Sense	5'-AGATGATTGGGAACAACGG-3'
	Antisense	5'-TAAGGCTTAGAGTTAGGGC-3'
COX1	Sense	5'-CCTGAGCAGGAATAGTAGGG-3'
	Antisense	5'-AGTGGTACAAGTCAGTTCCC-3'
ND1	Sense	5'-TGAATCCGAGCATCCTACC-3'
	Antisense	5'-ATTCTGCTAGGAAAATTGG-3'
SOD2	Sense	5'-CAAGGGAGATGTTACAACCTCAGG-3'
	Antisense	5'-CTTAGGGCTCAGGTTTGCCA-3'
UCP2	Sense	5'-GAGATACCAGAGCACTGTCC-3'
	Antisense	5'-GCTCAGTACAGTTGACAAATGG-3'
F4/80	Sense	5'-TCCTCTCTGGGGCTTCAGT-3'
	Antisense	5'-CCATTGCTGGGCAGAAAACC-3'
IL-6	Sense	5'-TTCAGAGCAATACTGAAACCC-3'
	Antisense	5'-GATGGTCTGGTCTTAGCC-3'
Tubulin	Sense	5'-CTCTCTGTCGACTACGGAAAG-3'
	Antisense	5'-TGGTGAGGATGGAATTGTAGG-3'
Actin	Sense	5'-TAAGGAACAACCCAGCATCC-3'
	Antisense	5'-CAGTGAGGCCAGGATAGAGC-3'

Mitochondrial DNA Content (Study 1 and 2)

Relative mtDNA content in rat cortex and striatum samples was measured using real-time qPCR. Nuclear and mitochondrial, was isolated from tissues using the DNEasy Blood and Tissue Kit (Qiagen), 5 ng of cellular DNA was used to perform qPCR. Relative quantity of mtDNA was assessed by expression of NADH dehydrogenase 1 (ND1), a mitochondrial gene, and normalized to nuclear-encoded β -actin. Primer sequences for ND1 and β -actin were ND1 sense: 5'-TGAATCCGAGCATCCTACC-3'; ND1 antisense: 5'-ATTCTGCTAGGAAAATTGG-3'; β -actin sense: 5'-TAAGGAACAACCCAGCATCC-3'; and β -actin antisense: 5'-CAGTGAGGCCAGGATAGAGC-3'. The $\Delta\Delta$ -Ct analysis method was used to calculate fold changes in expression (Wills, Trager et al. 2012).

Immunoblot Analysis (Study 1 and 2)

Rat cortex and striatum tissue was homogenized in 150 μ L of protein lysis buffer and protease inhibitors (1% Triton X-100, 150 mM NaCl, 10 mM Tris-HCl, pH 7.4; 1 mM EDTA; 1 mM EGTA; 2 mM sodium orthovanadate; 0.2 mM phenylmethylsulfonyl fluoride; 1 mM HEPES, pH 7.6; 1 μ g/ml leupeptin; and 1 μ g/ml aprotinin) using a Polytron homogenizer. Then the samples were sonicated and centrifuged at 14,000 g for 15 min at 4°C. The supernatant was collected and protein quantified using a bicinchoninic acid kit (Sigma). Proteins (30 μ g) were separated on 4 to 20% gradient SDS-polyacrylamide gels and transferred to nitrocellulose membranes. Membranes were blocked in 5% BSA or milk in TBST (0.1% Tween 20 in 1 \times Tris-buffered saline) and incubated with primary antibodies overnight at 4°C. Primary antibodies used in this study included: COX1 (1:2000 Abcam); ND1 (1:2000, Abcam); NDUFS1 (1:2000, Abcam); cleaved caspase 3 (1:1000, Cell Signaling, Danvers); Caspase 3 (1:1000, Santa Cruz); GAP-43 (1:1000, Cell Signaling) and GAPDH (1:10000, Fitzgerald). After incubation for 1hr at room temperature with secondary rabbit (1:2000, Abcam) or mouse (1:20000, Abcam) antibodies conjugated with horseradish peroxidase, membranes were detected by chemiluminescence. Densitometric analysis was performed using ImageJ (Schneider, Rasband et al. 2012).

Immunohistochemistry (IHC) (Study 3)

Following 15 days of rehabilitation training (RT), a subset of animals were examined for changes in perilesional dendritic density. Animals were deeply anesthetized with pentobarbital (Euthasol, 100-150mg/kg, IP) and were intracardial perfused with 0.1M phosphate-buffer and 4% paraformaldehyde. Six serial rostral to caudal sets of 50 μ m coronal sections were produced using a vibratome and stored in cryoprotectant. Three sets of sections were processed for IHC to ascertain post-injury morphological changes in the surface density of dendrites in the perilesional motor cortex. As described previously

(Adkins, Voorhies et al. 2004), free-floating sections were processed for IHC. Tissue was incubated for 48 hr in primary antibody for dendrites (MAP2; 1:500 mouse monoclonal; Sigma-Aldrich). Following primary incubation, sections were rinsed and incubated for 2 hr in secondary antibody at a dilution of 1:200 (horse anti-mouse). Sections were incubated in peroxidase-linked avidin-biotin complex (ABC kit) for 2 hr. Immunoreactivity was visualized using 3,3' diaminobenzidine with nickel ammonium sulfate intensification. All animals were included in each batch of IHC processing and each batch included negative control sections without primary antibody.

The cycloid grid intersection method (Baddeley, Gundersen et al. 1986) was used to determine surface density for MAP2 immuno-reactive processes. We sampled tissue that was represented that included the forelimb area of the sensorimotor cortex. Data were obtained in three adjacent coronal sections (~600 μm apart) which included peri-lesional motor cortex (i.e., between approximately +1.2 and -0.26 mm anterior/posterior relative to bregma). Using ImageJ (National Institute of Mental Health, Bethesda, MD), cycloid arcs were overlaid on light microscopic images, taken at 100 \times oil immersion (final magnification=1,400 \times), of four sample regions, two adjacent sets (~250 μm) in layers II/III and two sets in layer V beginning at approximately 250 μm medial to the lesion core (towards midline), for 3 sections. Each immuno-reactive process that crossed an arc was counted. The surface density was calculated using the formula $S_v = 2(I/L)$, where S_v is the surface density, I is the total number of intersections and L is the sum of the cycloid arc lengths.

Estimated Lesion Size Analysis (Study 3)

Nissl stained sections for animals in the 0.1mg/kg+RT, vehicle+RT, 0.1mg/kg+NoRT, and vehicle+NoRT were used for lesion volume estimations. Seven 50 μm coronal sections 600 μm apart were analyzed for lesion volume estimation using

sections between approximately 2.7mm anterior to 1.3mm posterior to Bregma, which were determined using structural landmarks. Injury volumes of cortex were estimated for each subject using a grid overlay in ImageJ with an area/point of 100 pixels². Points in healthy cortex was counted in the lesion and non-lesion hemisphere. Lesion area was calculated as the difference between the injured and non-injured cortex. Volume was estimated as the product of lesion area multiplied by the distance between sections (600µm) and the distance between points (0.824mm).

$$\text{Equation: Volume} = \Sigma(\text{Points} \times \text{Distance}^2 \times \text{Distance between sections})$$

Statistical Analysis

All data are reported as group means with \pm standard error of the mean (S.E.M.). Repeated analysis of variance (rANOVA) was used to test for behavioral differences with post-hoc comparisons for each post-operative day in all experiments. Single comparison of molecular data was performed using the Student t-test, whereas data found to not have a normal distribution were subjected to a Mann-Whitney U-test in experiment one and two. Data were considered statistically significantly different at $p \leq 0.05$.

Results

Study 1: Mitochondria Dysfunction Following Acute Stroke

Stroke Induced Motor Impairment

As demonstrated previously, unilateral ET-1 lesions to the forelimb area of the SMC result in lasting impairments in the forelimb opposite the lesion (Metz and Whishaw 2009). Animals exhibited more limb placement errors while walking across a horizontal ladder with their impaired limb at 24 hrs ($p < 0.005$), 72 hrs ($p < 0.005$), and 144 hrs ($p < 0.005$) post-injury compared to sham animals (**Figure 4.1**). There were no differences seen with the non-impaired forelimb compared to sham animals or pre-stroke number of errors.

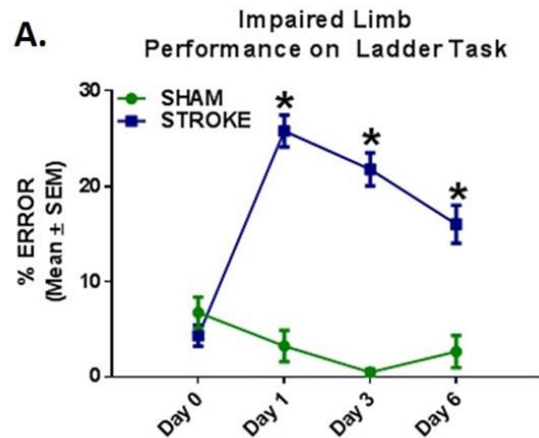


Figure 4.1 Stroke Induced Motor Impairment.

A. Following injury, animals made significantly more errors with their impaired forelimb compared to sham controls. Values are reported as mean \pm SEM. * $p < 0.005$.

Decreased respiratory chain gene expression and mtDNA content in ipsilesional motor and sensory cortex.

Mitochondrial dysfunction is a major contributor to neuronal death following ischemic stroke (Bayir and Kagan 2008). Therefore, we assessed mRNA expression of PGC-1 α , and components of the electron transport chain, nuclear-encoded NADH dehydrogenase (ubiquinone) Fe-S protein 1 (NDUFS1), and mitochondrial-encoded cytochrome c oxidase subunit 1 (COX1) and ND1. As seen in Figure 3.2, there was a non-significant downward trend ($p = 0.056$) in PGC-1 α mRNA expression 24 hrs post-stroke. NDUFS1 mRNA expression was decreased at 24 hrs and did not return to sham levels until 144 hrs post-stroke. Additionally, there was a robust reduction of COX1 and ND1 transcript levels at 72 hrs and remained suppressed at 144 hrs following injury. Mitochondrial DNA copy number was assessed as a marker of mitochondrial content. There was a persistent suppression of mtDNA copy number at 24, 72, 144 hrs post-stroke. Taken together, these findings reveal disruption in transcriptional regulation of

mitochondrial proteins involved in oxidative phosphorylation and mitochondrial content following ET-1 induction of cerebral ischemia.

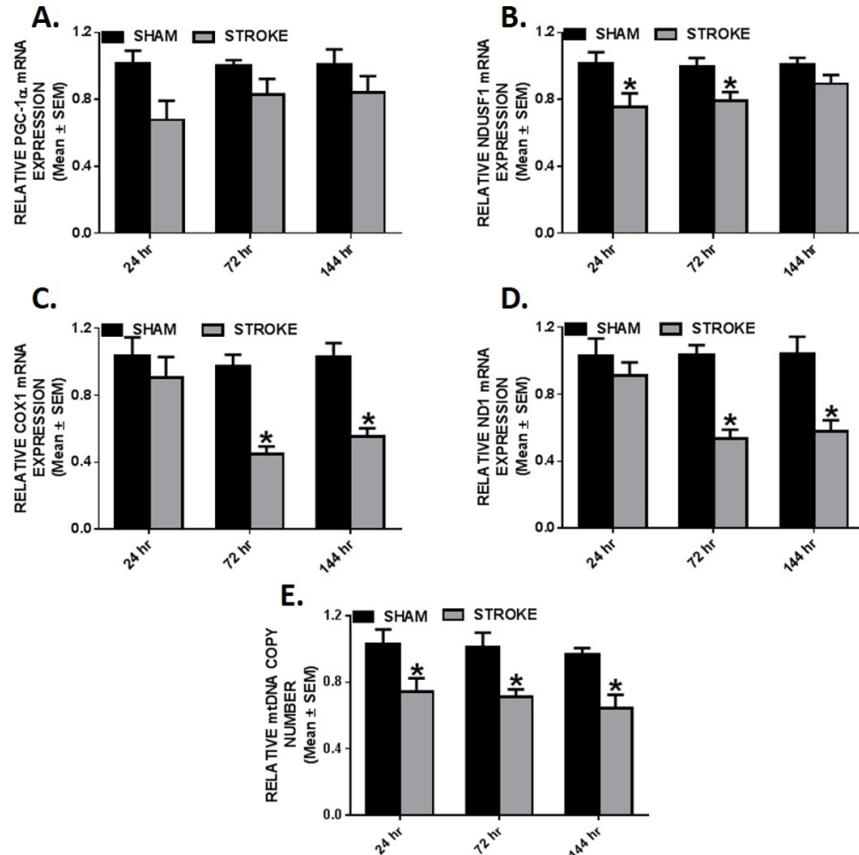


Fig. 4.2. Decreased respiratory chain gene expression and mtDNA content in ipsilesional motor and sensory cortex. PGC-1 α (a), NDUFS1 (b) COX1 (c), and ND1 (d) mRNA expression was measured by qRT-PCR using tubulin as a control gene in stroke and sham animals. mtDNA copy number (e) was measured by qRT-PCR using ND1 for the mtDNA gene and β -actin as the nuclear control gene. These markers were measured in the ipsilesional cortex 24, 72, and 144 hrs. Values reported as mean \pm SEM. *p < 0.05.

Transitory changes of mitochondrial encoded transcripts in ipsilesional striatum.

We screened for mitochondria damage in the ipsilesional striatum following ET-1 ischemic damage due to secondary injury in this area (Carmichael and Chesselet 2002). There were no changes in PGC-1 α and NDUFS1 mRNA expression in the striatum at any time point examined. However, we did observe a transitory decrease in COX1 and ND1 mRNA expression at 72 hrs (p<0.05) post-stroke and by 144 hrs mRNA levels recovered back to sham levels. At 24 hrs (p<0.05), there was a brief reduction of mitochondrial DNA

copy number in the ipsilesional striatum which returned to sham levels at 72 hrs (**Figure 4.3**). These results reveal that ET-1 induced SMC lesions result in subacute and transitory mitochondrial changes after stroke.

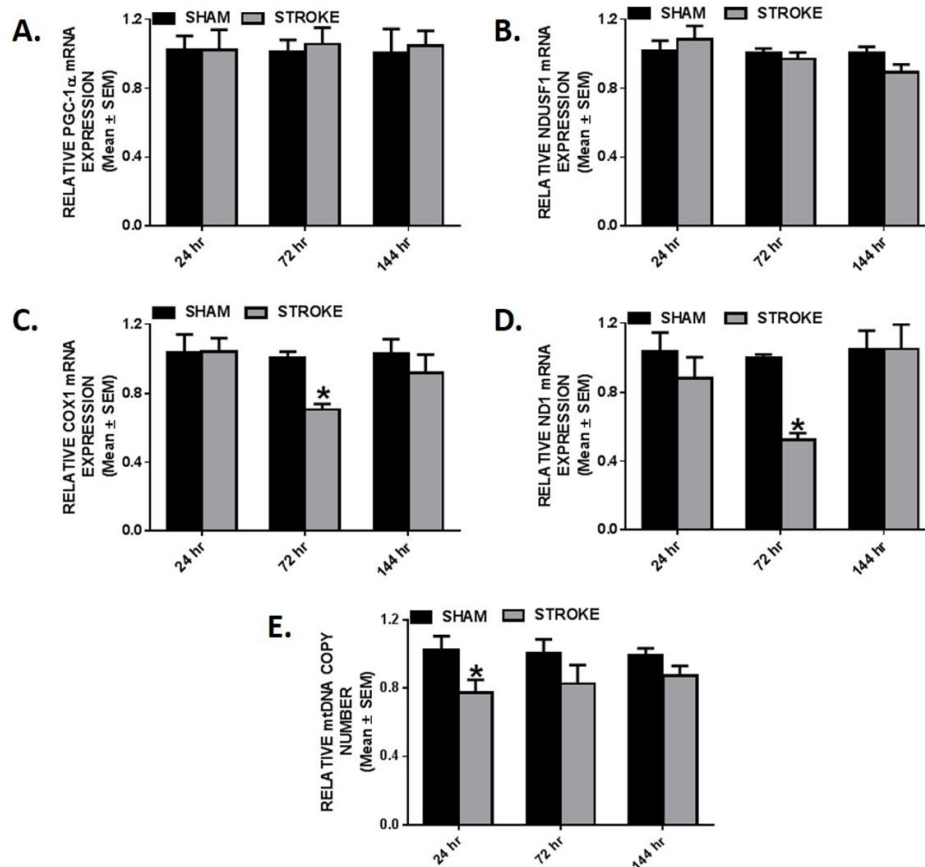


Figure 4.3. Transitory changes of mitochondrial encoded transcripts in ipsilesional striatum. PGC-1 α (a), NDUFS1 (b), COX1(c) and ND1 (d) mRNA expression was determined by qRT-PCR using tubulin as a control gene. mtDNA copy number (e) was determined by qRT-PCR, using ND1 for the mtDNA gene and β -actin for the nuclear control gene. These markers were measured in the ipsilesional striatum 24, 72, and 144 hrs. Values reported as mean \pm SEM. *p < 0.05.

Reduced mitochondrial encoded protein expression in the ipsilesional cortex and striatum.

To assess if ET-1 disrupts the translation of mitochondrial genes we also measured protein levels of COX1, ND1, and NDUFS1 at 144 hrs (**Figure 4.4**). Immunoblot analysis revealed that at 144 hrs, COX1 and ND1 were decreased compared to sham levels in the ipsilesional cortex (p<0.05). COX1 and ND1 protein expression were also decreased in the ipsilesional striatum compared to sham animals (p<0.05). NDUFS1

remained at sham control levels at this 144 hrs time point. These data reveal that in our model of cerebral ischemia mitochondrial-encoded genes are more sensitive to transcriptional/translational disruption than nuclear-encoded genes.

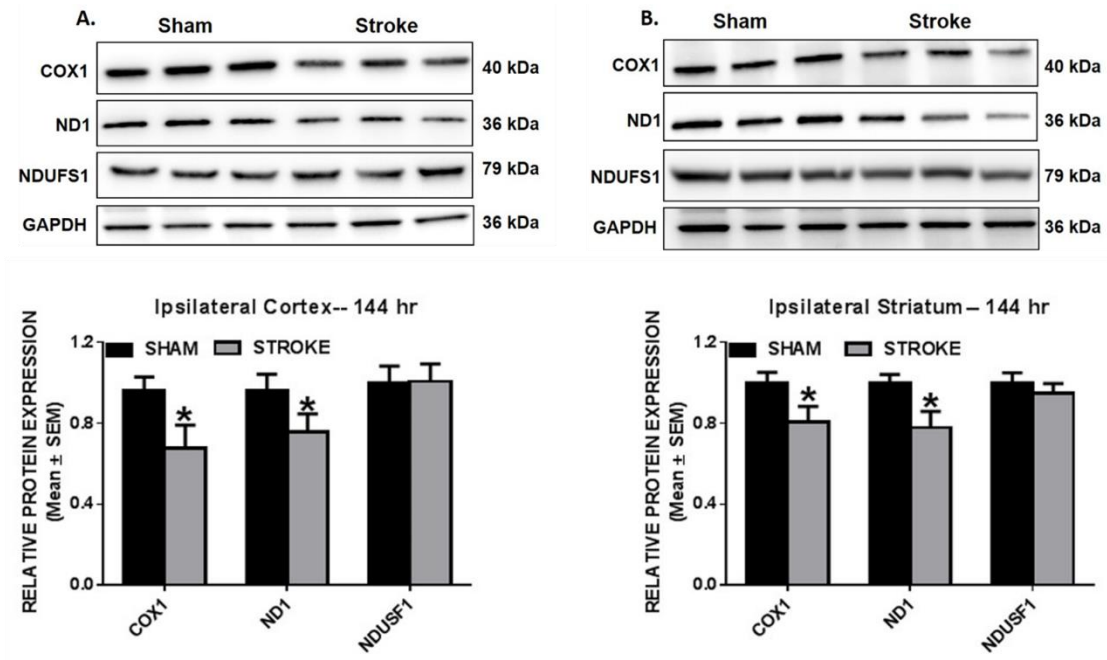


Figure 4.4. Reduced mitochondrial encoded protein expression in the ipsilesional cortex and striatum. COX1, ND1, and NDUFS1 protein expression was determined by immunoblot analysis. These markers were measured in protein isolated from ipsilesional cortex (a) and striatum (b) 144 hrs following ET-1 exposure. GAPDH is used as loading control. Values reported as mean ± SEM. *p < 0.05.

UCP2 activation in the ipsilesional cortex and striatum.

Excessive reactive oxygen species (ROS) generation can induce the up regulation of mitochondrial ROS detoxifying enzymes, manganese superoxide dismutase 2 (SOD2) and the uncoupling protein 2 (UCP2) to neutralize the detrimental effects initiated by oxidative stress. Along with its uncoupling role to mitigate ROS production, UCP2 has been implicated in neuroprotection by suppressing pro-inflammatory cytokines and elevating anti-apoptotic mediator, Bcl2 (Haines and Li 2012). Therefore, we measured SOD2 and UCP2 in ipsilesional cortex and striatum (**Figure 4.5**). Interestingly, there was only a modest decrease of SOD2 transcript at 72 hrs (p<0.05) in the cortex and SOD2 mRNA levels remained unchanged in the striatum. In contrast, cortical UCP2 transcript

levels increased within 24 hrs and further increased by 72 hrs which persisted to 144 hrs ($p < 0.05$). In the ipsilesional striatum, UCP2 increased compared to sham control at 72 hrs and remained elevated at 144 hrs ($p < 0.05$). These data reveal that ET-1 mediates sustained increases in UCP2 in cortex and striatum.

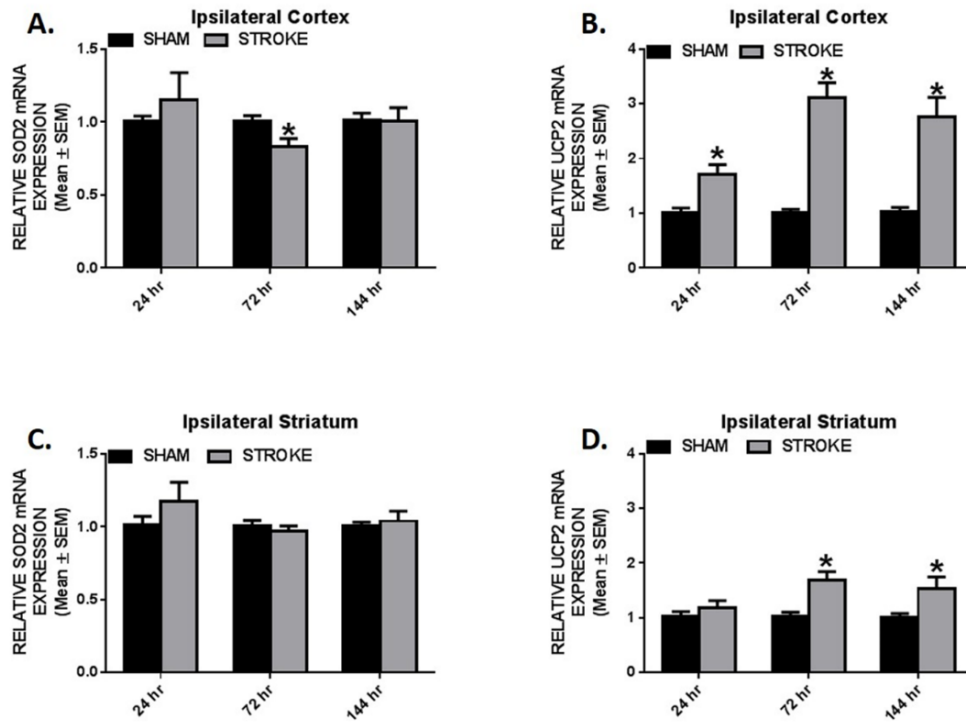


Figure 4.5. UCP2 activation in the ipsilesional cortex and striatum. Cortical (a,b) and striatal (c,d) SOD2 and UCP2 mRNA expression was determined by qRT-PCR using tubulin as a control gene. These markers were measured 24, 72, and 144 hrs following ET-1 exposure. Values reported as mean ± SEM. * $p < 0.05$.

Gene expression of inflammatory mediators and macrophages in the ipsilesional cortex and striatum.

Since macrophages are known to be involved in innate immune response following ischemic injury (Jin, Yang et al. 2010), we examined the transcriptional expression of F4/80, a surface marker for mature macrophages (**Figure 4.6**). We observed an increase in cortical F4/80 mRNA expression over sham animals at 72 and 144 hrs. Additionally, we observed significant increases in cortical interleukin-6 (IL-6) transcripts at 24, 72, and 144 hrs. There was a transitory increase in F4/80 at 72 hrs that returned to sham levels by 144

hrs in the striatum. IL-6 induced an increase at 24 hrs and remained elevated at 72 hrs in the striatum. Our data demonstrate that mitochondrial changes are occurring in peri-infarct tissue that is undergoing inflammatory responses over the 144 hrs examined. The pro-inflammatory environment in both the sensorimotor cortex and striatum further demonstrate continued stroke induced pathology in connected brain regions outside the primary stroke region and likely contribute mitochondria disruption.

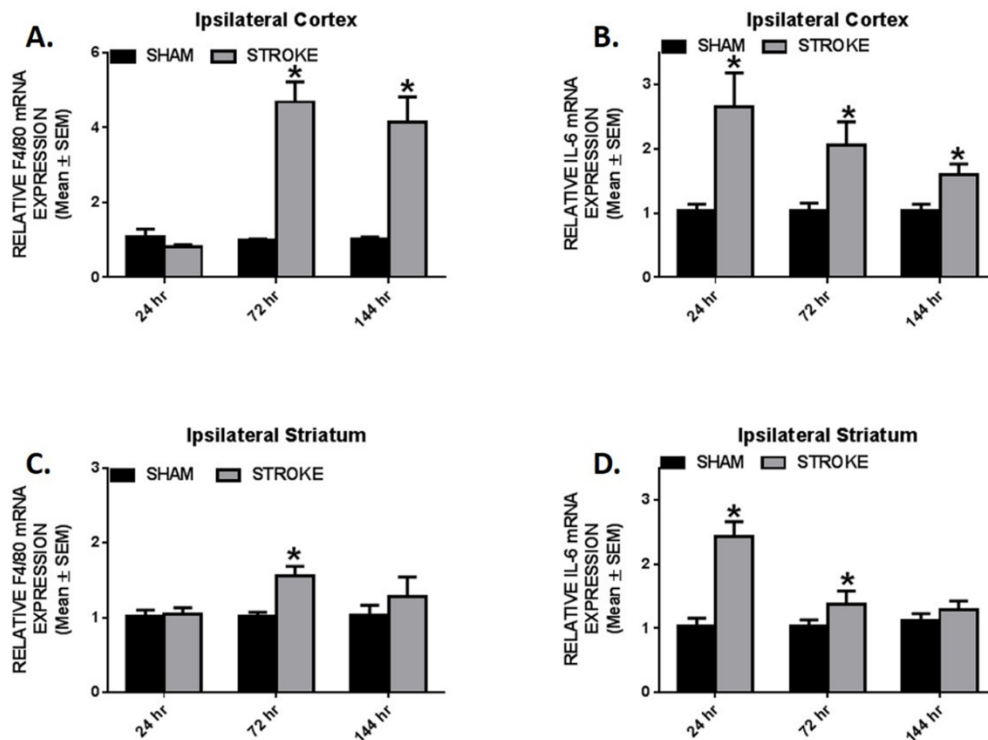


Figure 4.6. Gene expression of inflammatory mediators and macrophages in the ipsilesional cortex and striatum. Cortical (a,b) and striatal (c,d) F4/80 and IL6 mRNA expression was determined by qRT-PCR using tubulin as a control gene. These markers were measured 24, 72, and 144 hrs following ET-1 exposure. Values reported as mean ± SEM. *p < 0.05.

Caspase 3 cleavage and GAP43 expression in ipsilateral cortex and striatum.

Rodent models of neurodegenerative diseases implicate caspase dependent apoptosis as an important contributor to neuronal and tissue damage (Chen, Ona et al. 2000, Li, Ona et al. 2000, Ferrer, Friguls et al. 2003, Louneva, Cohen et al. 2008). Immunoblot analysis was used to assess the level of caspase 3 activation by measuring the cleaved form of caspase 3 following ET-1 induced stroke (**Figure 4.7**). Cleaved

caspace 3 was detected in the ipsilateral cortex, but not in the ipsilateral striatum 144 hrs following stroke. These data demonstrate that there is a range of pathological effects on brain regions neuronally connected to the primary site of stroke and that direct cell death, indicated by increased activation of cleaved caspase 3, may be the consequence of mitochondria disruption.

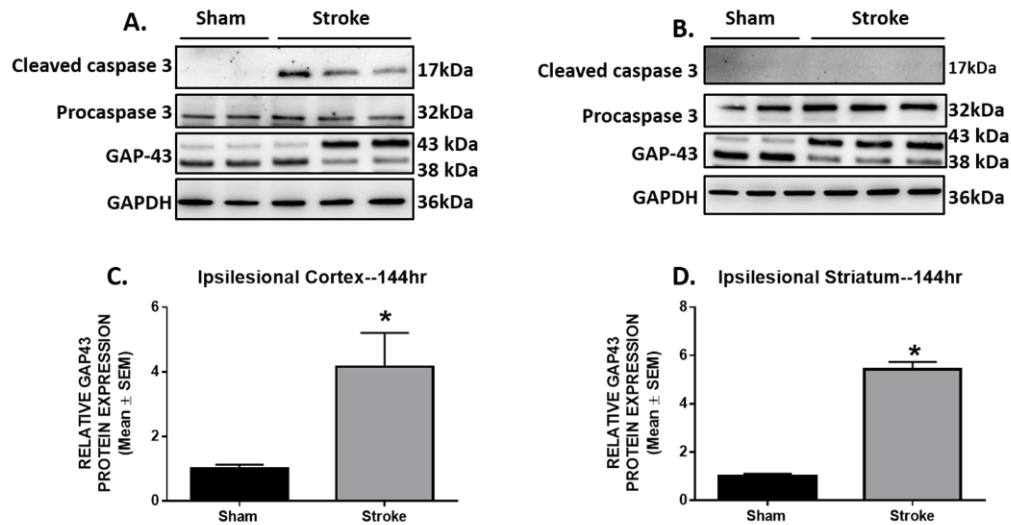


Figure 4.7. Caspase 3 cleavage and GAP43 expression in ipsilateral cortex and striatum. Cleaved caspase 3, procaspase 3, and GAP-43 protein expression was determined by immunoblot analysis. Protein was isolated from ipsilesional cortex (a) and striatum (b) 144 hrs post- injury. Cortical (c) and striatal (d) GAP-43 protein expression was quantified. GAPDH was used as loading control. Values reported as mean ± SEM. *p < 0.05.

Sensorimotor cortex and striatum are key areas that undergo neural regrowth and reorganization after following motor cortical damage (Carmichael and Chesselet 2002, Jones In Press). We measured axonal regeneration and outgrowth of growth-associated protein 43 (GAP-43). GAP-43 increases during periods of axonal sprouting and within the first week post-stroke in areas surrounding the primary site of injury (Stroemer, Kent et al. 1995, Benowitz and Carmichael 2010). In line with previous reports, we observed an increase in GAP-43 protein expression in the ipsilesional cortex at 144 hrs (**Figure 4.7**). We also detected an increase in the striatum at 144 hrs post-stroke. These data reveal that sufficient cell injury occurs in the early stages post-stroke to activate regenerative

processes and that this process occurs when mitochondria homeostasis is still disrupted in both striatum and cortex.

Study 2: Mitochondria Homeostasis Following Formoterol Treatment

Behavioral impairment post-stroke and formoterol treatment.

All animals that underwent an ET-1 induced ischemic lesion showed greater impairment on day 1, 3 and 6 post-stroke compared to pre-operative levels. There was not a significant difference in the percentage of errors performed between animals that received vehicle or formoterol at any time point post-stroke. Through slow-video replay exact forelimb placements can be scored on a scale from 0 (total miss) to 6 (correct placement). When examining correct (6's) and slightly incorrect placements (5's), there was a difference between vehicle and formoterol treated animals. Animals that received formoterol had significantly more 5's than vehicle animals and significantly less 6's. These results may indicate that formoterol treatment improves the use of better compensatory paw placement or poor placement adjustments.

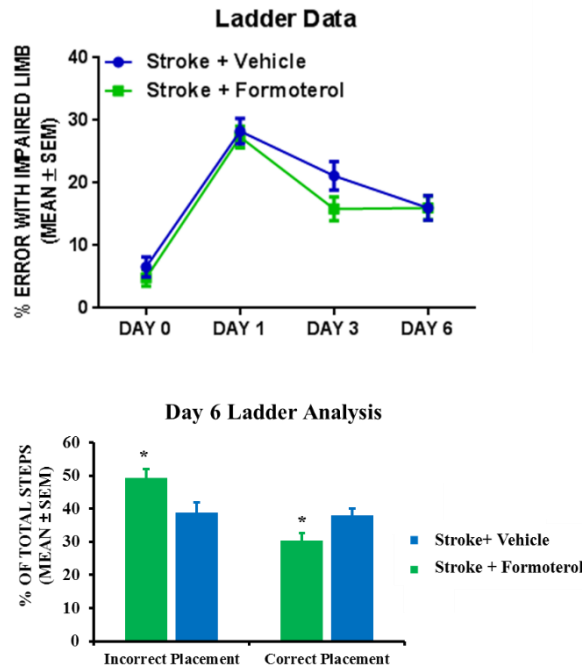


Figure 4.8. Behavioral Performance after Formoterol Treatment. A. There was not a significant difference in errors between animals given vehicle or formoterol. B. Animals given formoterol had more incorrect placements and less correct placements. Values are mean \pm SEM. * $p < 0.05$.

Partial recovery of respiratory chain gene expression in ipsilesional motor and sensory cortex.

In *study 1*, we demonstrated a decrease in respiratory chain gene expression in ND1, COX1, and NDUFS1. We replicated these results in our stroke+vehicle animals. Animals that received formoterol still showed a reduction of ND1 transcript levels at 72 hrs, however show a partial recovery at 144 hrs by no longer being significantly decreased from sham animals. COX1 mRNA expression in formoterol animals was not significantly different from sham animals at 72 hrs or 144 hrs, however was not significantly increased from stroke+vehicle animals. Finally, NDUSF1 transcript levels were no longer significantly different at 72 hrs in formoterol animals compared to sham animals. The modest decrease seen in NDUSF1 at 72 hrs in the stroke+vehicle animals has recovered by 144hrs. Taken together, these findings support that formoterol has a modest effect at the primary site of injury, the motor and sensory cortex, following stroke.

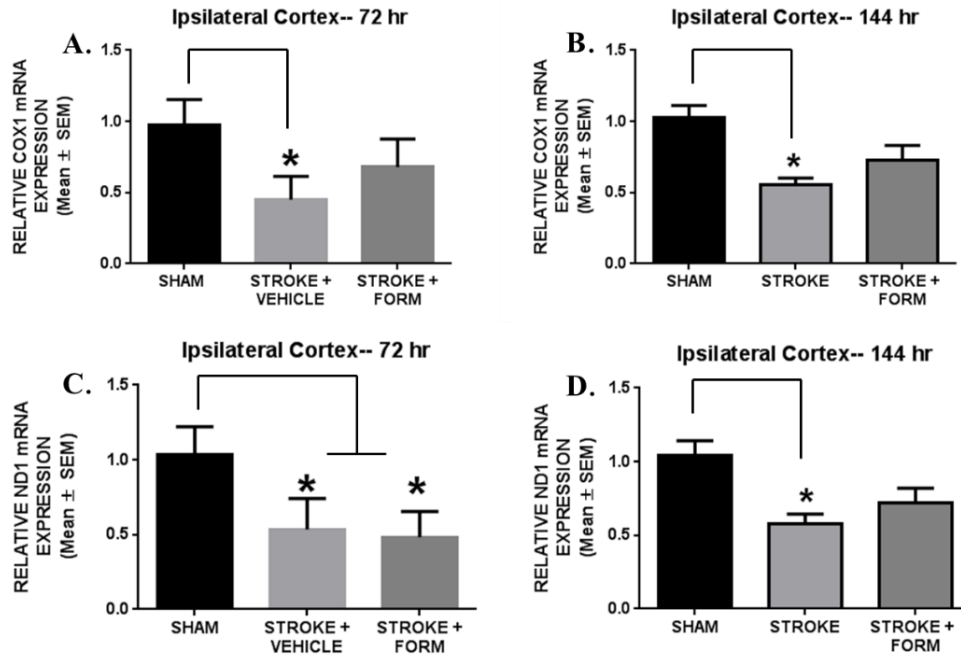


Figure 4.9. Ipsilateral motor and sensory cortex markers following formoterol treatment. COX1 (a. and b.) and ND1 (c. and d.) were examined at 72 hrs and 144 hrs after stroke. Animals were given vehicle or 0.1mg/kg of formoterol starting at 24 hrs post-stroke. Values are means \pm SEM. *p < 0.05.

Recovery of mitochondrial encoded transcripts in ipsilesional striatum.

We examined mitochondria transcripts in the ipsilesional striatum after stroke because secondary injury occurs in this area (Carmichael and Chesselet 2002). Since there was not a change in NDUSF1 in the stroke+vehicle animals compared to shams, we also did not detect a change in the stroke+formoterol animals compared to sham animals. In stroke+vehicle animals, there was a transitory decrease in COX1 and ND1 transcript levels that recovers at 144 hrs. Animals that were treated with formoterol showed a significant increase in both COX1 and ND1 mRNA levels compared to stroke+vehicle back to sham control levels at 72 hrs. These results show that formoterol promotes recovery of mitochondria homeostasis transcript levels early in the striatum, the secondary site of injury. This rescue of mitochondria encoded electron transport chain transcripts could aid in functional recovery post-stroke.

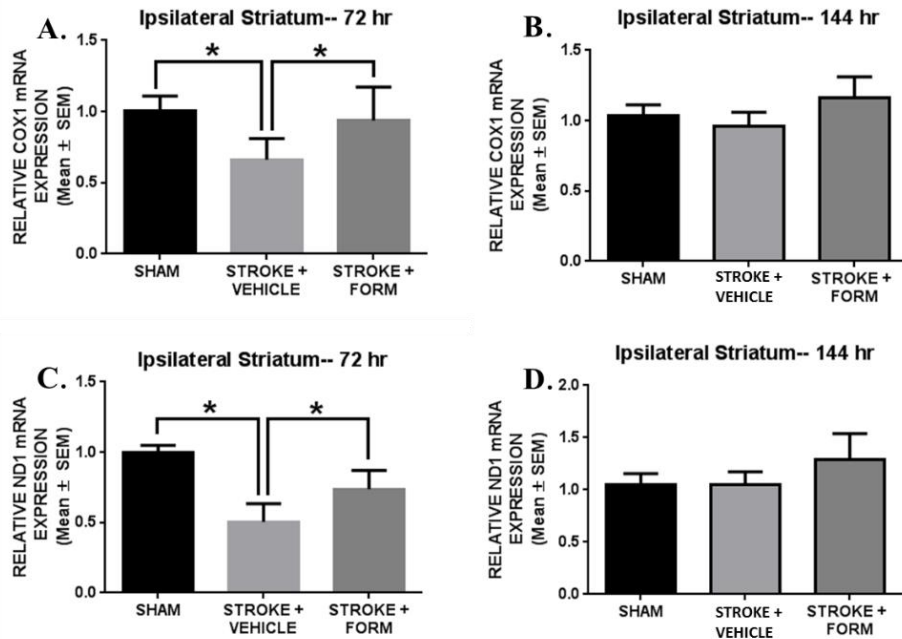


Figure 4.10. Ipsilateral striatum markers following formoterol treatment. COX1 (a. and b.) and ND1 (c. and d.) were examined at 72 hrs and 144 hrs after stroke. Animals given formoterol had increased COX1 (a.) and ND1 (c.) back to sham levels and significantly increased from vehicle animals at 72hrs. Values are means ± SEM. *p < 0.05.

Mitochondrial encoded protein expression in the ipsilesional cortex and striatum reflects transcript levels.

To assess if formoterol effects the translation of mitochondrial genes we measured protein levels of COX1, ND1, and NDUFS1 at 72 hrs and 144 hrs. Immunoblot analysis at 72 hrs and 144 hrs showed no change in NDUSF1 compared to sham animals in vehicle and formoterol animals. At 72 hrs and 144 hrs post-stroke in the motor and sensory cortex, COX1 and ND1 protein levels were significantly decreased in both vehicle and formoterol animals compared to sham animals. Formoterol treatment did not affect mitochondria protein levels in the cortex, the primary site of injury. In the striatum, formoterol treatment rescued both COX1 and ND1 protein levels at 72 hrs; animals were no longer significantly decreased compared to sham animals and were significantly increased compared to

vehicle animals. At 144 hrs post-stroke formoterol treatment also rescued COX1 protein levels in the striatum. However, formoterol treated animals show a significant decrease in ND1 protein level compared to sham animals at 144 hrs. Taken together, protein expression in the cortex and striatum reflect mRNA levels at 72 and 144 hrs.

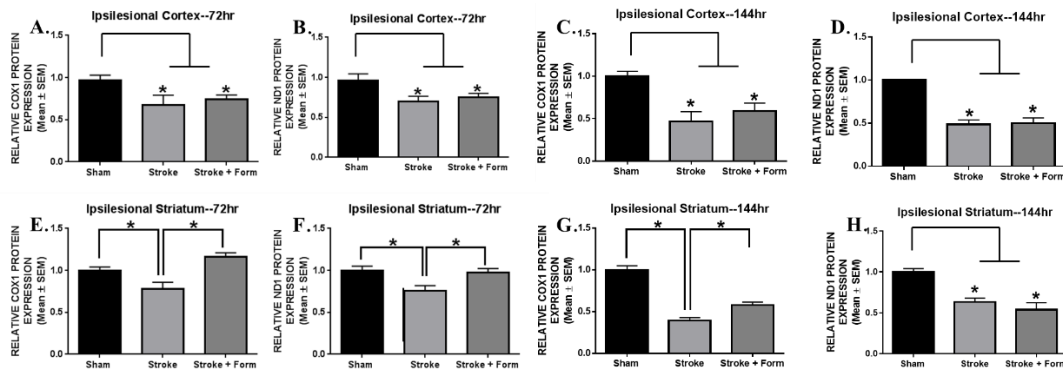


Figure 4.11. Protein Expression Acutely After Formoterol Treatment. There was no change in COX1 or ND1 protein levels in the cortex following formoterol treatment (a-d). Protein levels reflect mRNA expression changes in the striatum after formoterol treatment (e-h). Values are means \pm SEM. * $p < 0.05$.

UCP2 transcript levels in the ipsilesional cortex and striatum following formoterol treatment.

Mitochondria ROS detoxifying enzyme, UCP2, is used to neutralize the detrimental effects initiated by oxidative stress. UCP2 may also be neuroprotective (Haines and Li 2012). Animals that were given formoterol after stroke saw no change in UCP2 levels at 144 hrs compared to stroke+vehicle animals in the cortex or striatum (**Figure 4.12**). All animals with a stroke had significantly higher levels compared to sham animals.

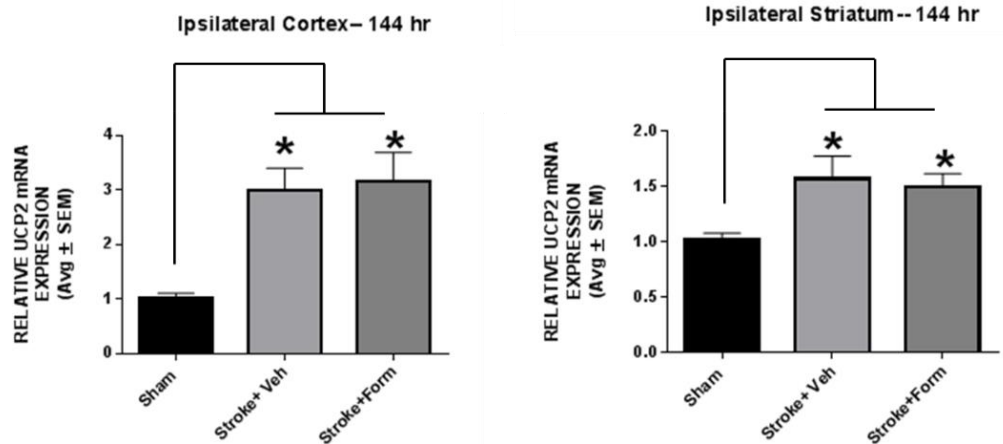


Figure 4.12. UCP2 transcript levels following formoterol treatment. At 144 hrs, there was no change in UCP2 in animals given formoterol. Values are means ± SEM. * $p < 0.05$.

Gene expression of inflammatory mediators and macrophages in the ipsilesional cortex and striatum.

Formoterol, in asthma and COPD models, was shown to have an anti-inflammatory effect (Whelan, Johnson et al. 1993, Bathoorn, Liesker et al. 2008). Since macrophages are known to be involved in innate immune response following ischemic injury (Jin, Yang et al. 2010), we examined the transcriptional expression of F4/80, a surface marker for mature macrophages after formoterol treatment. In the cortex, there was an increase in F4/80 in stroke+vehicle animals compared to sham animals. There was a partial recovery of F4/80 in animals treated with formoterol, whereas they were no longer different from sham controls. F4/80 levels in the striatum had returned to sham levels by 144 hrs in all stroke animals. Interleukin-6 (IL-6) showed a similar trend by returning to sham levels in the striatum by 144 hrs. Animals given formoterol showed a partial reduction in IL-6 in the cortex at 144 hrs to a level no different from sham animals. Formoterol is able to effect the pro-inflammatory environment following ET-1 lesions in the SMC.

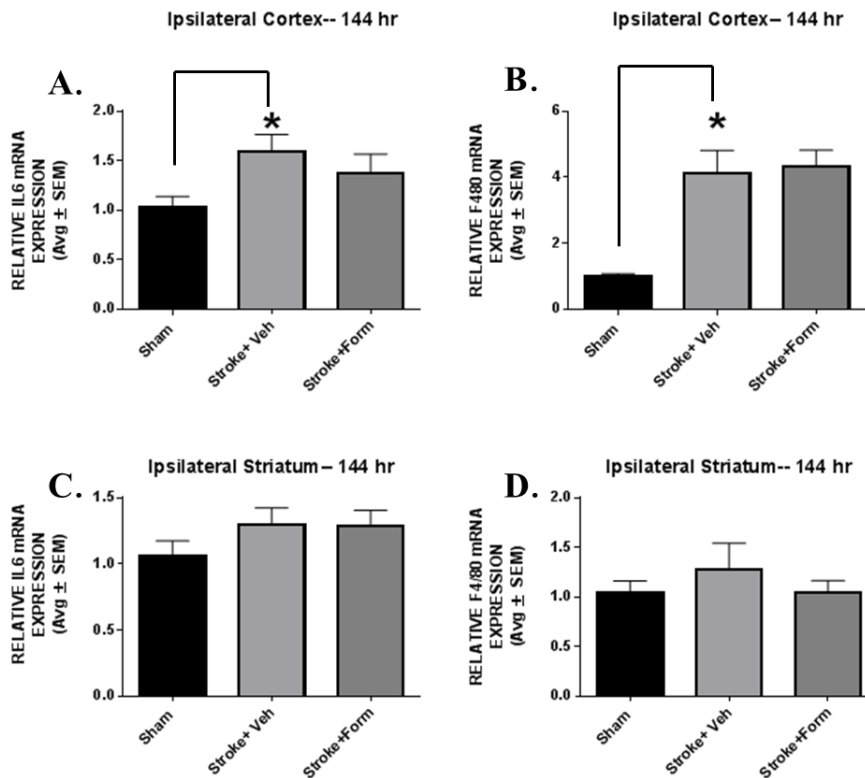


Figure 4.13. IL-6 and F4/80 transcript levels following formoterol treatment. At 144 hrs, both IL-6 and F4/80 show partial recovery in the cortex. There is no significant increase in stroke animals at 144 hrs in the striatum. Values are means \pm SEM. * $p < 0.05$.

Caspase 3 cleavage and GAP43 expression in ipsilateral cortex and striatum following formoterol treatment.

Protein expression analysis showed cleaved caspase 3 activation in all animals that had a stroke in the ipsilateral cortex and not the striatum. Animals treated with formoterol did not have a different level of caspase 3 cleavage than vehicle treated animals. All animals showed an increase in caspase 3 cleavage out to 144 hrs after stroke.

Growth-associated protein 43 (GAP-43) increases within the first week post-stroke surrounding the primary site of injury in areas of axonal sprouting (Carmichael, Archibeque et al. 2005). All animals that had an ET-1 stroke showed an increase in GAP-43 in the

cortex and not in the striatum. Formoterol treatment did not change the level of GAP-43 protein in either the cortex or striatum. It is important to note that there was a less robust increase in GAP-43 in the cortex in animals that had a stroke in this set of studies. Also, in *study 1* there was a very significant increase in GAP-43 in the striatum at 144 hrs; however, in *study 2* we do not. This may indicate that stroke-induced increases of GAP-43 were delayed in *study 2*, due to lesion progression and size.

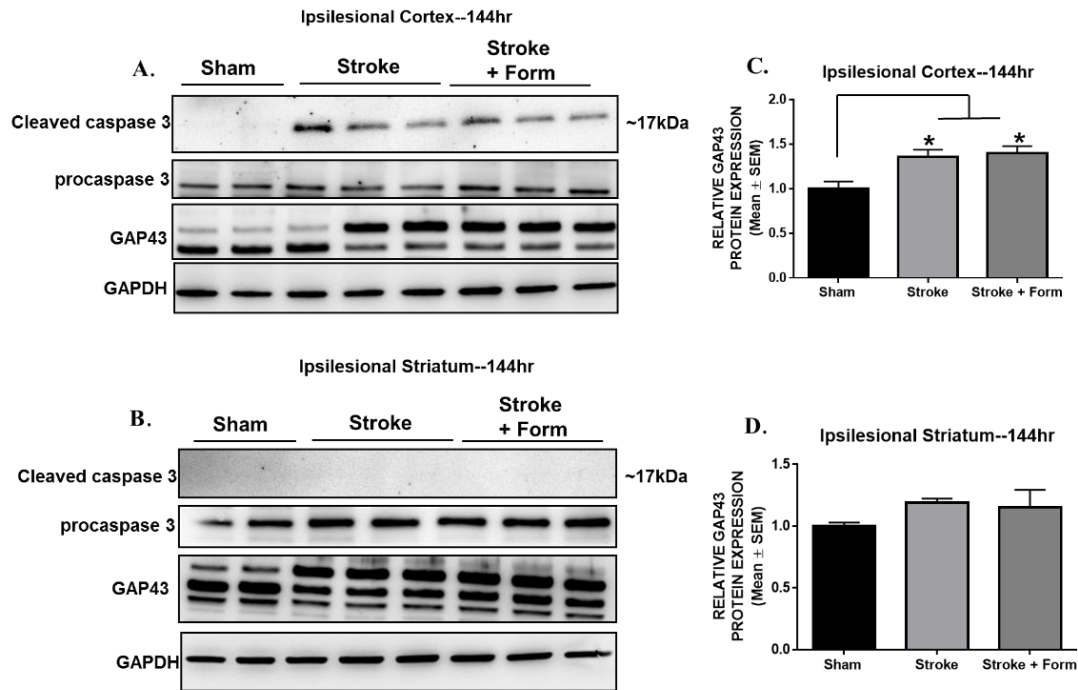


Figure 4.14. Cleaved caspase 3 and GAP-43 expression after formoterol treatment. At 144 hrs, all animals who had a stroke showed cleaved caspase 3 levels in the cortex and not the striatum. GAP-43 levels are increased in the cortex in stroke animals and there is no change from shams in the striatum. Values are means ± SEM. * $p < 0.05$.

Study 3: Formoterol Enhances Motor Recovery Following Stroke and Rehabilitative Training

Formoterol Enhanced Behavioral Recovery.

Animals were treated with three different doses (0.1mg/kg, 0.5mg/kg, or 1.0mg/kg) of formoterol or vehicle starting 24 hrs after injury and underwent 15 days of either rehabilitation training (RT) or control behaviors (No-RT). All animals that were given RT significantly improved after 15 days than animals that did not have RT ($p < 0.001$). There

were no behavioral differences between No-RT animals that received different formoterol doses. Animals in the 0.5mg/kg+RT ($F_{16}=0.726$, $p=0.766$) and 1.0mg/kg+RT ($F_{16}=0.841$, $p=0.638$) groups were not significantly differently from vehicle+RT animals (**Figures 4.15 and 4.16**). However, animals given 0.1mg/kg+RT significantly improved over time compared to vehicle+RT animals ($F_{16}=1.965$, $p=0.016$). Specifically on rehabilitation days 3 ($p=0.042$), 4 ($p=0.002$), 6 ($p=0.014$), 9 ($p=0.007$), and 12 ($p=0.008$) 0.1mg/kg+RT animals performed the SPR task significantly better than vehicle+RT (**Figure 4.17**).

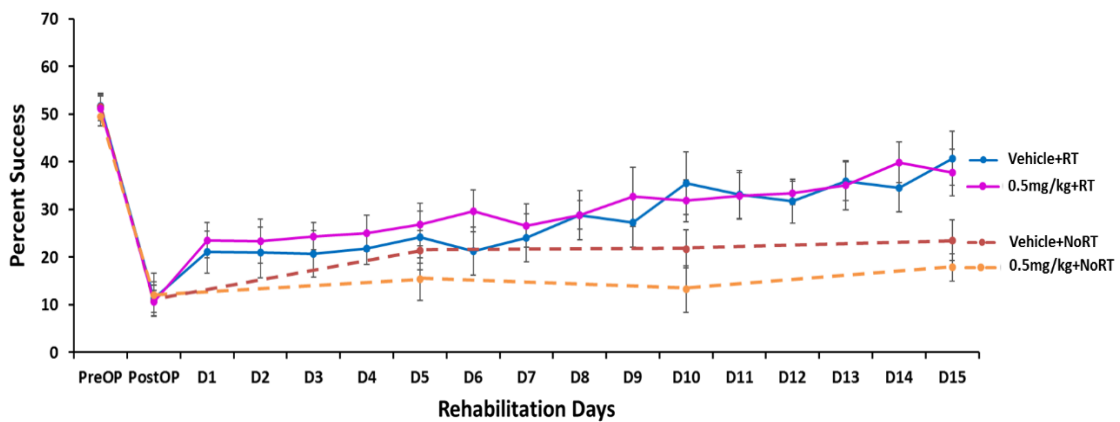


Figure 4.15. 0.5mg/kg formoterol and RT was not different from vehicle. Animals that received formoterol (0.5mg/kg) were no different than animals that received vehicle. Both groups that underwent RT showed better improvement than No-RT animals. Values are means \pm SEM.

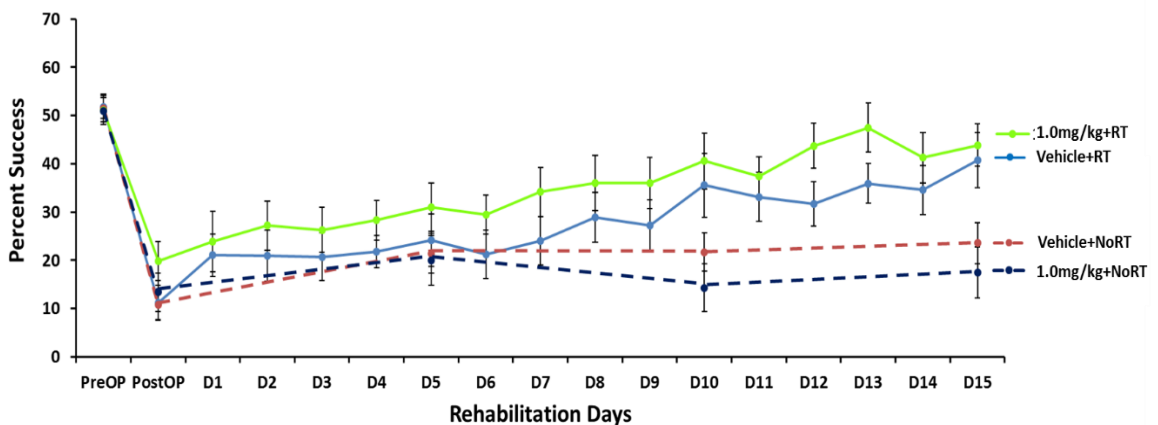


Figure 4.16. 1.0mg/kg formoterol and RT was not different from vehicle. Animals that received formoterol (1.0mg/kg) were no different than animals that received vehicle. Both groups that underwent RT showed better improvement than No-RT animals. Values are means \pm SEM.

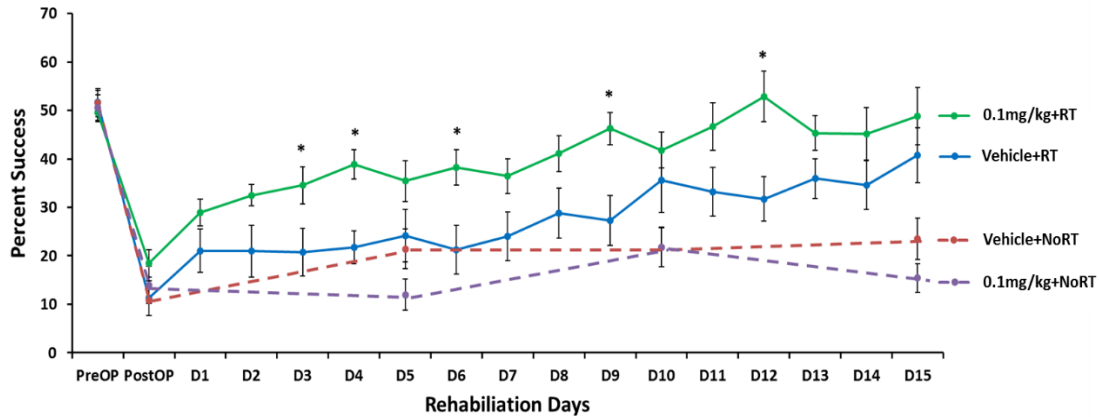


Figure 4.17. 0.1mg/kg formoterol and RT was most effective to enhance motor recovery.

Animals that received formoterol (0.1mg/kg) did significantly better on the SPR task than animals that received vehicle. Both groups that underwent RT showed better improvement than No-RT animals. Values are means \pm SEM. *p < 0.05.

Density of Dendritic Processes after Formoterol Treatment.

Formoterol promotes changes in dendritic complexity in a down syndrome model (Dang, Medina et al. 2014). Since there was a behavioral difference between animals that received 0.1mg/kg+RT compared to vehicle+RT animals, we attempted to determine dendritic density changes between these two groups of animals by using stereological processes. In previous studies, animals that have undergone RT show an increase in dendritic density compared to untrained animals (Jones, Chu et al. 1999). Increases in dendritic density is one example of enhanced neuroplasticity following RT that contributes to enhanced behavioral performance. There was not a difference in dendritic surface density between vehicle+RT and 0.1mg/kg+RT animals. However, this immunohistochemical technique might not have been the best way to capture changes in dendritic complexity changes following formoterol treatment. On the other hand, in our model formoterol may not be changing dendritic complexity and possibility acting through a different mechanism to enhance motor recovery compared to vehicle animals.

Formoterol as a Neuroprotectant.

Previous research has suggested that β_2 -adrenergic receptor agonists can act as a neuroprotectant in a focal ischemia model (Junker, Becker et al. 2002). It has not been

examined whether formoterol effects lesion size when given after the injury has occurred. Our goal was to examine whether formoterol reduced lesion size. We quantified lesion size between the 0.1mg/kg+RT and vehicle+RT groups. Using a point counting method explained above, we determined there was not a difference in lesion size between the two groups. In our hands, formoterol does not change lesion size and is therefore likely acting along another mechanism to enhance motor recovery when administered 24h after stroke. These results are in agreement with the cleaved caspase 3 levels in vehicle and formoterol treated animals explored in *study 2*. We were able to show no difference in caspase 3 levels between drug and vehicle treated animals and therefore would expect no change in lesion size between the two groups.

Discussion

Several studies have demonstrated that mitochondrial dysfunction is a common consequence of cerebral ischemia (Anderson and Sims 1999, Sims and Anderson 2002, Hoppins 2014). Disrupted mitochondrial homeostasis has been linked to detrimental pathways such as ROS production, calcium dysregulation, inflammation, and intrinsic apoptotic cell death (Sciamanna, Zinkel et al. 1992, Dirnagl, Iadecola et al. 1999, Chan 2005, Sims and Mwyderman 2010). These complex pathophysiological pathways have been intimately described following ischemic stroke and it is hypothesized that mitochondria are crucial initiators and targets of these diverse inflammatory and aberrant metabolic pathways. In addition, it is possible but, untested, that mitochondrial dysfunction may be related to a reduction in neuronal function, altering sensory and behavioral outcomes following stroke. Many of these effects occur immediately post-injury; therefore, elucidation of the pathways and key proteins linked to mitochondrial dysfunction following insult and over time may provide targets for pharmacological intervention.

The results of *study 1* demonstrated mitochondrial disruption, activation of inflammatory pathways, cell death and initiation of regenerative pathways within the first week of ischemic stroke in a focal ET-1 induced rat stroke model. In the cortex, there was decreased mRNA and protein expression of nuclear and mitochondrial encoded subunits of complex I and IV as well as depletion of mitochondrial DNA number. Concomitantly, mitochondrial DNA copy number was suppressed early and persistently in the ipsilesional cortex following ischemia. There was only reduced protein expression in mitochondrial-encoded proteins which may be due to the increased sensitivity of mtDNA damage compared to nuclear DNA. Following ischemic injury, chronic ROS production causes extensive mtDNA damage and the inability to monitor and repair mtDNA damage is due to the less efficient mitochondrial DNA repair mechanisms that become overwhelmed in the presence of excessive oxidative stress (Yakes and Van Houten 1997). It is expected that mtDNA damage may lead to inactive electron transport chain activity, thereby affecting normal mitochondrial function.

As demonstrated in *study 2*, formoterol treatment had minimal effects on restoring mitochondria function and reducing inflammatory activation during the first week post-stroke in the primary site of injury, the cortex, which was unexpected. In mitochondrial encoded subunits of complex I and IV of the electron transport chain and inflammatory markers, there was a partial rescue of function. In an earlier study by our lab, naïve animals given formoterol did not show an increase in PGC-1 α or mitochondria copy number in the cortex, but did show an increase in both markers in the striatum. We hypothesized that no change in the cortex could be due to a ceiling effect and once injury had occurred, formoterol would increase these factors in the cortex. Our data indicates a biogenetic effect in the striatum in naïve animals and following stroke. The minimal effects seen in the cortex are not because formoterol is not crossing the blood brain barrier or

unable to promote MB. In previous studies formoterol induced MB following ischemia in the kidney, therefore drug treatment has shown MB in other disease models. Additionally, studies have shown that β_2 -adrenergic receptors are located within the cerebral cortex (Nicholas, Pieribone et al. 1993). Even though we saw dramatic mitochondria dysfunction in the cortex, we did not detect MB in the cortex following ischemic stroke of the SMC.

Study 1 identified mitochondrial deficits in the secondary site of injury, the striatum. There was decreased striatal mitochondrial content, as measured by mtDNA copy number, mtDNA transcripts and protein. Acute and transient reduction of mitochondrial DNA and mRNA expression of ND1 and COX1 in the striatum were seen. While the biochemical and cellular mechanisms that comprise secondary injury are not entirely understood, we hypothesize that the disturbance in mitochondrial DNA and gene regulation is based on the functional connectivity between the cortex and striatum. The striatal changes are transient, with mtDNA and mitochondrial RNA changes recovering to control levels by 72 hrs and 144 hrs, respectively, suggesting the damage to the striatum is less severe compared to the primary site of injury and is recoverable. Future investigation into the role of cellular stress responses and the dynamic interplay of multiple pathophysiological cascades in secondary injury, that go beyond both the initial ischemic insult and the disruption of cerebral circulation are needed (Veenith, Goon et al. 2009).

Although the striatum revealed transient decreases formoterol was able to accelerate recovery of mitochondria homeostasis proteins back to control levels by 72 hrs post stroke. Formoterol promoted MB and recovery in the striatum, which was less severely damaged, demonstrated by the lack of cell death pathway, measured by cleaved caspase 3 protein levels. Therefore, these data suggest that formoterol might be most effective with mild injuries under the same dosing and administration timing examined since formoterol is effective in the striatum, which is a secondary location of injury.

Formoterol is likely inducing reparative processes in the striatum shown by recovery of mitochondrial homeostasis proteins. Other reparative processes that promote functional recovery after stroke have been seen acutely in the striatum. For example, axon sprouting in the striatum begins 2-3 days after cortical stroke leading to new cortical-striatum synaptic connections and increases in multiple synaptic boutons within the striatum (McNeill, Brown et al. 2003).

It is important to note that although in *study 1* there was not a significant decrease in PGC-1 α mRNA expression in either the cortex or striatum, we hypothesize that the PGC-1 α transcript levels are reduced abruptly following injury and recover rapidly to control levels to regulate compensatory mechanisms such as antioxidant production. Under normal physiological conditions, mitochondrial respiratory complexes are a source of ROS generation (Bayir and Kagan 2008). When respiratory enzymes are damaged following injury, these complexes produce an excessive amount of ROS which can lead to protein, lipid, and DNA damage, subsequently contributing to mitochondrial damage and dysfunction. Therefore, mRNA level of the mitochondrial antioxidant gene, SOD2 as a marker of oxidative stress was assessed. Surprisingly, we only observed a decrease in SOD2 transcript at 72 hrs post-stroke in the cortex, which recovered to sham control levels by 144 hrs and SOD2 mRNA levels remained unchanged in the striatum. Numerous studies have reported SOD2 is a direct downstream target of PGC-1 α (Marmolino, Manto et al. 2010, Xiong, MacColl Garfinkel et al. 2015); therefore, we predict that SOD2 mRNA levels transiently decreased in response to the modest suppression of PGC-1 α in the cortex at 24 hrs.

Recently, an increasing number of studies have focused on the various physiological and pathological roles of UCP2 (Brand and Esteves 2005, Chen, Wu et al. 2006, Dietrich, Andrews et al. 2008, Wojtczak, Lebedzinska et al. 2011), which has been

described to have a role in mediating lipid peroxidation within the mitochondrial matrix due to ROS formation. When UCP2 detects elevated levels of mitochondrial ROS, a feedback loop is activated to induce UCP2 expression in the inner mitochondrial membrane (Dietrich, Andrews et al. 2008). It is well documented that the primary role of UCP2 is to dissipate the proton gradient across the inner membrane to prevent ATP synthesis and transport superoxide radicals across the inner mitochondrial membrane, thus decreasing the effect of ROS produced by the respiratory chain (Brand and Esteves 2005). Interestingly, UCP2 mRNA expression was persistently increased in both the ispilesional cortex and striatum in *study one*. Formoterol treatment did not change the increase in UCP2 in the cortex or striatum at 144 hrs post-stroke. Several reports have demonstrated that β -adrenergic receptors activate UCP2 in other disease states (Pearen, Ryall et al. 2009), however this has yet to be examined in a stroke model until these studies. UCP2 has also been reported to perform other functions such as regulating neuroinflammation and apoptosis following ischemic stroke. *Haines, et al.*, demonstrated that the overexpression of UCP2 alleviated the ischemia-induced increase in IL-6 mRNA which may reduce the deleterious effects of prolonged inflammation. Overexpression of UCP2 also rescued diminished pro-survival markers such as Bcl-2, cyclin G2, and HSP90 (Haines and Li 2012). Furthermore, UCP2 has been documented to be neuroprotective via its involvement in neurogenesis and synaptogenesis, suggesting a role in neuronal growth and development (Dietrich, Andrews et al. 2008, Simon-Areces, Dietrich et al. 2012). Future studies are needed to explore the potential roles of UCP2 in our cerebral ischemic model.

Consistent with cortical mitochondrial deficits, the presence of neuroinflammation during the first days of experimental stroke was confirmed by the elevated mRNA expression of macrophage marker, F4/80 and inflammatory mediator cytokine, IL-6.

Interestingly, cortical IL-6 transcript levels were induced earlier than F4/80, with a 3-fold increase in expression that remained persistently elevated above sham control levels. Furthermore, the maximal expression of F4/80 and IL-6 in the cortex corresponds to the maximal expression of both transcripts in the striatum, suggesting that neuroinflammation may have a greater role in development of secondary damage post-stroke than previously anticipated. Elevated macrophage and cytokine markers, suggest that cortical and striatal compensatory pathways are insufficient to blunt neuroinflammatory responses following ischemic stroke. This may be due to the potentiation of the activation of cellular injury cascade by prolonged mitochondrial dysregulation in the cortex. Together, these findings support the implication that ischemic injury causes detrimental effects in surrounding tissue days after the initial stroke; therefore treatment with formoterol should improve these neuroinflammatory responses.

In the cortex, there was a minimal recovery of IL-6 and F4/80 transcripts after formoterol treatment. By 144 hrs post-stroke, there was no longer an increase of transcripts in the striatum and no effect of formoterol. Formoterol is FDA approved to treat asthma and COPD, therefore there has been extensive work examining the effect of formoterol on inflammation. Reports have shown that giving formoterol alone, instead of in combination with a steroid, has no effect on IL-6 levels in the cardiovascular system (Suda, Tsuruta et al. 2011). In the cortex and hippocampus, formoterol was shown to increase other cytokines that are anti-inflammatory (McNamee, Ryan et al. 2010), however pro-inflammatory cytokines such as IL-6 were not examined in these studies. Although, an extensive number of groups have examined cytokine expression after formoterol treatment, very little work has been done to examine formoterol's interaction with macrophage expression which are innate immune cells. One group was able to show that IL-6 is linked with macrophage activation (Fernando, Reyes et al. 2014), which

may be why we saw the same effect in both IL-6 and F4/80 transcript levels after formoterol treatment. A few reports have attempted to understand how formoterol interacts with microglia in the brain (Qian, Wu et al. 2011).

Cell death in peri-infarct cortex is, in part, a consequence of mitochondrial dysfunction as evidenced by caspase 3 cleavage in the cortex. One of the most common forms of cell death in neurodegeneration is through the intrinsic mitochondrial apoptotic pathway. Following initiation of the intrinsic pathway, cytochrome c is released from the mitochondria and works with other apoptotic factors to process the inactive form of procaspase 3 to the cleaved, active form (Vila and Przedborski 2003). Cleaved caspase 3 in turn induces cellular changes including chromatin condensation, DNA fragmentation, and formation of apoptotic bodies, leading finally to cell death (Hengartner 2000, Galluzzi, Morselli et al. 2009). These studies revealed that cerebral ischemia induced caspase 3 cleavage in the peri-infarct region of ipsilateral cortex 144 hrs post-stroke, in concert with increases in GAP-43 in both cortex and striatum. GAP-43 is associated with neurite outgrowth, axon growth cone formation and axonal sprouting post -injury and may play an important role in experience-dependent plasticity (Benowitz and Routtenberg 1997, Carmichael 2016). After onset of stroke, one of the most prominent regenerative events is axonal sprouting in the penumbra, which is accompanied by expression of GAP- 43 (Goto, Yamada et al. 1994, Carmichael, Archibeque et al. 2005). Additionally, GAP-43 is a recently discovered postsynaptic substrate of caspase 3 and caspase 3 has also been demonstrated to be involved in the formation of new synaptic contacts; therefore, it has been hypothesized that caspase 3 and GAP- 43 are part of a common molecular pathway involved in tissue response after stroke (Han, Jiao et al. 2013, Wang, Chen et al. 2014). Our data are consistent with this hypothesis as evidenced by caspase 3 cleavage and increased GAP-43 protein expression, which demonstrates that sufficient cell injury occurs

in the early stages post-stroke to activate regenerative processes needed to preserve and restore neuronal function.

Finally, after acute formoterol treatment, we examined whether formoterol would decrease cell death or increase reparative processes. Formoterol did not affect cleaved caspase 3 or GAP-43 levels 144 hrs after stroke. We hypothesized that formoterol would promote MB and thus improve cell survival, however we did not see this. There is very little evidence in the literature to support changes to caspase 3 or GAP-43 levels after formoterol treatment. There is conflicting evidence to support both β -adrenergic receptor activation promoting and blocking cell death pathways in other disease models (Gannon, Che et al. 2015). Therefore, it was unknown whether formoterol would have any effect on cell death following stroke. In the heart, β -adrenergic receptor blockers showed inhibition of axonal growth (Clarke, Bhattacharjee et al. 2010). These treatments were not done with β_2 agonists, but rather with β_1 antagonists which are primarily found in the heart and agonists have not been examined. Treatment with the β_2 -adrenergic agonist, Clenbuterol, increases regeneration of motor neurons and improves synaptic function in mice with motor neuron degeneration (Zeman, Peng et al. 2004). These two studies taken together suggest that activation of β_2 -adrenergic receptors via formoterol may lead to reparative processes after injury. Although we were unable to show an increase in GAP-43 compared to vehicle animals acutely, formoterol could be activating other pathways promoting repair mechanism. Further work needs to be done to examine these mechanisms.

Formoterol and Rehabilitation Training Enhanced Motor Recovery

To determine whether formoterol would enhance RT after stroke, animals underwent rehabilitative training on the single pellet reaching task. Skilled reaching alone is known to sub-optimally improve motor function following a motor cortical stroke. In line

with previous work, all animals in the RT group showed significant improvements compared to untrained animals (No-RT). In *study 3*, our goal was to promote mitochondria biogenesis via formoterol to enhance functional recovery early after stroke and lead to long-lasting behavioral improvements. To determine the most effective dose, three doses of formoterol were examined. In a similar brain injury model, our group initially found that between 0.01 mg/kg, 0.1mg/kg, and 0.3mg/kg, that 0.1mg/kg was the most effective in increasing mitochondrial linked markers in rat cortex. Consistent with previous research and our work, 0.1mg/kg dose of formoterol was the most effective to enhance motor performance post stroke when combined with the single pellet reaching task.

Formoterol improves cognitive memory and enhances dendritic plasticity in a down syndrome model (Dang, Medina et al. 2014). Otherwise, very few studies have examined the effect of formoterol induced MB in the brain. Therefore, we first examined dendritic density in our most efficacious group (0.1mg/kg) after 15 days of RT. Previous groups have demonstrated that animals that have undergone RT show an increase in dendritic density in perilesional cortex (Jones, Chu et al. 1999). Increases in dendritic density is one example of enhanced neuroplasticity following stroke that contributes to enhanced behavioral performance and we hypothesized these neuroplasticity events could be part of the mechanism behind increased behavioral recovery in formoterol treated animals. We did not detect a difference in dendritic density using our immunohistochemistry approach. Secondly, we did not see a difference in lesion size following formoterol treatment. No change in lesion size aligns with no change in cleaved caspase 3 protein levels within a week after stroke. In our hands, formoterol does not appear to be causing a change in cell death rates which we originally hypothesized. Taken together, we showed that formoterol is not neuroprotective nor stimulating dendritic growth to enhance

behavioral recovery following ischemic stroke. However, formoterol did stimulate MB in the striatum.

Meshul and colleagues found that following cortical lesions, there is an increase in sensorimotor striatal glutamatergic function and an increase in synaptic terminals in the striatum (Meshul, Cogen et al. 2000). These increases in synaptic terminals and glutamatergic function are found up to 30 days after stroke and are linked to an increase in behavioral recovery. Research groups have shown that β -adrenergic receptors can modulate glutamate transition in other areas of the brain (Egli, Kash et al. 2005). Therefore, formoterol activation of β -adrenergic receptors in the striatum may lead to enhanced cortical function and plasticity, which results in an enhancement of motor recovery following a stroke in these studies. The most likely explanation is that there are a combination of factors (i.e. dosing, timing, injury size and severity) and mechanisms that are leading to our behavioral result which have yet to be examined by our group.

Conclusion

We hypothesized that promoting mitochondria biogenesis would lead to better functional recovery and induce structural and functional plasticity following rehabilitative training. In conclusion, ET-1-induced focal experimental stroke to the SMC leads to mitochondrial dysregulation, inflammatory cell infiltration, and cell death during the first week of injury which lasts for days following initial injury in peri-infarct cortex and striatum. Further, mitochondrial disruptions occur in accordance with marked motor impairment in the ladder task, which assesses both cortical and striatal injury. We also observed transient alterations in the pathways in the striatum, a secondary site of damage. The presence of mitochondrial suppression in the cortex and striatum depicts how pathogenic mechanisms can affect adjacent cells, intensifying the damaging effects of ischemic stroke. Formoterol treatment to stimulate mitochondria biogenesis leads to a rescue of

mitochondrial encoded subunits of complex I and IV of the electron transport chain in the striatum. All other markers of injury had mild to no effects following treatment acutely with formoterol. The ladder task also showed no change in performance between animals given vehicle or formoterol indicating a more sensitive task must be used to determine motor improvement after injury. A commonly studied dose of formoterol did show enhancement of motor recovery when given in combination with rehabilitation training. These results supported our hypothesis, however we were unable to show a change in functional and structural plasticity. A direct mechanism of action for motor improvement is still unknown and needs to be investigated in subsequent studies. Given the significance of mitochondria in regulation of neuronal function and survival, more studies are warranted to explore the relationship between mitochondrial function and behavior outcomes following stroke.

CHAPTER 5: DISCUSSION AND CONCLUSIONS

Ischemic stroke is a leading cause of death in the world and a majority of stroke survivors are left with long-lasting motor deficits. The primary goals of these studies was to enhance recovery of motor function following stroke via pharmacology enhancement and to understand the relationship between dMRI measures and the cellular, functional, and behavioral changes acutely and chronically. These studies have been promising for stroke recovery and understanding early biomarkers post stroke. Our hypothesis was ***that dMRI would be a sensitive tool to identify microstructural changes acutely and chronically following stroke and that promoting mitochondria biogenesis would lead to better functional recovery and induce structural and functional plasticity following rehabilitative training.***

The original conclusion and culmination of this work was to investigate dMRI metrics following pharmacologically enhanced rehabilitation training with formoterol. However, as shown in Chapter 3, dMRI was not able to detect a difference between animals who underwent RT versus control procedures, be more specific. Both diffusivity and kurtosis measures have been used to understand mitochondria function and health. DTI has been used to image patients with mitochondrial dysfunction disorders to determine lesion severity and monitor the overall progress of the lesion (Gropman 2013). Changes in mitochondria function have been found to be strongly correlated with DKI metrics, indicating dMRI is a viable technique to monitor changes in mitochondria function and health in rodents (D. S. Rosenberger 2014, Xingju Nie 2015). Future work will be necessary to determine optimal training parameters to create long lasting neuroplasticity changes visible with dMRI.

Diffusion MRI Used as a Predictor After Stroke

Roughly one-third of patients who suffer a stroke are left with persistent long-term motor deficits (Kelly-Hayes, Robertson et al. 1998, Association 2015). However, currently

there is not a way to determine who will recover motor function following a stroke and to what extent. Many patients will have a MRI to diagnose stroke occurrence and it has become common to use DTI. There are characteristic changes in dMRI metrics in the stroke core that several investigators are continuing to examine and determine the underlying neural changes. To date, although several hypotheses have been proposed to explain dMRI ischemic stroke lesion core changes, none are without debate and most lack direct causal evidence. Thus these dissertation studies were meant to understand the underlying structural changes and to investigate the sensitivity of dMRI to these changes in perilesional motor cortex. Numerous studies have discovered that MD decreases within hours of an ischemic stroke and begins to renormalize 5-7 days post lesion (Alexander, Lee et al. 2007). Neuronal beading, swelling and osmotic imbalance in neurons following stroke, have all been shown to restrict water movement and is currently hypothesized to be one of the leading causes for the reduction of MD in the lesion core (Budde and Frank 2010). This hypothesis is debated in the field, so we attempted to examine other structural protein changes that could cause changes in water diffusion following a stroke in the perilesional area. More recently discovered, less studied and understood is the increase in mean kurtosis (MK) seen hours following stroke compared to the non-stroke hemisphere seen in animal models persists at least one week following stroke (Hui, Du et al. 2012). Very few studies have begun to examine MK acutely following stroke and currently structural changes underlying the increase in MK after stroke have not been directly examined. In Chapter 2 we were able to replicate these dramatic changes in MD and MK in the lesion core of a focal ischemia model, therefore concluding decreases in MD and increases in MK are consistent throughout models of stroke and species (Alexander, Lee et al. 2007, Hui, Du et al. 2012, Weber, Hui et al. 2015).

The use of dMRI techniques in perilesional grey matter has been under examined, however the perilesional remaining sensory and motor cortex undergoes stroke-related

and behavioral-induced plasticity that are important for recovery of function (Jones, Chu et al. 1999, Carmichael 2016). The goal of our studies (Chapter 2 and 3) was to determine if dMRI was sensitive to these changes and thus whether dMRI could be used as a biomarker to determine rehab-induced neural plasticity and thus help clinicians prescribe adequate or effective rehab doses, for example. Our findings suggest that dMRI metrics are sensitive enough to pick up changes in the perilesional area acutely following stroke and that glial infiltration at later time points (3-7 days) is likely contributing to dMRI metric changes. Although these dMRI changes in the perilesional area are not as robust as in the core of the lesion, these studies were first of their kind to attempt to understand the mechanism of dMRI metric changes acutely in the perilesional area following an acute stroke. Even though in both studies we found correlations between dMRI metrics and astrocyte upregulation, these studies did not determine causality. It is standard in the field to determine these connections with correlations, however that may not be the best approach. It would have been ideal to knock out or knock in GFAP-positive astrocytes and determine the effect on dMRI metrics. Further, there are several other processes that are occurring early after a stroke that happen concurrently as glial upregulation that may be causing the differences we see in dMRI compared to sham animals and the non-injured cortex. Within hours to days post stroke edema occurs, which has been shown in previous studies to correlate with changes in dMRI metrics within 8 hours after a middle cerebral artery occlusion in cats (Moseley, Cohen et al. 1990). Secondly, microglia upregulation is occurring early after a stroke (by 24hrs) and although less studied, microglia may be driving changes in diffusion properties in grey and white matter following an acute ischemic stroke (Indraswari, Wong et al. 2009). Links between level of microglia activation in white matter tracks and integrity of the white matter tracks measured by fractional anisotropy have been established (Thiel and Heiss 2011). Inflammation and cellular apoptosis are also likely to contribute to changes in dMRI metrics following stroke,

although these were not investigated in our studies (Moseley, Cohen et al. 1990, Budde, Janes et al. 2011, Umesh Rudrapatna, Wieloch et al. 2014).

Experiments in Chapter 3 aimed to examine dMRI metrics after rehabilitative training (RT) to determine if there were differences between animals who underwent rehabilitative training or not. In particular, the goal was to understand dMRI changes in perilesional grey matter and white matter integrity in the corpus callosum near the forelimb region of the sensorimotor cortex (SMC) following skilled rehabilitative training. Perilesional grey matter and white matter near the SMC undergo behavioral-induced plasticity changes that are important for recovery of function after rehabilitative training. We hypothesized that dMRI changes would correlate to these behavioral-induced plasticity changes and behavioral recovery measured by the single pellet reaching task and that we could determine biomarkers that would lead to refined and individualized rehabilitation. Unlike other reports reviewed by Johansen-Berg examining dMRI changes following injury and training (Johansen-Berg 2012), we did not see learning induced changes in grey or white matter following rehabilitation training after stroke.

Our animals were scanned at three time points: before injury but after initial training on the SPR, 4 days after injury, and after 21 days of RT. One possibility to explain our lack of findings was the schedule in which the animals underwent MRI scans. We had behavioral differences as early as the first week of RT, scanning them each week may have yielded a different result or provided more clarity of our results. Although, we expected that dMRI would be sensitive to long-term structural changes, such as growth of dendritic fields (Jones, Chu et al. 1999, Voorhies 2001, Kleim and Jones 2008), following RT, by imagining them following the last day of RT, we may have missed a more dynamic or robust change. Animals were imaged the day after the last day of RT, potentially scanning them on the last day of RT and within 90 minutes, which tends to be the window for upregulation of immediate early genes in active brain regions, might have revealed a

more robust difference leading to visualized changes with dMRI. Lastly, I was only able to discover one negative report in which the authors did not detect a difference MRI metrics and training on a motor task (Thomas, Marrett et al. 2009). Thomas and colleagues (2009) used a within-group study design in which human participants were trained on a visual-motor and imaged before training, after control procedures, and following motor training. No significant differences in dMRI metrics were found in grey matter after controlling for alignment biases and correct statistical analysis. There is a strong publication bias to only publish positive results, as a recent review indicated that far more negative reports could be observed and not reported (Johansen-Berg 2012); therefore it is hard to know how many studies did not find a connection between dMRI metrics and motor learning as we show.

Sampaio-Baptista and colleagues trained a group of animals on the SPR task for 11 consecutive days and demonstrated an increase in fractional anisotropy (FA) in the corpus callosum under the SMC compared to animals trained on an unskilled task and control animals (Sampaio-Baptista, Khrapitchev et al. 2013). This increase in FA was also correlated to the learning rate of animals on the SPR task. Since, we were unable to detect a difference in our stroke animals after undergoing 21 days of RT and in order to determine if we could replicate Sampaio-Baptista and colleagues, we examined control animals trained on the SPR task compared to naïve animals. For this comparison, we analyzed and compared the imaging data collected from our “pre-stroke” time period (Chapter 3, study 1). Thus, as described in in chapter methods, animals were pre-trained on the SPR task until they reached a criterion of 60%. Following asymptotic behavior, which took 6 days (± 0.53) (stable behavior when averaged over 3 days) animals then were returned to their home cage to await ischemic stroke injury. These trained animals were then compared to aged matched naïve animals (sham animals from Chapter 2, study 2) with no behavioral training.

Pre-trained animals from Chapter 3 study 1, had received a varying number of training days because all animals reach asymptotic behavior at a different pace. Animals on average were trained for 6 days ($SEM \pm 0.53$), with a maximum of 11 days for one animal, which is on average half of the number of days animals in the Sampaio-Baptista and colleagues manuscript were trained (Sampaio-Baptista, Khrapitchev et al. 2013). Additionally, in our study as the number of training days increased there was an increase in FA values in the external capsule region ($p=0.017$, $r=0.606$), where we detect an increase in FA in naïve animals compared to trained animals. When we compared FA averages, all of our animals were near control levels compared to this previous report. Our training paradigm was shorter in duration, therefore less intense compared to the Sampaio-Baprista et al., (2013) report and thus may account for the lack of white matter changes.

To further understand why naïve animals have greater FA in the external capsule, we used an analytical program to investigate white matter tract integrity (WMTI) parameters. White matter tract integrity assumes there are two compartments that do not exchange water: the intra-axonal space and the extra-axonal space (Fieremans, Jensen et al. 2011). There are four primary metrics we use in the WMTI: 1) Axonal water fraction is thought to measure axonal density; 2) The intrinsic diffusivity examines diffusion inside axons and might be a marker of axonal injury; 3) The axial and radial diffusivities are markers of isotropic changes in extra-axonal space; and 4) Radial diffusivity is a marker for changes in the extra-axonal diffusion transverse to the fibers which may link to myelin breakdown. By examining only highly aligned white matter tracts by applying a FA threshold of 0.36 (maximum of 1) in the WMTI, there were no longer significant voxels in the external capsule and we were unable to understand why naïve animals had significantly higher FA values in this region. The fact that the external capsule had FA values lower than 0.36 indicates white matter in that region is less highly aligned and

significant differences in the external capsule could be a statistical fluke. Naïve animals did show an increase in axonal water fraction in the corpus callosum directly under the forelimb region, suggesting an increase in axonal density without training. To determine axonal density changes, carefully designed histology analysis would need to be conducted. The other three metrics were not significantly different between groups. These results are inconclusive and require additional and redesigned studies to understand dMRI metrics after SPR training.

The results from this dissertation suggest that acutely dMRI is able to detect changes in the perilesional area, known to undergo stroke-related and behavioral-induced plasticity changes over time, and that astrocyte upregulation is playing a role. Although the causal role of astrocytes to alter water diffusion and thus dMRI was not investigated, future key experiments could be done by knocking out or knocking in astrocytes to determine the mechanism of diffusion changes in the perilesional area. In depth experiments and analysis did not show chronic dMRI metric changes after stroke animals underwent rehabilitation training. Future experiments with more intense behavioral training may be able to determine if dMRI metrics are sensitive to more robust learning-induced plasticity. Initially, we hypothesized that dMRI would be a sensitive tool to identify microstructural changes acutely and chronically following stroke. We can conclude that dMRI is a sensitive tool to identify changes acutely following stroke, although more work is necessary to determine if dMRI is sensitive to other types of structural changes not examined in these studies. We were unable to detect learning-induced dMRI changes chronically following stroke.

Formoterol as a Potential Pharmacotherapy Following Stroke

In Chapter 4, we performed three experiments to determine whether mitochondria are dysfunctional in a focal model of ischemic stroke, whether formoterol, a beta2 adrenergic drug found to increase MB in the periphery, would improve mitochondria

function acutely after stroke, and if formoterol and rehabilitative training would lead to enhanced behavioral recovery. We demonstrated in *study 1* that following focal ischemic stroke, there was dysfunction in three pathways: (1) sustained loss of mitochondrial proteins and mitochondrial DNA copy number in the cortex linked to decreased mitochondrial gene transcription; (2) early inflammatory response mediated by interleukin-6 followed by macrophages; (3) apoptosis in conjunction with the activation of regenerative pathways. Formoterol rescues mitochondrial dysfunction mRNA and proteins in the striatum within 72 hrs with partial recovery of cortical markers. Formoterol had little to no effect on other pathways such as inflammation, apoptosis, and regeneration. Although, there was not full recovery of mitochondria homeostasis markers in the cortex we continued by examined the effect of RT combined with formoterol treatment to determine whether partial recovery of these markers was sufficient to drive motor recovery. Animals that were treated with formoterol for 18 days in combination with RT for 15 days showed significantly greater behavioral recovery compared to animals that were given vehicle. Two other doses of formoterol were also examined to determine optimal dosing parameters, however 0.1mg/kg was the only dose to show a significant difference compared to vehicle treatment.

Throughout these studies, we chose to investigate the remaining motor and sensory cortex that did not include the lesion core (primary injury location and unlikely to survive) because these areas are highly connected to the primary area of injury, undergo secondary degeneration, and are important for recovery of sensorimotor function following caudal forelimb injuries and thus are targets for intervention (Jones, Chu et al. 1999, Nudo 2013). Unpublished data from the Schnellmann laboratory examined both the lesion core and perilesional area following spinal cord injury. After formoterol daily treatment for 7 days in the core of the spinal cord injury, there was partial recovery of mitochondria copy number and PGC1 α and no injury-induced change in ND1 and COX1. No deficits or

formoterol effect was seen in the perilesional area 7 days following injury. After 15 days post spinal cord injury, there was no longer an injury-induced deficit however there was a formoterol enhancement in both the lesion core and perilesional area. Examining the lesion core following our ischemic stroke along with the perilesional area may have given more insight to effect of formoterol in the perilesional motor cortex. Demonstrated by the unpublished data, examining mitochondria markers longer after injury may have been beneficial. Additionally, we examined the entire striatum because it is known to undergo functional plasticity following stroke and is thought to be critical to intervention (Carmichael and Chesselet 2002). Investigation of the dorsal-lateral striatum would have provided more targeted information and should be the focus of future experiments.

Initial studies from our group examining formoterol revealed that formoterol caused mitochondrial biogenetic changes solely in the striatum. Naïve animals dosed with 0.1mg/kg of formoterol showed a significant increase in PGC-1 α levels in the striatum with no change in the cortex (**Figure 5.1**). Daily injections of 0.1mg/kg formoterol did not increase in mitochondria copy number in the cortex or striatum. We hypothesized that injury would lower a potential ceiling effect and that we would see an effect of formoterol in the cortex following injury. In the early 1990s Nicholas and colleagues examined the disruption of β_2 -adrenergic receptors in the rat throughout the brain by using in situ hybridization. Receptors were located throughout the caudate and putamen, however

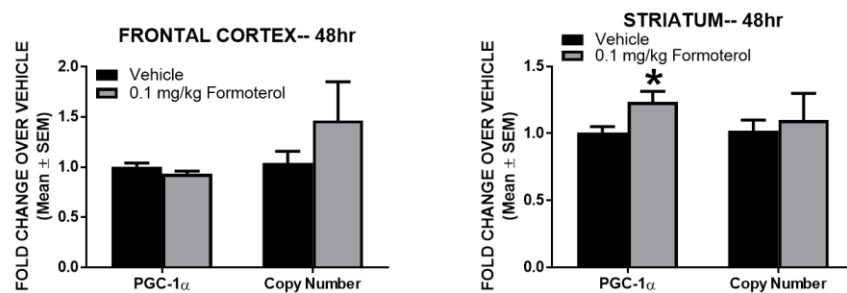


Figure 5.1. Naïve animals dosed with 0.1mg/kg of formoterol showed a significant increase in PGC-1 α levels in the striatum with no change in the cortex. Daily injections of 0.1mg/kg formoterol did not increase in mitochondria copy number in the cortex or striatum.

none were detected in the motor or sensory cortex (Nicholas, Pieribone et al. 1993). This may be one reason that the effect of formoterol in the cortex is minimal and fully recovery is seen in the striatum following stroke.

Proposed Mechanism of Action

From our results and previous reports, formoterol is likely modulating another neurotransmitter system or causing changes in the striatum leading to decreased motor impairments. In Chapter 3, experiment 2 we found that formoterol stimulated mitochondria biogenesis (MB) in the striatum. β_2 -adrenergic receptors are located throughout the caudate and putamen and have been shown to modulate glutamate transition in the brain (Nicholas, Pieribone et al. 1993, Egli, Kash et al. 2005). Meshul and colleagues found that following cortical lesions, there is an increase in sensorimotor striatal glutamatergic function and an increase in synaptic terminals in the striatum (Meshul, Cogen et al. 2000). These increases 30 days after stroke are linked to an increase in behavioral recovery.

Thus, MB is likely not the key mechanism in formoterol-induced enhancement of motor recovery. Formoterol activation of β_2 -adrenergic receptors in the striatum may be a more likely candidate. G-coupled protein receptors, such as β_2 -adrenergic receptors, activate a large cascade of proteins (adenylate cyclase, cyclic AMP, protein kinase A) that could stimulate motor recovery. Formoterol may induce better motor recovery by activating β_2 -adrenergic receptors which then modulate oxidative metabolism, lipolysis, glucose transport, and glucose oxidation (Wills, Trager et al. 2012). Although a clear synaptic mechanism remains to be determined, it is probable that formoterol acts within the striatum to enhance motor recovery. Future studies could begin to elucidate this mechanism by directly infusing formoterol into the dorsal lateral striatum near the forelimb motor area or use β_2 -adrenergic receptors antagonists to determine mitochondria homeostasis effects and effects on motor recovery.

Future Directions

To determine the direct cause of dMRI metric changes in the perilesional area post stroke, more direct and less correlative studies need to be done. Knocking in or knocking out GFAP-positive astrocytes for example would help to determine the role of astrocyte increases post stroke to dMRI metrics. Although, not as direct of analysis, pharmacological studies with agonists and/or antagonists may also be conducted to elucidate a causal relationship. These same experiments could be done to understand other mechanisms (edema, microglia upregulation, inflammation, etc.) that could be contributing to changes in dMRI acutely following stroke. In attempt to visualize RT effects with dMRI, a more intense RT must be used. Combining multiple skilled learning tasks may be the most beneficial and create a more robust change in structural proteins after stroke. Some studies post stroke have used exercise training instead of skilled learning tasks, it would be beneficial to examine the differences between exercise-induced and skilled learning-induced dMRI changes.

Unpublished data suggests that examining formoterol acutely several weeks, instead of days, post-injury would give more insight into changes in the mitochondria homeostasis pathway. These studies did not look at changes after 6 days post stroke, however it may be more beneficial to extend these analysis to 14-21 days after injury. To further understand the mechanism by which formoterol enhances motor recovery an antagonists could be given and/or directly infusing formoterol to specific brain regions of interest.

Conclusions

We hypothesized ***that dMRI would be a sensitive tool to identify microstructural changes acutely and chronically following stroke and that promoting mitochondria biogenesis would lead to better functional recovery and induce structural and functional plasticity following rehabilitative training.*** To accomplish these studies, we used a combination of sensitive behavioral,

immunohistochemical, mitochondrial related molecular markers, and diffusion magnetic resonance imaging (dMRI) to investigate the time course of acute and chronic stroke effects. In summary, we found that dMRI is a sensitive tool to identify microstructural changes acutely following stroke. We were unable to detect differences in dMRI metrics chronically following rehabilitation training. Lastly, we found that formoterol lead to better functional recovery when combined with rehabilitation training through an undetermined mechanism.

References

- Adkins-Muir, D. L. and T. A. Jones (2003). "Cortical electrical stimulation combined with rehabilitative training: enhanced functional recovery and dendritic plasticity following focal cortical ischemia in rats." Neurol Res **25**(8): 780-788.
- Adkins, D. L., J. Boychuk, M. S. Remple and J. A. Kleim (2006). "Motor training induces experience-specific patterns of plasticity across motor cortex and spinal cord." J Appl Physiol (1985) **101**(6): 1776-1782.
- Adkins, D. L., P. Campos, D. Quach, M. Borromeo, K. Schallert and T. A. Jones (2006). "Epidural cortical stimulation enhances motor function after sensorimotor cortical infarcts in rats." Exp Neurol **200**(2): 356-370.
- Adkins, D. L., J. E. Hsu and T. A. Jones (2008). "Motor cortical stimulation promotes synaptic plasticity and behavioral improvements following sensorimotor cortex lesions." Exp Neurol **212**(1): 14-28.
- Adkins, D. L. and T. A. Jones (2005). "D-amphetamine enhances skilled reaching after ischemic cortical lesions in rats." Neurosci Lett **380**(3): 214-218.
- Adkins, D. L., A. C. Voorhies and T. A. Jones (2004). "Behavioral and neuroplastic effects of focal endothelin-1 induced sensorimotor cortex lesions." Neuroscience **128**(3): 473-486.
- Aicardi, G., E. Argilli, S. Cappello, S. Santi, M. Riccio, H. Thoenen and M. Canossa (2004). "Induction of long-term potentiation and depression is reflected by corresponding changes in secretion of endogenous brain-derived neurotrophic factor." Proc Natl Acad Sci U S A **101**(44): 15788-15792.
- Alaverdashvili, M. and I. Q. Whishaw (2013). "A behavioral method for identifying recovery and compensation: hand use in a preclinical stroke model using the single pellet reaching task." Neurosci Biobehav Rev **37**(5): 950-967.
- Alexander, A. L., J. E. Lee, M. Lazar and A. S. Field (2007). "Diffusion tensor imaging of the brain." Neurotherapeutics **4**(3): 316-329.
- Alexander, D. C., G. J. Barker and S. R. Arridge (2002). "Detection and modeling of non-Gaussian apparent diffusion coefficient profiles in human brain data." Magn Reson Med **48**(2): 331-340.
- Allen, K. L., A. Almeida, T. E. Bates and J. B. Clark (1995). "Changes of respiratory chain activity in mitochondrial and synaptosomal fractions isolated from the gerbil brain after graded ischaemia." J Neurochem **64**(5): 2222-2229.
- Allred, R. P., S. Y. Kim and T. A. Jones (2014). "Use it and/or lose it-experience effects on brain remodeling across time after stroke." Front Hum Neurosci **8**: 379.
- Anderson, M. F. and N. R. Sims (1999). "Mitochondrial respiratory function and cell death in focal cerebral ischemia." J Neurochem **73**(3): 1189-1199.

- Ankarcrona, M., J. M. Dypbukt, E. Bonfoco, B. Zhivotovsky, S. Orrenius, S. A. Lipton and P. Nicotera (1995). "Glutamate-induced neuronal death: a succession of necrosis or apoptosis depending on mitochondrial function." Neuron **15**(4): 961-973.
- Association, A. H. (2014). "Post-Stroke Rehabilitation ", 2016.
- Association, A. H. (2015). "Impact of Stroke (Stroke statistics)." Retrieved July 14, 2015.
- Baddeley, A. J., H. J. Gundersen and L. M. Cruz-Orive (1986). "Estimation of surface area from vertical sections." J Microsc **142**(Pt 3): 259-276.
- Bathoorn, E., J. J. Liesker, D. S. Postma, M. Boorsma, E. Bondesson, G. H. Koeter, H. F. Kauffman, A. J. van Oosterhout and H. A. Kerstjens (2008). "Anti-inflammatory effects of combined budesonide/formoterol in COPD exacerbations." COPD **5**(5): 282-290.
- Bayir, H. and V. E. Kagan (2008). "Bench-to-bedside review: Mitochondrial injury, oxidative stress and apoptosis--there is nothing more practical than a good theory." Crit Care **12**(1): 206.
- Bell, J. A., M. L. Wolke, R. C. Ortez, T. A. Jones and A. L. Kerr (2015). "Training Intensity Affects Motor Rehabilitation Efficacy Following Unilateral Ischemic Insult of the Sensorimotor Cortex in C57BL/6 Mice." Neurorehabil Neural Repair **29**(6): 590-598.
- Benowitz, L. I. and S. T. Carmichael (2010). "Promoting axonal rewiring to improve outcome after stroke." Neurobiol Dis **37**(2): 259-266.
- Benowitz, L. I. and A. Routtenberg (1997). "GAP-43: an intrinsic determinant of neuronal development and plasticity." Trends Neurosci **20**(2): 84-91.
- Biernaskie, J., D. Corbett, J. Peeling, J. Wells and H. Lei (2001). "A serial MR study of cerebral blood flow changes and lesion development following endothelin-1-induced ischemia in rats." Magn Reson Med **46**(4): 827-830.
- Bonzano, L., A. Tacchino, G. Brichetto, L. Roccatagliata, A. Dessypris, P. Feraco, M. L. Lopes De Carvalho, M. A. Battaglia, G. L. Mancardi and M. Bove (2014). "Upper limb motor rehabilitation impacts white matter microstructure in multiple sclerosis." Neuroimage **90**: 107-116.
- Borgens, R. B. and P. Liu-Snyder (2012). "Understanding secondary injury." Q Rev Biol **87**(2): 89-127.
- Brand, M. D. and T. C. Esteves (2005). "Physiological functions of the mitochondrial uncoupling proteins UCP2 and UCP3." Cell Metab **2**(2): 85-93.
- Brown, C. E., J. D. Boyd and T. H. Murphy (2010). "Longitudinal in vivo imaging reveals balanced and branch-specific remodeling of mature cortical pyramidal dendritic arbors after stroke." J Cereb Blood Flow Metab **30**(4): 783-791.

- Budde, M. D. and J. A. Frank (2010). "Neurite beading is sufficient to decrease the apparent diffusion coefficient after ischemic stroke." Proc Natl Acad Sci U S A **107**(32): 14472-14477.
- Budde, M. D., L. Janes, E. Gold, L. C. Turtzo and J. A. Frank (2011). "The contribution of gliosis to diffusion tensor anisotropy and tractography following traumatic brain injury: validation in the rat using Fourier analysis of stained tissue sections." Brain **134**(Pt 8): 2248-2260.
- Carmichael, S. T. (2003). "Plasticity of cortical projections after stroke." Neuroscientist **9**(1): 64-75.
- Carmichael, S. T. (2005). "Rodent models of focal stroke: size, mechanism, and purpose." NeuroRx **2**(3): 396-409.
- Carmichael, S. T. (2016). "Emergent properties of neural repair: elemental biology to therapeutic concepts." Ann Neurol **79**(6): 895-906.
- Carmichael, S. T., I. Archibeque, L. Luke, T. Nolan, J. Momiy and S. Li (2005). "Growth-associated gene expression after stroke: evidence for a growth-promoting region in peri-infarct cortex." Exp Neurol **193**(2): 291-311.
- Carmichael, S. T. and M. F. Chesselet (2002). "Synchronous neuronal activity is a signal for axonal sprouting after cortical lesions in the adult." J Neurosci **22**(14): 6062-6070.
- Carmichael, S. T., B. Kathirvelu, C. A. Schweppe and E. H. Nie (2016). "Molecular, cellular and functional events in axonal sprouting after stroke." Exp Neurol.
- Carmichael, S. T., L. Wei, C. M. Rovainen and T. A. Woolsey (2001). "New patterns of intracortical projections after focal cortical stroke." Neurobiol Dis **8**(5): 910-922.
- Chan, P. H. (2005). "Mitochondrial dysfunction and oxidative stress as determinants of cell death/survival in stroke." Ann N Y Acad Sci **1042**: 203-209.
- Cheeran, B., P. Talelli, F. Mori, G. Koch, A. Suppa, M. Edwards, H. Houlden, K. Bhatia, R. Greenwood and J. C. Rothwell (2008). "A common polymorphism in the brain-derived neurotrophic factor gene (BDNF) modulates human cortical plasticity and the response to rTMS." J Physiol **586**(23): 5717-5725.
- Chen, J., K. Jin, M. Chen, W. Pei, K. Kawaguchi, D. A. Greenberg and R. P. Simon (1997). "Early detection of DNA strand breaks in the brain after transient focal ischemia: implications for the role of DNA damage in apoptosis and neuronal cell death." J Neurochem **69**(1): 232-245.
- Chen, M., V. O. Ona, M. Li, R. J. Ferrante, K. B. Fink, S. Zhu, J. Bian, L. Guo, L. A. Farrell, S. M. Hersch, W. Hobbs, J. P. Vonsattel, J. H. Cha and R. M. Friedlander (2000). "Minocycline inhibits caspase-1 and caspase-3 expression and delays mortality in a transgenic mouse model of Huntington disease." Nat Med **6**(7): 797-801.

- Chen, S. D., H. Y. Wu, D. I. Yang, S. Y. Lee, F. Z. Shaw, T. K. Lin, C. W. Liou and Y. C. Chuang (2006). "Effects of rosiglitazone on global ischemia-induced hippocampal injury and expression of mitochondrial uncoupling protein 2." Biochem Biophys Res Commun **351**(1): 198-203.
- Chen, Z. Y., D. Jing, K. G. Bath, A. Ieraci, T. Khan, C. J. Siao, D. G. Herrera, M. Toth, C. Yang, B. S. McEwen, B. L. Hempstead and F. S. Lee (2006). "Genetic variant BDNF (Val66Met) polymorphism alters anxiety-related behavior." Science **314**(5796): 140-143.
- Cheng, A., Y. Hou and M. P. Mattson (2010). "Mitochondria and neuroplasticity." ASN Neuro **2**(5): e00045.
- Cheung, J. S., E. Wang, E. H. Lo and P. Z. Sun (2012). "Stratification of heterogeneous diffusion MRI ischemic lesion with kurtosis imaging: evaluation of mean diffusion and kurtosis MRI mismatch in an animal model of transient focal ischemia." Stroke **43**(8): 2252-2254.
- Clarke, G. L., A. Bhattacharjee, S. E. Tague, W. Hasan and P. G. Smith (2010). "ss-adrenoceptor blockers increase cardiac sympathetic innervation by inhibiting autoreceptor suppression of axon growth." J Neurosci **30**(37): 12446-12454.
- Clay Montier, L. L., J. J. Deng and Y. Bai (2009). "Number matters: control of mammalian mitochondrial DNA copy number." J Genet Genomics **36**(3): 125-131.
- Costa, R. M., D. Cohen and M. A. Nicolelis (2004). "Differential corticostriatal plasticity during fast and slow motor skill learning in mice." Curr Biol **14**(13): 1124-1134.
- Cui, L., H. Jeong, F. Borovecki, C. N. Parkhurst, N. Tanese and D. Krainc (2006). "Transcriptional repression of PGC-1alpha by mutant huntingtin leads to mitochondrial dysfunction and neurodegeneration." Cell **127**(1): 59-69.
- D. S. Rosenberger, W. S., F. Falangola, A. Ledreux, D. Wynn, A. Granholm (2014). Role of Mitochondrial Transition Pore (MTP) Channel Protein VDAC1 in Middle-ages Rodents Exposed to Midazolam. International Anesthesia Research Society.
- Dang, M. T., F. Yokoi, H. H. Yin, D. M. Lovinger, Y. Wang and Y. Li (2006). "Disrupted motor learning and long-term synaptic plasticity in mice lacking NMDAR1 in the striatum." Proc Natl Acad Sci U S A **103**(41): 15254-15259.
- Dang, V., B. Medina, D. Das, S. Moghadam, K. J. Martin, B. Lin, P. Naik, D. Patel, R. Nosheny, J. Wesson Ashford and A. Salehi (2014). "Formoterol, a long-acting beta2 adrenergic agonist, improves cognitive function and promotes dendritic complexity in a mouse model of Down syndrome." Biol Psychiatry **75**(3): 179-188.
- Dietrich, M. O., Z. B. Andrews and T. L. Horvath (2008). "Exercise-induced synaptogenesis in the hippocampus is dependent on UCP2-regulated mitochondrial adaptation." J Neurosci **28**(42): 10766-10771.
- Dirnagl, U., C. Iadecola and M. A. Moskowitz (1999). "Pathobiology of ischaemic stroke: an integrated view." Trends Neurosci **22**(9): 391-397.

- Doyon, J. and H. Benali (2005). "Reorganization and plasticity in the adult brain during learning of motor skills." Curr Opin Neurobiol **15**(2): 161-167.
- Duchen, M. R. (2000). "Mitochondria and calcium: from cell signalling to cell death." J Physiol **529 Pt 1**: 57-68.
- Egan, M. F., M. Kojima, J. H. Callicott, T. E. Goldberg, B. S. Kolachana, A. Bertolino, E. Zaitsev, B. Gold, D. Goldman, M. Dean, B. Lu and D. R. Weinberger (2003). "The BDNF val66met polymorphism affects activity-dependent secretion of BDNF and human memory and hippocampal function." Cell **112**(2): 257-269.
- Egli, R. E., T. L. Kash, K. Choo, V. Savchenko, R. T. Matthews, R. D. Blakely and D. G. Winder (2005). "Norepinephrine modulates glutamatergic transmission in the bed nucleus of the stria terminalis." Neuropsychopharmacology **30**(4): 657-668.
- Ekstrand, M. I., M. Falkenberg, A. Rantanen, C. B. Park, M. Gaspari, K. Hultenby, P. Rustin, C. M. Gustafsson and N. G. Larsson (2004). "Mitochondrial transcription factor A regulates mtDNA copy number in mammals." Hum Mol Genet **13**(9): 935-944.
- Falangola, M. F., D. N. Guilfoyle, A. Tabesh, E. S. Hui, X. Nie, J. H. Jensen, S. V. Gerum, C. Hu, J. LaFrancois, H. R. Collins and J. A. Helpert (2014). "Histological correlation of diffusional kurtosis and white matter modeling metrics in cuprizone-induced corpus callosum demyelination." NMR Biomed **27**(8): 948-957.
- Featherstone, R. E. and R. J. McDonald (2005). "Lesions of the dorsolateral striatum impair the acquisition of a simplified stimulus-response dependent conditional discrimination task." Neuroscience **136**(2): 387-395.
- Fernando, M. R., J. L. Reyes, J. Iannuzzi, G. Leung and D. M. McKay (2014). "The pro-inflammatory cytokine, interleukin-6, enhances the polarization of alternatively activated macrophages." PLoS One **9**(4): e94188.
- Ferrer, I., B. Friguls, E. Dalfo, C. Justicia and A. M. Planas (2003). "Caspase-dependent and caspase-independent signalling of apoptosis in the penumbra following middle cerebral artery occlusion in the adult rat." Neuropathol Appl Neurobiol **29**(5): 472-481.
- Fieremans, E., A. Benitez, J. H. Jensen, M. F. Falangola, A. Tabesh, R. L. Deardorff, M. V. Spampinato, J. S. Babb, D. S. Novikov, S. H. Ferris and J. A. Helpert (2013). "Novel white matter tract integrity metrics sensitive to Alzheimer disease progression." AJNR Am J Neuroradiol **34**(11): 2105-2112.
- Fieremans, E., J. H. Jensen and J. A. Helpert (2011). "White matter characterization with diffusional kurtosis imaging." Neuroimage **58**(1): 177-188.
- Figurov, A., L. D. Pozzo-Miller, P. Olafsson, T. Wang and B. Lu (1996). "Regulation of synaptic responses to high-frequency stimulation and LTP by neurotrophins in the hippocampus." Nature **381**(6584): 706-709.

- Fiskum, G., A. N. Murphy and M. F. Beal (1999). "Mitochondria in neurodegeneration: acute ischemia and chronic neurodegenerative diseases." J Cereb Blood Flow Metab **19**(4): 351-369.
- Franklin, J. L. (2011). "Redox regulation of the intrinsic pathway in neuronal apoptosis." Antioxid Redox Signal **14**(8): 1437-1448.
- Galluzzi, L., E. Morselli, O. Kepp and G. Kroemer (2009). "Targeting post-mitochondrial effectors of apoptosis for neuroprotection." Biochim Biophys Acta **1787**(5): 402-413.
- Gannon, M., P. Che, Y. Chen, K. Jiao, E. D. Roberson and Q. Wang (2015). "Noradrenergic dysfunction in Alzheimer's disease." Front Neurosci **9**: 220.
- Gleeson, L. C., K. J. Ryan, E. W. Griffin, T. J. Connor and A. Harkin (2010). "The beta2-adrenoceptor agonist clenbuterol elicits neuroprotective, anti-inflammatory and neurotrophic actions in the kainic acid model of excitotoxicity." Brain Behav Immun **24**(8): 1354-1361.
- Goto, S., K. Yamada, N. Inoue, S. Nagahiro and Y. Ushio (1994). "Increased expression of growth-associated protein GAP-43/B-50 following cerebral hemitranssection or striatal ischemic injury in the substantia nigra of adult rats." Brain Res **647**(2): 333-339.
- Gropman, A. L. (2013). "Neuroimaging in mitochondrial disorders." Neurotherapeutics **10**(2): 273-285.
- Guglielmetti, C., J. Veraart, E. Roelant, Z. Mai, J. Daans, J. Van Audekerke, M. Naeyaert, G. Vanhoutte, Y. P. R. Delgado, J. Praet, E. Fieremans, P. Ponsaerts, J. Sijbers, A. Van der Linden and M. Verhoye (2016). "Diffusion kurtosis imaging probes cortical alterations and white matter pathology following cuprizone induced demyelination and spontaneous remyelination." Neuroimage **125**: 363-377.
- Haines, B. and P. A. Li (2012). "Overexpression of mitochondrial uncoupling protein 2 inhibits inflammatory cytokines and activates cell survival factors after cerebral ischemia." PLoS One **7**(2): e31739.
- Han, M. H., S. Jiao, J. M. Jia, Y. Chen, C. Y. Chen, M. Gucek, S. P. Markey and Z. Li (2013). "The novel caspase-3 substrate Gap43 is involved in AMPA receptor endocytosis and long-term depression." Mol Cell Proteomics **12**(12): 3719-3731.
- Harmon, J. L., W. S. Gibbs, R. M. Whitaker, R. G. Schnellmann and D. L. Adkins (2016). "Striatal Mitochondrial Disruption following Severe Traumatic Brain Injury." J Neurotrauma.
- Harms, K. J., M. S. Rioult-Pedotti, D. R. Carter and A. Dunaevsky (2008). "Transient spine expansion and learning-induced plasticity in layer 1 primary motor cortex." J Neurosci **28**(22): 5686-5690.
- Hengartner, M. O. (2000). "The biochemistry of apoptosis." Nature **407**(6805): 770-776.

- Hodgson, R. A., Z. Ji, S. Standish, T. E. Boyd-Hodgson, A. K. Henderson and R. J. Racine (2005). "Training-induced and electrically induced potentiation in the neocortex." Neurobiol Learn Mem **83**(1): 22-32.
- Hoppins, S. (2014). "The regulation of mitochondrial dynamics." Curr Opin Cell Biol **29**: 46-52.
- Hui, E. S., F. Du, S. Huang, Q. Shen and T. Q. Duong (2012). "Spatiotemporal dynamics of diffusional kurtosis, mean diffusivity and perfusion changes in experimental stroke." Brain Res **1451**: 100-109.
- Indraswari, F., P. T. Wong, E. Yap, Y. K. Ng and S. T. Dheen (2009). "Upregulation of Dpysl2 and Spna2 gene expression in the rat brain after ischemic stroke." Neurochem Int **55**(4): 235-242.
- Jander, S., M. Schroeter and G. Stoll (2000). "Role of NMDA receptor signaling in the regulation of inflammatory gene expression after focal brain ischemia." J Neuroimmunol **109**(2): 181-187.
- Jensen, J. H. and J. A. Helpern (2010). "MRI quantification of non-Gaussian water diffusion by kurtosis analysis." NMR Biomed **23**(7): 698-710.
- Jensen, J. H., J. A. Helpern, A. Ramani, H. Lu and K. Kaczynski (2005). "Diffusional kurtosis imaging: the quantification of non-gaussian water diffusion by means of magnetic resonance imaging." Magn Reson Med **53**(6): 1432-1440.
- Jiang, Q., Z. G. Zhang and M. Chopp (2010). "MRI of stroke recovery." Stroke **41**(2): 410-414.
- Jin, R., G. Yang and G. Li (2010). "Inflammatory mechanisms in ischemic stroke: role of inflammatory cells." J Leukoc Biol **87**(5): 779-789.
- Johansen-Berg, H. (2012). "The future of functionally-related structural change assessment." Neuroimage **62**(2): 1293-1298.
- Jones, T. A. and D. L. Adkins (2015). "Motor System Reorganization After Stroke: Stimulating and Training Toward Perfection." Physiology (Bethesda) **30**(5): 358-370.
- Jones, T. A., C. J. Chu, L. A. Grande and A. D. Gregory (1999). "Motor skills training enhances lesion-induced structural plasticity in the motor cortex of adult rats." J Neurosci **19**(22): 10153-10163.
- Jones, T. A. and S. C. Jefferson (2011). "Reflections of experience-expectant development in repair of the adult damaged brain." Dev Psychobiol **53**(5): 466-475.
- Jones, T. A. a. A., D. A. (In Press). "Brain Reorganization after Stroke - Stimulating and Training towards Perfection." Journal of Neurophysiology.

- Junker, V., A. Becker, R. Huhne, M. Zembatov, A. Ravati, C. Culmsee and J. Kriegstein (2002). "Stimulation of beta-adrenoceptors activates astrocytes and provides neuroprotection." Eur J Pharmacol **446**(1-3): 25-36.
- Kann, O. and R. Kovacs (2007). "Mitochondria and neuronal activity." Am J Physiol Cell Physiol **292**(2): C641-657.
- Karl, J. M. and I. Q. Whishaw (2013). "Different evolutionary origins for the reach and the grasp: an explanation for dual visuomotor channels in primate parietofrontal cortex." Front Neurol **4**: 208.
- Kelly-Hayes, M., J. T. Robertson, J. P. Broderick, P. W. Duncan, L. A. Hershey, E. J. Roth, W. H. Thies and C. A. Trombly (1998). "The American Heart Association Stroke Outcome Classification." Stroke **29**(6): 1274-1280.
- Kleim, J. A., S. Barbay and R. J. Nudo (1998). "Functional reorganization of the rat motor cortex following motor skill learning." J Neurophysiol **80**(6): 3321-3325.
- Kleim, J. A., R. Bruneau, K. Calder, D. Pocock, P. M. VandenBerg, E. MacDonald, M. H. Monfils, R. J. Sutherland and K. Nader (2003). "Functional organization of adult motor cortex is dependent upon continued protein synthesis." Neuron **40**(1): 167-176.
- Kleim, J. A., S. Chan, E. Pringle, K. Schallert, V. Procaccio, R. Jimenez and S. C. Cramer (2006). "BDNF val66met polymorphism is associated with modified experience-dependent plasticity in human motor cortex." Nat Neurosci **9**(6): 735-737.
- Kleim, J. A., J. H. Freeman, Jr., R. Bruneau, B. C. Nolan, N. R. Cooper, A. Zook and D. Walters (2002). "Synapse formation is associated with memory storage in the cerebellum." Proc Natl Acad Sci U S A **99**(20): 13228-13231.
- Kleim, J. A., T. M. Hogg, P. M. VandenBerg, N. R. Cooper, R. Bruneau and M. Remple (2004). "Cortical synaptogenesis and motor map reorganization occur during late, but not early, phase of motor skill learning." J Neurosci **24**(3): 628-633.
- Kleim, J. A. and T. A. Jones (2008). "Principles of experience-dependent neural plasticity: implications for rehabilitation after brain damage." J Speech Lang Hear Res **51**(1): S225-239.
- Kleim, J. A., E. Lussnig, E. R. Schwarz, T. A. Comery and W. T. Greenough (1996). "Synaptogenesis and Fos expression in the motor cortex of the adult rat after motor skill learning." J Neurosci **16**(14): 4529-4535.
- Krakauer, J. W. (2006). "Motor learning: its relevance to stroke recovery and neurorehabilitation." Curr Opin Neurol **19**(1): 84-90.
- Labat-gest, V. and S. Tomasi (2013). "Photothrombotic ischemia: a minimally invasive and reproducible photochemical cortical lesion model for mouse stroke studies." J Vis Exp(76).

- Le Bihan, D. (2003). "Looking into the functional architecture of the brain with diffusion MRI." Nat Rev Neurosci **4**(6): 469-480.
- Le Bihan, D., E. Breton, D. Lallemand, P. Grenier, E. Cabanis and M. Laval-Jeantet (1986). "MR imaging of intravoxel incoherent motions: application to diffusion and perfusion in neurologic disorders." Radiology **161**(2): 401-407.
- Li, M., V. O. Ona, C. Guegan, M. Chen, V. Jackson-Lewis, L. J. Andrews, A. J. Olszewski, P. E. Stieg, J. P. Lee, S. Przedborski and R. M. Friedlander (2000). "Functional role of caspase-1 and caspase-3 in an ALS transgenic mouse model." Science **288**(5464): 335-339.
- Li, S., J. J. Overman, D. Katsman, S. V. Kozlov, C. J. Donnelly, J. L. Twiss, R. J. Giger, G. Coppola, D. H. Geschwind and S. T. Carmichael (2010). "An age-related sprouting transcriptome provides molecular control of axonal sprouting after stroke." Nat Neurosci **13**(12): 1496-1504.
- Lin, J., P. H. Wu, P. T. Tarr, K. S. Lindenberg, J. St-Pierre, C. Y. Zhang, V. K. Mootha, S. Jager, C. R. Vianna, R. M. Reznick, L. Cui, M. Manieri, M. X. Donovan, Z. Wu, M. P. Cooper, M. C. Fan, L. M. Rohas, A. M. Zavacki, S. Cinti, G. I. Shulman, B. B. Lowell, D. Krainc and B. M. Spiegelman (2004). "Defects in adaptive energy metabolism with CNS-linked hyperactivity in PGC-1alpha null mice." Cell **119**(1): 121-135.
- Lin, M. T. and M. F. Beal (2006). "Mitochondrial dysfunction and oxidative stress in neurodegenerative diseases." Nature **443**(7113): 787-795.
- Linnik, M. D., J. A. Miller, J. Sprinkle-Cavallo, P. J. Mason, F. Y. Thompson, L. R. Montgomery and K. K. Schroeder (1995). "Apoptotic DNA fragmentation in the rat cerebral cortex induced by permanent middle cerebral artery occlusion." Brain Res Mol Brain Res **32**(1): 116-124.
- Liu, F. and L. D. McCullough (2011). "Middle cerebral artery occlusion model in rodents: methods and potential pitfalls." J Biomed Biotechnol **2011**: 464701.
- Liu, Z., Y. Li, L. Zhang, H. Xin, Y. Cui, L. R. Hanson, W. H. Frey, 2nd and M. Chopp (2012). "Subacute intranasal administration of tissue plasminogen activator increases functional recovery and axonal remodeling after stroke in rats." Neurobiol Dis **45**(2): 804-809.
- Louneva, N., J. W. Cohen, L. Y. Han, K. Talbot, R. S. Wilson, D. A. Bennett, J. Q. Trojanowski and S. E. Arnold (2008). "Caspase-3 is enriched in postsynaptic densities and increased in Alzheimer's disease." Am J Pathol **173**(5): 1488-1495.
- Lu, H., J. H. Jensen, A. Ramani and J. A. Helpert (2006). "Three-dimensional characterization of non-gaussian water diffusion in humans using diffusion kurtosis imaging." NMR Biomed **19**(2): 236-247.
- Maldonado, M. A., R. P. Allred, E. L. Felthouser and T. A. Jones (2008). "Motor skill training, but not voluntary exercise, improves skilled reaching after unilateral

- ischemic lesions of the sensorimotor cortex in rats." Neurorehabil Neural Repair **22**(3): 250-261.
- Malpass, K. (2013). "Neurodegenerative disease: defective mitochondrial dynamics in the hot seat-a therapeutic target common to many neurological disorders?" Nat Rev Neurol **9**(8): 417.
- Manley, G. T., M. Fujimura, T. Ma, N. Noshita, F. Filiz, A. W. Bollen, P. Chan and A. S. Verkman (2000). "Aquaporin-4 deletion in mice reduces brain edema after acute water intoxication and ischemic stroke." Nat Med **6**(2): 159-163.
- Marchal, G., A. R. Young and J. C. Baron (1999). "Early postischemic hyperperfusion: pathophysiological insights from positron emission tomography." J Cereb Blood Flow Metab **19**(5): 467-482.
- Marmolino, D., M. Manto, F. Acquaviva, P. Vergara, A. Ravella, A. Monticelli and M. Pandolfo (2010). "PGC-1alpha down-regulation affects the antioxidant response in Friedreich's ataxia." PLoS One **5**(4): e10025.
- Martinowich, K., H. Manji and B. Lu (2007). "New insights into BDNF function in depression and anxiety." Nat Neurosci **10**(9): 1089-1093.
- McNamee, E. N., K. M. Ryan, E. W. Griffin, R. E. Gonzalez-Reyes, K. J. Ryan, A. Harkin and T. J. Connor (2010). "Noradrenaline acting at central beta-adrenoceptors induces interleukin-10 and suppressor of cytokine signaling-3 expression in rat brain: implications for neurodegeneration." Brain Behav Immun **24**(4): 660-671.
- McNeill, T. H., S. A. Brown, E. Hogg, H. W. Cheng and C. K. Meshul (2003). "Synapse replacement in the striatum of the adult rat following unilateral cortex ablation." J Comp Neurol **467**(1): 32-43.
- Mergenthaler, P., U. Lindauer, G. A. Dienel and A. Meisel (2013). "Sugar for the brain: the role of glucose in physiological and pathological brain function." Trends Neurosci **36**(10): 587-597.
- Meshul, C. K., J. P. Cogen, H. W. Cheng, C. Moore, L. Krentz and T. H. McNeill (2000). "Alterations in rat striatal glutamate synapses following a lesion of the cortico-and/or nigrostriatal pathway." Exp Neurol **165**(1): 191-206.
- Metz, G. A. and I. Q. Whishaw (2009). "The ladder rung walking task: a scoring system and its practical application." J Vis Exp(28).
- Miura, S., Y. Kai, Y. Kamei and O. Ezaki (2008). "Isoform-specific increases in murine skeletal muscle peroxisome proliferator-activated receptor-gamma coactivator-1alpha (PGC-1alpha) mRNA in response to beta2-adrenergic receptor activation and exercise." Endocrinology **149**(9): 4527-4533.
- Moseley, M. E., Y. Cohen, J. Mintorovitch, L. Chileuitt, H. Shimizu, J. Kucharczyk, M. F. Wendland and P. R. Weinstein (1990). "Early detection of regional cerebral ischemia in cats: comparison of diffusion- and T2-weighted MRI and spectroscopy." Magn Reson Med **14**(2): 330-346.

- Mostany, R., T. G. Chowdhury, D. G. Johnston, S. A. Portonovo, S. T. Carmichael and C. Portera-Cailliau (2010). "Local hemodynamics dictate long-term dendritic plasticity in peri-infarct cortex." J Neurosci **30**(42): 14116-14126.
- Nakagomi, S., S. Kiryu-Seo and H. Kiyama (2000). "Endothelin-converting enzymes and endothelin receptor B messenger RNAs are expressed in different neural cell species and these messenger RNAs are coordinately induced in neurons and astrocytes respectively following nerve injury." Neuroscience **101**(2): 441-449.
- Neafsey, E. J., E. L. Bold, G. Haas, K. M. Hurley-Gius, G. Quirk, C. F. Sievert and R. R. Terrence (1986). "The organization of the rat motor cortex: a microstimulation mapping study." Brain Res **396**(1): 77-96.
- Nicholas, A. P., V. A. Pieribone and T. Hokfelt (1993). "Cellular localization of messenger RNA for beta-1 and beta-2 adrenergic receptors in rat brain: an in situ hybridization study." Neuroscience **56**(4): 1023-1039.
- Niizuma, K., H. Endo and P. H. Chan (2009). "Oxidative stress and mitochondrial dysfunction as determinants of ischemic neuronal death and survival." J Neurochem **109** **Suppl 1**: 133-138.
- Nudo, R. J. (1997). "Remodeling of cortical motor representations after stroke: implications for recovery from brain damage." Mol Psychiatry **2**(3): 188-191.
- Nudo, R. J. (2006). "Mechanisms for recovery of motor function following cortical damage." Curr Opin Neurobiol **16**(6): 638-644.
- Nudo, R. J. (2013). "Recovery after brain injury: mechanisms and principles." Front Hum Neurosci **7**: 887.
- Nudo, R. J., G. W. Milliken, W. M. Jenkins and M. M. Merzenich (1996). "Use-dependent alterations of movement representations in primary motor cortex of adult squirrel monkeys." J Neurosci **16**(2): 785-807.
- Palikaras, K. and N. Tavernarakis (2014). "Mitochondrial homeostasis: the interplay between mitophagy and mitochondrial biogenesis." Exp Gerontol **56**: 182-188.
- Pavlidis, C., E. Miyashita and H. Asanuma (1993). "Projection from the sensory to the motor cortex is important in learning motor skills in the monkey." J Neurophysiol **70**(2): 733-741.
- Pearen, M. A., J. G. Ryall, G. S. Lynch and G. E. Muscat (2009). "Expression profiling of skeletal muscle following acute and chronic beta2-adrenergic stimulation: implications for hypertrophy, metabolism and circadian rhythm." BMC Genomics **10**: 448.
- Plautz, E. J., S. Barbay, S. B. Frost, K. M. Friel, N. Dancause, E. V. Zoubina, A. M. Stowe, B. M. Quaney and R. J. Nudo (2003). "Post-infarct cortical plasticity and behavioral recovery using concurrent cortical stimulation and rehabilitative training: a feasibility study in primates." Neurol Res **25**(8): 801-810.

- Qian, L., H. M. Wu, S. H. Chen, D. Zhang, S. F. Ali, L. Peterson, B. Wilson, R. B. Lu, J. S. Hong and P. M. Flood (2011). "beta2-adrenergic receptor activation prevents rodent dopaminergic neurotoxicity by inhibiting microglia via a novel signaling pathway." J Immunol **186**(7): 4443-4454.
- Riban, V. and M. F. Chesselet (2006). "Region-specific sprouting of crossed corticofugal fibers after unilateral cortical lesions in adult mice." Exp Neurol **197**(2): 451-457.
- Riout-Pedotti, M. S., J. P. Donoghue and A. Dunaevsky (2007). "Plasticity of the synaptic modification range." J Neurophysiol **98**(6): 3688-3695.
- Riout-Pedotti, M. S., D. Friedman and J. P. Donoghue (2000). "Learning-induced LTP in neocortex." Science **290**(5491): 533-536.
- Sakamoto, T., K. Arissian and H. Asanuma (1989). "Functional role of the sensory cortex in learning motor skills in cats." Brain Res **503**(2): 258-264.
- Sakamoto, T., L. L. Porter and H. Asanuma (1987). "Long-lasting potentiation of synaptic potentials in the motor cortex produced by stimulation of the sensory cortex in the cat: a basis of motor learning." Brain Res **413**(2): 360-364.
- Sampaio-Baptista, C., A. A. Khrapitchev, S. Foxley, T. Schlagheck, J. Scholz, S. Jbabdi, G. C. DeLuca, K. L. Miller, A. Taylor, N. Thomas, J. Kleim, N. R. Sibson, D. Bannerman and H. Johansen-Berg (2013). "Motor skill learning induces changes in white matter microstructure and myelination." J Neurosci **33**(50): 19499-19503.
- Schallert, T., S. M. Fleming, J. L. Leasure, J. L. Tillerson and S. T. Bland (2000). "CNS plasticity and assessment of forelimb sensorimotor outcome in unilateral rat models of stroke, cortical ablation, parkinsonism and spinal cord injury." Neuropharmacology **39**(5): 777-787.
- Schneider, C. A., W. S. Rasband and K. W. Eliceiri (2012). "NIH Image to ImageJ: 25 years of image analysis." Nat Methods **9**(7): 671-675.
- Schroeter, M., S. Jander, I. Huitinga, O. W. Witte and G. Stoll (1997). "Phagocytic response in photochemically induced infarction of rat cerebral cortex. The role of resident microglia." Stroke **28**(2): 382-386.
- Sciamanna, M. A., J. Zinkel, A. Y. Fabi and C. P. Lee (1992). "Ischemic injury to rat forebrain mitochondria and cellular calcium homeostasis." Biochim Biophys Acta **1134**(3): 223-232.
- Simon-Areces, J., M. O. Dietrich, G. Hermes, L. M. Garcia-Segura, M. A. Arevalo and T. L. Horvath (2012). "UCP2 induced by natural birth regulates neuronal differentiation of the hippocampus and related adult behavior." PLoS One **7**(8): e42911.
- Sims, N. R. and M. F. Anderson (2002). "Mitochondrial contributions to tissue damage in stroke." Neurochem Int **40**(6): 511-526.

- Sims, N. R. and H. Muyderman (2010). "Mitochondria, oxidative metabolism and cell death in stroke." Biochim Biophys Acta **1802**(1): 80-91.
- Smith, J. A., L. J. Stallons, J. B. Collier, K. D. Chavin and R. G. Schnellmann (2015). "Suppression of mitochondrial biogenesis through toll-like receptor 4-dependent mitogen-activated protein kinase kinase/extracellular signal-regulated kinase signaling in endotoxin-induced acute kidney injury." J Pharmacol Exp Ther **352**(2): 346-357.
- Smith, S. M., M. Jenkinson, H. Johansen-Berg, D. Rueckert, T. E. Nichols, C. E. Mackay, K. E. Watkins, O. Ciccarelli, M. Z. Cader, P. M. Matthews and T. E. Behrens (2006). "Tract-based spatial statistics: voxelwise analysis of multi-subject diffusion data." Neuroimage **31**(4): 1487-1505.
- Soares, J. M., P. Marques, V. Alves and N. Sousa (2013). "A hitchhiker's guide to diffusion tensor imaging." Front Neurosci **7**: 31.
- Sofroniew, M. V. and H. V. Vinters (2010). "Astrocytes: biology and pathology." Acta Neuropathol **119**(1): 7-35.
- Soliman, F., C. E. Glatt, K. G. Bath, L. Levita, R. M. Jones, S. S. Pattwell, D. Jing, N. Tottenham, D. Amso, L. H. Somerville, H. U. Voss, G. Glover, D. J. Ballon, C. Liston, T. Teslovich, T. Van Kempen, F. S. Lee and B. J. Casey (2010). "A genetic variant BDNF polymorphism alters extinction learning in both mouse and human." Science **327**(5967): 863-866.
- Stallons, L. J., R. M. Whitaker and R. G. Schnellmann (2014). "Suppressed mitochondrial biogenesis in folic acid-induced acute kidney injury and early fibrosis." Toxicol Lett **224**(3): 326-332.
- Steiner, J. L., E. A. Murphy, J. L. McClellan, M. D. Carmichael and J. M. Davis (2011). "Exercise training increases mitochondrial biogenesis in the brain." J Appl Physiol (1985) **111**(4): 1066-1071.
- Stinear, C. (2010). "Prediction of recovery of motor function after stroke." Lancet Neurol **9**(12): 1228-1232.
- Stroemer, R. P., T. A. Kent and C. E. Hulsebosch (1995). "Neocortical neural sprouting, synaptogenesis, and behavioral recovery after neocortical infarction in rats." Stroke **26**(11): 2135-2144.
- Suda, K., M. Tsuruta, J. Eom, C. Or, T. Mui, J. E. Jaw, Y. Li, N. Bai, J. Kim, J. Man, D. Ngan, J. Lee, S. Hansen, S. W. Lee, S. Tam, S. P. Man, S. Van Eeden and D. D. Sin (2011). "Acute lung injury induces cardiovascular dysfunction: effects of IL-6 and budesonide/formoterol." Am J Respir Cell Mol Biol **45**(3): 510-516.
- Tabesh, A., J. H. Jensen, B. A. Ardekani and J. A. Helpert (2011). "Estimation of tensors and tensor-derived measures in diffusional kurtosis imaging." Magn Reson Med **65**(3): 823-836.

- Tennant, K. A., D. L. Adkins, M. D. Scalco, N. A. Donlan, A. L. Asay, N. Thomas, J. A. Kleim and T. A. Jones (2012). "Skill learning induced plasticity of motor cortical representations is time and age-dependent." Neurobiol Learn Mem **98**(3): 291-302.
- Tennant, K. A., A. L. Kerr, D. L. Adkins, N. Donlan, N. Thomas, J. A. Kleim and T. A. Jones (2015). "Age-dependent reorganization of peri-infarct "premotor" cortex with task-specific rehabilitative training in mice." Neurorehabil Neural Repair **29**(2): 193-202.
- Thiel, A. and W. D. Heiss (2011). "Imaging of microglia activation in stroke." Stroke **42**(2): 507-512.
- Thomas, A. G., S. Marrett, Z. S. Saad, D. A. Ruff, A. Martin and P. A. Bandettini (2009). "Functional but not structural changes associated with learning: an exploration of longitudinal voxel-based morphometry (VBM)." Neuroimage **48**(1): 117-125.
- Turner, R., D. Le Bihan, J. Maier, R. Vavrek, L. K. Hedges and J. Pekar (1990). "Echo-planar imaging of intravoxel incoherent motion." Radiology **177**(2): 407-414.
- Umesh Rudrapatna, S., T. Wieloch, K. Beirup, K. Ruscher, W. Mol, P. Yanev, A. Leemans, A. van der Toorn and R. M. Dijkhuizen (2014). "Can diffusion kurtosis imaging improve the sensitivity and specificity of detecting microstructural alterations in brain tissue chronically after experimental stroke? Comparisons with diffusion tensor imaging and histology." Neuroimage **97**: 363-373.
- Ungerleider, L. G., J. Doyon and A. Karni (2002). "Imaging brain plasticity during motor skill learning." Neurobiol Learn Mem **78**(3): 553-564.
- van der Blik, A. M., Q. Shen and S. Kawajiri (2013). "Mechanisms of mitochondrial fission and fusion." Cold Spring Harb Perspect Biol **5**(6).
- Veenith, T., S. Goon and R. M. Burnstein (2009). "Molecular mechanisms of traumatic brain injury: the missing link in management." World J Emerg Surg **4**: 7.
- Ventura-Clapier, R., A. Garnier and V. Veksler (2008). "Transcriptional control of mitochondrial biogenesis: the central role of PGC-1alpha." Cardiovasc Res **79**(2): 208-217.
- Vidoni, E. D., N. E. Acerra, E. Dao, S. K. Meehan and L. A. Boyd (2010). "Role of the primary somatosensory cortex in motor learning: An rTMS study." Neurobiol Learn Mem **93**(4): 532-539.
- Vila, M. and S. Przedborski (2003). "Targeting programmed cell death in neurodegenerative diseases." Nat Rev Neurosci **4**(5): 365-375.
- Voorhies, A. C., Adkins, D. L., Jones, T. A. (2001). "Cortical Structural Plasticity and Behavioral Deficits Following Endothelin-1 Induced Ischemic Lesions of the Sensorimotor Cortex." Society for Neuroscience Abstract: 190.

- Wang, J. Y., F. Chen, X. Q. Fu, C. S. Ding, L. Zhou, X. H. Zhang and Z. G. Luo (2014). "Caspase-3 cleavage of dishevelled induces elimination of postsynaptic structures." Dev Cell **28**(6): 670-684.
- Wang, S., E. X. Wu, D. Qiu, L. H. Leung, H. F. Lau and P. L. Khong (2009). "Longitudinal diffusion tensor magnetic resonance imaging study of radiation-induced white matter damage in a rat model." Cancer Res **69**(3): 1190-1198.
- Wang, X., M. Casadio, K. A. Weber, 2nd, F. A. Mussa-Ivaldi and T. B. Parrish (2013). "White matter microstructure changes induced by motor skill learning utilizing a body machine interface." Neuroimage **88C**: 32-40.
- Weber, R. A., E. S. Hui, J. H. Jensen, X. Nie, M. F. Falangola, J. A. Helpert and D. L. Adkins (2015). "Diffusional kurtosis and diffusion tensor imaging reveal different time-sensitive stroke-induced microstructural changes." Stroke **46**(2): 545-550.
- Whelan, C. J., M. Johnson and C. J. Vardey (1993). "Comparison of the anti-inflammatory properties of formoterol, salbutamol and salmeterol in guinea-pig skin and lung." Br J Pharmacol **110**(2): 613-618.
- Whishaw, I. Q. and S. M. Pellis (1990). "The structure of skilled forelimb reaching in the rat: a proximally driven movement with a single distal rotatory component." Behav Brain Res **41**(1): 49-59.
- Whishaw, I. Q., S. M. Pellis, B. P. Gorny and V. C. Pellis (1991). "The impairments in reaching and the movements of compensation in rats with motor cortex lesions: an endpoint, videorecording, and movement notation analysis." Behav Brain Res **42**(1): 77-91.
- Wills, L. P., R. E. Trager, G. C. Beeson, C. C. Lindsey, Y. K. Peterson, C. C. Beeson and R. G. Schnellmann (2012). "The beta2-adrenoceptor agonist formoterol stimulates mitochondrial biogenesis." J Pharmacol Exp Ther **342**(1): 106-118.
- Wise, R. S. a. S. P. (2005). Computational Neurobiology of Reaching and Pointing: A Foundation for Motor Learning. Cambridge MA, MIT Press.
- Wojtczak, L., M. Lebedzinska, J. M. Suski, M. R. Wieckowski and P. Schonfeld (2011). "Inhibition by purine nucleotides of the release of reactive oxygen species from muscle mitochondria: indication for a function of uncoupling proteins as superoxide anion transporters." Biochem Biophys Res Commun **407**(4): 772-776.
- Wolpert, D. M., Z. Ghahramani and J. R. Flanagan (2001). "Perspectives and problems in motor learning." Trends Cogn Sci **5**(11): 487-494.
- Woodruff, T. M., J. Thundyil, S. C. Tang, C. G. Sobey, S. M. Taylor and T. V. Arumugam (2011). "Pathophysiology, treatment, and animal and cellular models of human ischemic stroke." Mol Neurodegener **6**(1): 11.
- Wu, Z., P. Puigserver, U. Andersson, C. Zhang, G. Adelmant, V. Mootha, A. Troy, S. Cinti, B. Lowell, R. C. Scarpulla and B. M. Spiegelman (1999). "Mechanisms controlling

mitochondrial biogenesis and respiration through the thermogenic coactivator PGC-1." Cell **98**(1): 115-124.

Xingju Nie, D. R., Aurelie Ledreux, Ann-Charlotte Granholm, Heather Boger, Maria Falangola (2015). Preliminary Evidence of Midazolam Effect in Brain Microstructure using Diffusional Kurtosis Imaging

Xiong, W., A. E. MacColl Garfinkel, Y. Li, L. I. Benowitz and C. L. Cepko (2015). "NRF2 promotes neuronal survival in neurodegeneration and acute nerve damage." J Clin Invest **125**(4): 1433-1445.

Xu, T., X. Yu, A. J. Perlik, W. F. Tobin, J. A. Zweig, K. Tennant, T. Jones and Y. Zuo (2009). "Rapid formation and selective stabilization of synapses for enduring motor memories." Nature **462**(7275): 915-919.

Yakes, F. M. and B. Van Houten (1997). "Mitochondrial DNA damage is more extensive and persists longer than nuclear DNA damage in human cells following oxidative stress." Proc Natl Acad Sci U S A **94**(2): 514-519.

Zatorre, R. J., R. D. Fields and H. Johansen-Berg (2012). "Plasticity in gray and white: neuroimaging changes in brain structure during learning." Nat Neurosci **15**(4): 528-536.

Zeman, R. J., H. Peng and J. D. Etlinger (2004). "Clenbuterol retards loss of motor function in motor neuron degeneration mice." Exp Neurol **187**(2): 460-467.

Zhang, Q., Y. Wu, P. Zhang, H. Sha, J. Jia, Y. Hu and J. Zhu (2012). "Exercise induces mitochondrial biogenesis after brain ischemia in rats." Neuroscience **205**: 10-17.

Zhuo, J., S. Xu, J. L. Proctor, R. J. Mullins, J. Z. Simon, G. Fiskum and R. P. Gullapalli (2012). "Diffusion kurtosis as an in vivo imaging marker for reactive astrogliosis in traumatic brain injury." Neuroimage **59**(1): 467-477.